STRUCTURE-FUNCTION STUDIES ON THE FLAVOCYTOCHROME CELLOBIOSE DEHYDROGENASE FROM *PHANEROCHAETE CHRYSOSPORIUM*

Frederik A. J. Rotsaert
M.S., Technological University of Delft, 1996

A dissertation to the faculty of the
OGI School of Science and Engineering
at Oregon Health & Science University
in partial fulfillment of the requirements
for the degree
Doctor of Philosophy
in
Biochemistry and Molecular Biology

August 2003

The dissertation "Structure–Function Studies on the Flavocytochrome Cellobiose Dehydrogenase from *Phanerochaete chrysosporium*" by Frederik A. J. Rotsaert has been examined and approved by the following Examination Committee:

V. Renganathan, Advisor
Associate Professor

Pierre Moënne-Loccoz
Assistant Professor

Paul Tratnyek
Associate Professor

James W. Whittaker
Associate Professor

ACKNOWLEDGEMENTS

First, I would like to thank my advisors, Professors Michael H. Gold and V. Renganathan, who took me as a student in my second year at OGI, for the academic freedom I was given over the years and for their constant support, especially at the end of my thesis. Second, thanks to Professor Emeritus Joanne Sanders-Loehr for letting me start as a graduate student in her laboratory, for her support and her effort to bring the "Rieske project" to a successful end. Third, thanks to my thesis committee members, Professors Pierre Moënne-Loccoz, James W. Whittaker and Paul G. Tratnyek, for thoroughly reading my thesis.

Nancy and Terrie have made the small bureaucracy of OGI even smaller, being always available and helpful. Many thanks. Terrie's critical eye over the many versions of papers and the thesis brought all to a successful end. Thanks.

My thesis would have not been possible without the help of several collaborators: Thanks to Pierre Moenne-Loccoz for his critical input into the RR study and the thesis (and also or the many hours we have spent on and off the tennis court), Simon de Vries for his hospitality and for putting me in contact with OGI, and Christina Divne and Martin Hallberg for their outstanding work on the heme variant.

The daily work would not have been so enjoyable without the presence of my many lab-mates over the years, Heather, Biao, Maarten, Mary, Sridhar, Lakshmi, Vijay, and Shen Lu. Their friendship and helpfulness made OGI a great place to be, as well as to spent time outside of work (drinking an Oregon beer, camping trips and hitting the cross-country slopes with the BMB students).

Thanks to the friends I have made over the many years: Shailesh, Ashish, Bridget, John, Heleen, Sabrina, Esther, Willow, Ash, Phillip, Pam, Mike Amol, Eleina, Michela, Iavor. The camping, biking, and hiking throughout Oregon and the partying in Portland made the more than six year unforgettable. In particular, I want

to thank, my roommates for five years, Montse and Johan, for their support over the years; they have been the best friends. Thanks to Sergey for his friendship and for the many biking and hiking trips.

Last, moeke and papa, I cannot thank them enough for the love and support from the beginning till end, during high and low times. Thanks to Isabelle, Marc and Michiel for visiting me so many times, despite the distance between Portland and Holland.

TABLE OF CONTENTS

LIST OF TABLES

LIST OF FIGURES

ABSTRACT

Structure-Function Studies on the Flavocytochrome Cellobiose Dehydrogenase from *Phanerochaete chrysosporium*

Frederik A.J. Rotsaert, M.S.

Ph.D., OGI School of Science & Engineering
at Oregon Health & Science University
August 2003

Thesis Advisor: Dr. V. Renganathan

Cellobiose dehydrogenase (CDH) is a unique extracellular flavocytochrome, produced under cellulolytic conditions by the white-rot fungus *Phanerochaete chrysosporium*. This enzyme consists of a flavin domain and a *b*-type cytochrome domain connected via a short linker peptide. This enzyme catalyzes the oxidation of cellobiose to cellobionolactone, which is followed by the transfer of electrons to an electron acceptor, either directly by the flavin domain or via the cytochrome domain.

The residues Met65, His114, and His163 were targeted for alanine mutation to identify the axial heme ligands. The spectral and kinetic characteristics of H114A were similar to that of wild-type CDH. In contrast, M65A and H163A yielded mainly 70-kDa flavoproteins and very little of the whole 90-kDa flavocytochromes. This strongly suggests Met65 and His163 as ligands, and in the absence of either of the ligands the cytochrome domain is unstable and susceptible to degradation.

To further investigate the role of Met65 in modulating the reactivity of the cytochrome domain, a second CDH variant of Met65, M65H, was produced. The flavin reactivity is retained in M65H, but the inter-domain electron transfer is

essentially abolished, most likely due to a decrease in the redox potential of the heme. The electronic absorption and resonance Raman spectroscopy data support a *bis*-histidyl coordination. The tertiary structure of the cytochrome M65H variant shows the first example of an iron—N^{δ} His bond in a *b*-type heme protein.

The residues His689 and N732 in the flavin domain were substituted with Gln, Asn, Glu, Asp, Val, Ala and/or His to examine the role of these residues in catalysis. An over 1000-fold decrease in reactivity with cellobiose is observed for all H689 variants, suggesting that this residue acts as a general base in catalysis. The oxidation and binding of substrate by the different N732 variants varies over one to three orders of magnitude, suggesting a role for N732 in the productive binding of the substrate. In addition, the proximity of a neutral residue, such as N732, to the H689 and isoalloxazine ring appears to modulate the acidity of the general base and the electrostatic environment around the flavin ring, respectively.

CHAPTER 1
INTRODUCTION

1.1 FUNGAL DEGRADATION OF CELLULOSE

1.1.1 Wood and Cellulose

Wood (xylem), the hard, fibrous substance of the tree, is primarily a matrix of plant cell walls. During cell division and cell enlargement, the primary cell wall is formed and is further thickened by the deposit of the secondary cell wall, a composite of cellulose fibrils within a matrix of amorphous hemicelluloses and lignin (lignocellulose matrix) [Thomas, 1991]. Upon maturation, most of the plant cells die, and these cells and their cell walls function as mechanical support for the tree. Newly formed xylem also transports nutrients and water through the trunk and limbs.

Cellulose comprises 40–55% of the lignocellulosic material of woody plant cells, and is a long chain of 10^2–10^4 β-D-glucose subunits (Fig. 1.1) linked together via (1→4) glycosidic bonds [Okamura, 1991]. The β-configuration imposes a rotation of 180° on alternating units, so that the basic unit is cellobiose (Fig. 1.1). This configuration results in a stiff and straight cellulose chain, different from the α-linked amylose fraction of starch, which forms a helical conformation. The linearity of cellulose chains contributes to the strong van der Waals interactions between chains, as well as the formation of numerous inter- and intramolecular hydrogen bonds (Fig. 1.1). These interactions result in the formation of rigid, insoluble and semi-crystalline microfibrils, which contain several hundred parallel-oriented cellulose chains [Beguin and Aubert, 1994; Teeri, 1997; Bayer et al., 1998]. At the surface, the crystalline regions are interspersed by disordered amorphous or paracrystalline regions.

A

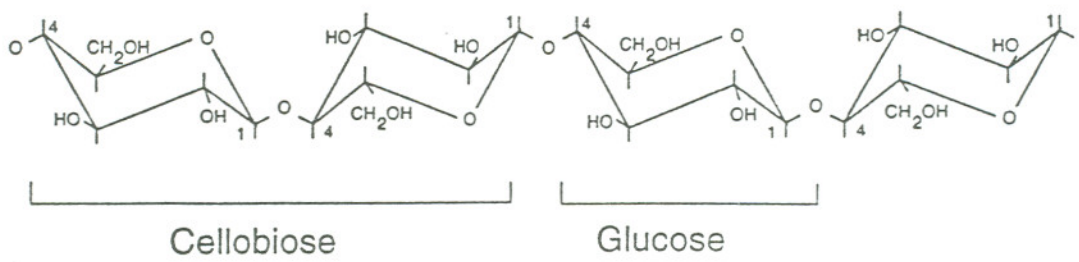

B

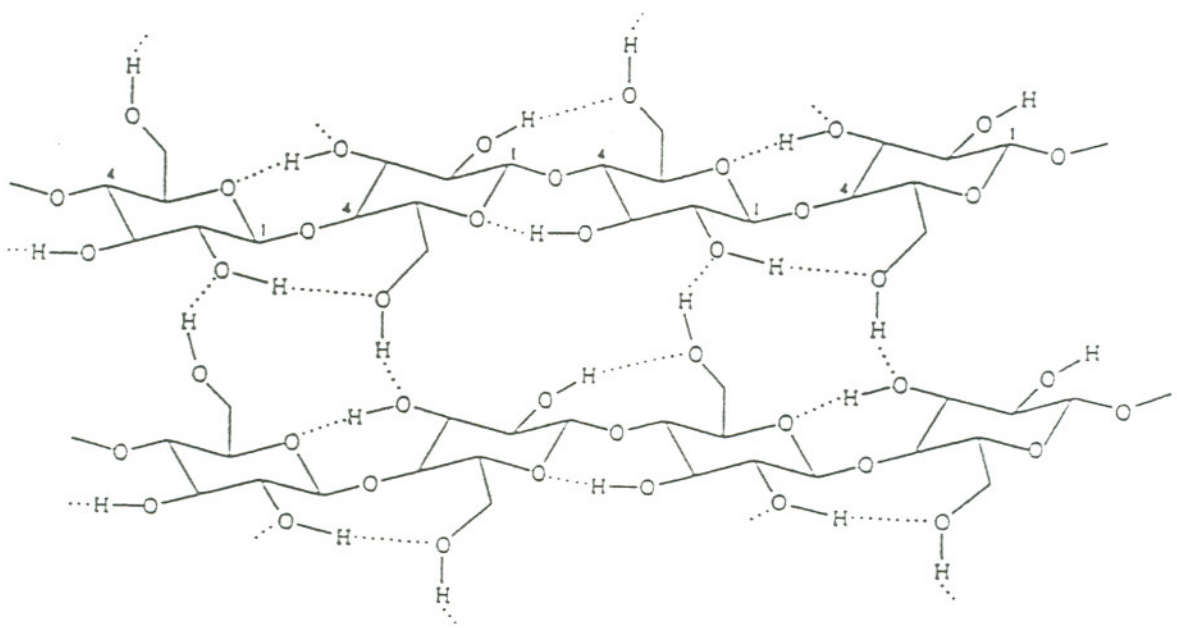

Fig. 1.1 Structure of cellulose. (**A**) β-Glucosidic bonds. (**B**) Hydrogen bond network in cellulose.

1.1.2 Cellulolytic Microorganisms

Annually, about 50% of all carbon dioxide that is converted to biomass by photosynthetic fixation is sequestered in cellulose fibers (10^9–10^{11} tons). The carbon stored in cellulose needs to be returned to the atmosphere in order to complete the carbon cycle. This is predominantly achieved through microbial degradation of cellulose [Eriksson et al., 1990]. Wood-rot fungi contribute significantly to wood degradation. They are classified into three different groups: white-rot, brown-rot, and soft-rot fungi [Eriksson et al., 1990]. This classification is based on the texture and morphological appearance of the decayed wood. Almost all white-rot fungi belong to the Basidiomycotina, which include *Phanerochaete chrysosporium*, *Dichomitus squalens*, and *Trametes versicolor*. They are the only organisms that can completely degrade all three wood biopolymers—cellulose, hemicellulose and lignin—to CO_2. Some strains selectively remove lignin, resulting in bleaching of wood where the residual white color comes from the cellulosic and hemicellulosic backbone. Brown-rot fungi, such as *Conophora puteana* and *Gloeophyllum trabeum*, also are classified as Basidiomycotina. They degrade wood to a brown-colored, amorphous, and crumbly residue. The brown-rots apparently selectively degrade cellulose, leaving lignin essentially intact or with some modifications. The brown color of rotted wood comes from residual lignin. The third class is composed of the soft-rot fungi. They are mostly Ascomycetes and Deuteromycetes, and include *Trichoderma reesei* and *Sporotrichum thermophile*. These fungi attack wood with a high moisture content and, like the brown-rot fungi, primarily decompose cellulose and hemicellulose.

1.1.3 *Phanerochaete chrysosporium*

The morphological characteristics of the white-rot fungus *Phanerochaete chrysosporium* were first described by H.H. Burdsall in 1974 [Burdsall and Eslyn, 1974]. It does not form mushrooms but flat fruiting bodies that appear as a crust on decaying wood. This basidiomycete serves as a model organism for white-rot degradation of wood for the following reasons [Gold and Alic, 1993]: it can degrade all three wood biopolymers simultaneously as well as selectively; it is thermo-tolerant;

it can be cultured under laboratory conditions; and it produces sexual basidiospores and asexual conidia spores, which are essential for genetic manipulation [Burdsall and Eslyn, 1974; Gold and Cheng, 1978]. In 2001, a draft of the 30 million base-pair genome of *P. chrysosporium*, strain BKM-F-1767, was reported using a whole-genome shotgun approach [White-Rot Genome Project, 2002]. The complete genome should further advance the understanding of microbial degradation of wood. From an industrial perspective, this organism has attracted the attention of the paper and pulp industry. Pulping (delignification) of wood chips is an energy-intensive and chemical process-intensive step in the production of paper from wood. A specific lignin-degrading fungus, such as *P. chrysosporium*, could be an environmental alternative (biopulping) or could be used as a pretreatment step, reducing the energy and chemical (alkaline) requirements. At the moment, several lignocellulolytic enzymes, including cellulases and xylananses, are commercially used in several steps of the production of paper (*de novo* and recycled), as well as the treatment of waste streams [Pratima and Bajpai, 2001]. In addition, the fungus has potential application in bioremediation due to its capability to mineralize many toxic and recalcitrant aromatic compounds, such as pesticides, polycyclic and chlorinated aromatic compounds [Field et al., 1993; Cameron et al., 2000; Reddy and Gold, 2000].

1.2 EXTRACELLULAR FUNGAL CELLULOLYTIC ENZYMES

1.2.1 Fungal Cellulases and Their Catalytic Action

Filamentous fungi secrete a range of redox and hydrolytic enzymes to degrade wood to utilizable carbon and energy sources [Eriksson et al., 1990]. The extracellular enzymes decompose polymeric substrates to small, soluble compounds that are taken up by the cells. Cellulases, β-1,4-glycoside hydrolases, form the major group of extracellular cellulolytic enzymes [Bisaria and Mishra, 1989; Beguin and Aubert, 1994]. The action of these enzymes on the polymeric substrate cellulose can be described as an endo– or exo-type of attack. Endo-β-1,4-glucanases (endoglucanase) cleave glycoside bonds within the cellulose chains. Cellobiohydrolases (exo-β-1,4-glucanase) initiate their action from the end of the

chains, releasing predominantly cellobiose [Teeri, 1997]. β-Glucosidase, the third member of the cellulases, hydrolyzes cellobiose to glucose, thus completing cellulose hydrolysis. An oxidative enzyme, cellobiose dehydrogenase, is also implicated in the degradation of cellulose (see Section 1.3).

Individually, endoglucanases and cellobiohydrolases can modify cellulose, but cannot efficiently solubilize it. Endoglucanases can rapidly decrease the degree of polymerization (DP), but release soluble products only slowly [Kleman-Leyer et al., 1994]. Cellobiohydrolases can attack crystalline areas of the cellulose surface, producing primarily cellobiose from the end of the cellulose chains, but decrease the DP only slowly [Teeri, 1997]. β-Glucosidase cannot attack cellulose directly. However, the three components, which are simultaneously secreted by cellulolytic organisms, can cooperatively act on cellulose (Fig. 1.2). In the simplest model, the cellulases bind to cellulose, and this tight absorption is linked with catalytic activity on the solid substrate [Klyosov, 1990]. The endoglucanases randomly cleave within the cellulose chain, preferentially the amorphous regions, thus creating reducing and non-reducing ends. The cellobiohydrolases then remove cellobiose. This endo–exo attack can explain the synergy between the two enzymes [Beguin and Aubert, 1994]. In addition, initial cleavage creates new substrate binding sites, and it is apparent that fungi secrete a number of isozymes of each type of cellulases with different specificities. For example, five endoglucanases [Eriksson and Pettersson, 1975] and three cellobiohydrolases [Uzcategui et al., 1991; Henriksson et al., 1999] have been purified from *P. chrysosporium* (although some may be holoenzyme degradation products). Cloning revealed six genes coding for cellobiohydrolases I (Cel7), of which two may have different substrate specificity [Munoz et al., 2001]. Finally, β-glucosidase hydrolyzes cellobiose, reducing cellobiose-dependent inhibition of other cellulases and completing the depolymerization of cellulose [Beguin and Aubert, 1994].

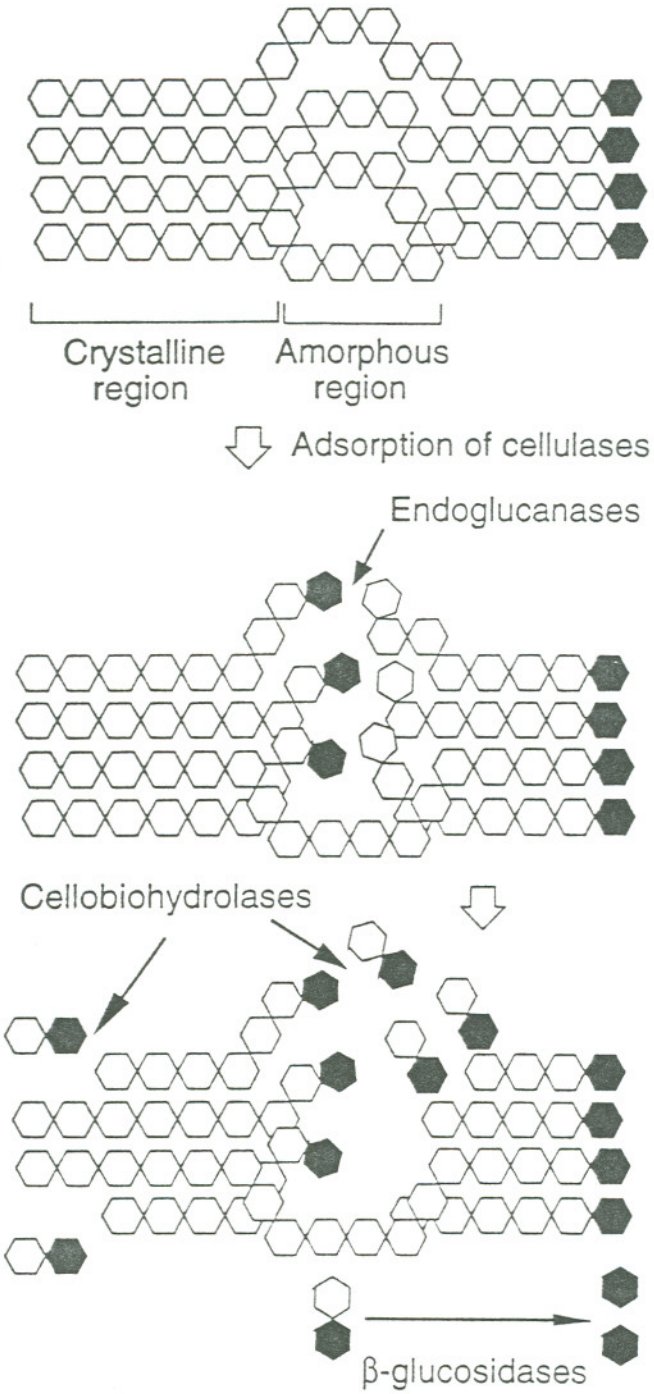

Fig. 1.2 Cellulose degradation by fungal cellulase system.

1.2.2 Catalytic Domain

Cellulases are modular enzymes composed of multiple functionally and structurally distinct units. They generally consist of a catalytic domain connected by an extended linker (30–40 amino acids) to one or more cellulose binding domains (CBDs) [Henrissat et al., 1998]. The linker is rich in Ser and Thr residues [Gilkes et al., 1991], which are often heavily glycosylated [Lindner and Teeri, 1997]. Separate domains can be obtained by treatment of the holoenzyme with an appropriate protease. The catalytic domain belongs to the group of glycoside hydrolases, which are classified into 88 families [Henrissat and Bairoch, 1993; Henrissat and Bairoch, 1996; Bourne and Henrissat, 2001] (see *http://afmb.cnrs-mrs.fr/~cazy/CAZY/acc.html* for updated list). Comparison of amino acid sequences of cellulases with other hydrolases suggests that fungal cellulases are distributed in five families.

The last decade has seen rapid advances in our understanding of cellulases via genetic engineering, protein engineering, and crystallographic studies. Although the crystallization of a holo cellulase has not been reported to date, likely due to the flexible linker, a number of catalytic domain structures have been solved [Bayer et al., 1998; Schulein, 2000]. These structural studies have probed various questions, such as the structural origin for the catalytic mechanism of hydrolysis, the substrate specificity of endoglucanases and cellobiohydrolases, and the binding to the cellulose substrate. Cellulose hydrolysis involves acid–base catalysis [Koshland, 1953; Zechel and Withers, 2000], and, in accordance with that, two acidic amino acid residues (Glu or Asp) are found in the active side of cellulases [Schulein, 2000]. Endoglucanases make internal cuts in the cellulose chain and typically display an open substrate-binding cleft [Kleywegt et al., 1997]. Cellobiohydrolases in contrast cleave from the ends and act progressively on the chain, i.e., after cleavage of cellobiose they slide further along the chain to position themselves for the release of subsequent cellobiose units [Rouvinen et al., 1990; Divne et al., 1994]. For this reason, the active site is tunnel-shaped to bind a single cellulose chain. Different isozymes may display different substrate specificity; for example, the two cellobiohydrolases from *Trichoderma reesei*, Cel7A and Cel6A, formerly called CBHI and CBHII, act on reducing and non-reducing ends, respectively [Divne et al., 1998; Zou et al., 1999].

Recently, several three-dimensional models of cellulase–substrate complex were presented. One approach involved complex formation with a non-hydrolyzable substrate, an example of a non-hydrolyzable analogue of cellotetraose bound to cellobiohydrolase Cel6A from *T. reesei* [Zou et al., 1999]. It was also possible to bind cellodextrose to a catalytically inactive mutant of cellobiohydrolase Cel7A from *T. reesei* [Divne et al., 1998]. These models show that the substrate is bound to the enzyme via a large number of protein-mediated hydrogen bonds and via several hydrophobic stacking interactions with tryptophan, tyrosine, and phenylalanine residues.

1.2.3 Cellulose Binding Domain

The catalytic domain does not require the cellulose binding domain (CBD), to hydrolyze soluble oligosaccharides and soluble cellulose. However, when the CBD is proteolytically or genetically removed, activity towards insoluble cellulose is greatly reduced, concomitant with a reduction in cellulose binding [Klyosov, 1990; Lindner and Teeri, 1997]. Possible roles for the adsorption include increase of the effective enzyme concentration on the cellulose surface and solubilization of the cellulose chains by interaction between the CBD and cellulose surface [Lindner and Teeri, 1997]. In general, one or more CBDs are connected via the linker at the C- or N-terminus of the catalytic domain. The fungal CBDs consist of 30–40 residues and have a conserved protein sequence [Tomme et al., 1995]. The best-characterized fungal domain is from *T. reesei* Cel7A. The NMR structure [Kraulis et al., 1989] exhibits three antiparallel β-strands with an overall wedge shape. One face of the wedge is hydrophobic; the other is hydrophilic. Three highly conserved, structurally aligned tyrosine residues (Y5, Y31 and Y32) on the hydrophobic face are implicated in binding to crystalline cellulose by site-directed mutagenesis and NMR spectroscopy [Reinikainen et al., 1992; Linder et al., 1995; Mattinen et al., 1997]. Molecular modeling suggests that the tyrosine residues may be stacked onto every other glucose unit in the cellulose chain [Mattinen et al., 1997].

1.2.4 Cellulose Degradation by Brown-Rot Fungi

The mechanism of degradation of cellulose by brown-rot fungi, such as *Gloeophyllum trabeum* and *Tyromyces palustris*, appears to be different from that of the other two classes of wood-rot fungi. So far there is no report of the purification of a brown-rot cellobiohydrolase, suggesting no synergistic action between endoglucanases and cellobiohydrolases [Xu and Goodell, 2001]. Koenigs had proposed in early 1970 that hydroxyl radicals (·OH), powerful oxidants, are responsible for the rapid depolymerization of cellulose by brown-rot fungi [Koenig, 1974, 1975]. These radicals are produced via a Fenton reaction, the reduction of hydrogen peroxide by ferrous iron. Recently, a mechanism for the production of the Fenton reagents from oxygen and ferric iron by brown-rot fungi has been proposed (Fig. 1.3) [Kerem et al., 1999]. This involve the one-electron reduction reaction of Fe(III) and oxygen with hydroquinones and the regeneration of the hydroquinones by a fungal enzyme system. This mechanism is supported by the extraction of these hydroquinones [Paszczynski et al., 1999; Jensen et al., 2001] from the extracellular medium and the purification of an intracellular NADH:Quinone oxidoreductase from *G. trabeum*, active towards these quinones [Jensen et al., 2002].

1.3 CELLOBIOSE DEHYDROGENASE

An extracellular oxidoreductase was initially implicated in the degradation of cellulose by wood-rot fungi when Eriksson and coworkers demonstrated that the cell-free cultures of *P. chrysosporium*, *Polyporus adustus*, *Myrothecium verrucaria*, and *Trichoderma viride* degraded cellulose twice as fast in air compared with an anaerobic environment [Eriksson et al., 1974]. This group subsequently discovered two cellobiose oxidizing enzymes from *P. chrysosporium*, a flavocytochrome cellobiose dehydrogenase (CDH) and a flavin enzyme cellobiose:quinone oxidoreductase (CBQase). It is now accepted that CBQase is the flavin domain of CDH, formed by (proteolytic) cleavage of the holoenzyme [Wood and Wood, 1992; Habu et al., 1993; Raices et al., 2002]. The truncated cytochrome domain has also been purified from cellulolytic cultures of *P. chrysosporium*. [Hallberg et al., 2000].

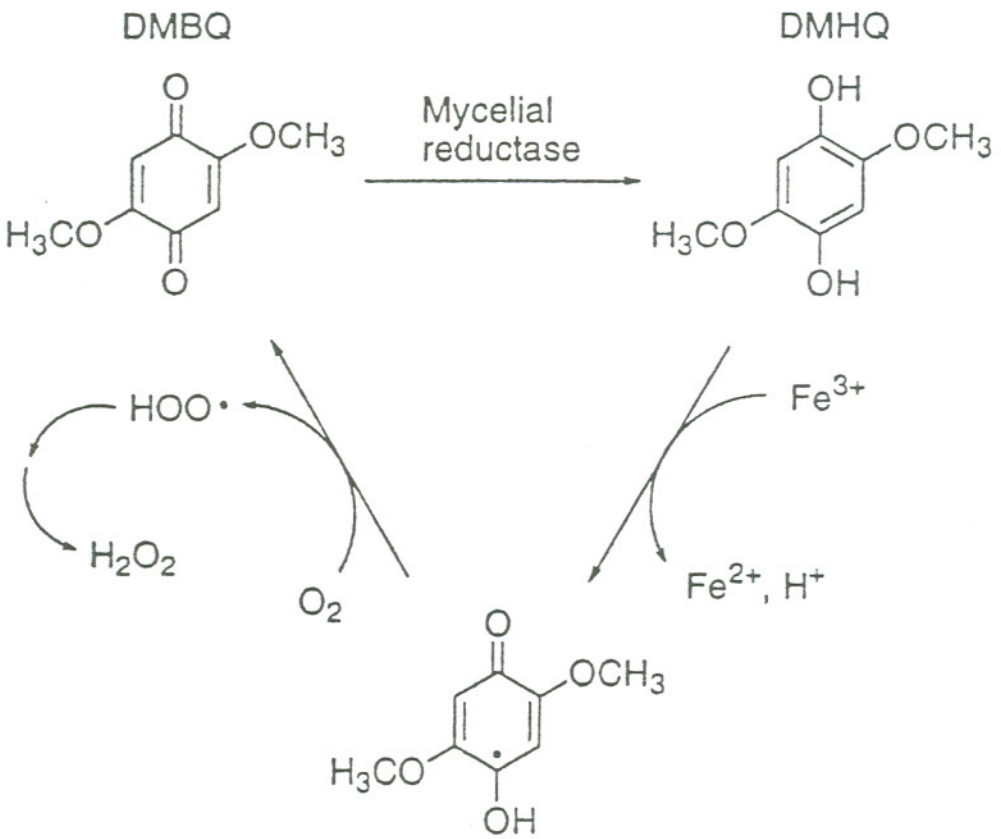

Fig. 1.3 Possible mechanism for the generation of Fenton reagents, Fe^{2+} and H_2O_2, by the brown-rot fungus, *G. trabeum*.

Cellobiose oxidizing activity has further been found in the cellulolytic culture medium of various lignocellulolytic fungi [Henriksson et al., 2000]. Furthermore, CDH has been purified from the white-rot fungi *Trametes versicolor* [Roy et al., 1996], *Pycnoporus cinnabarinus* [Temp and Eggert, 1999], and *Schizophyllum commune* [Fang et al., 1998]; the brown-rot fungus *Coneophora puteana* [Schmidhalter and Canevascini, 1993]; and the soft-rot fungi *Humicola insolens* [Schou et al., 1998], *Sporotrichum thermophile* (*Thielavia heterothallica*) [Coudray et al., 1982; Subramaniam et al., 1999], and *Sclerotium rolfsii* [Baminger et al., 2001]. All CDHs exhibit similar biochemical characteristics (catalytic activity, cofactors, structural organization) as is observed for CDH from *P. chrysosporium* (CDH_{PC}). The CBQase enzyme has also been purified from *Trametes versicolor* [Roy et al., 1996] and *Sclerotium rolfsii* [Sadana and Patil, 1985; Baminger et al., 2001].

1.3.1 Biochemical Characterization of Cellobiose Dehydrogenase

CDH_{PC} is purified as a monomeric glycoprotein with a relative molecular mass of approximately 90 kD [Ayers et al., 1978; Morpeth, 1985; Bao et al., 1993]. The enzyme contains a heme *b* and a flavin adenine dinucleotide (FAD), each non-covalently bound to distinct domains [Henriksson et al., 1991]. The native heme iron is in the ferric state, exhibiting electronic absorption maxima at 420, 530 and 570 nm [Bao et al., 1993]. Upon addition of cellobiose or dithionite, both cofactors are reduced and the heme-based maxima shift to 428, 532 and 534. Detailed resonance Raman, NMR, EPR and MCD spectroscopy demonstrated that the heme iron is low spin (LS) in both redox states and suggested that the iron is coordinated to a methionine and histidine residue [Cox et al., 1992; Cohen et al., 1997]. The flavin domain, purified from cellulolytic cultures or by proteolytic cleavage of the purified enzyme, has a molecular weight of approximately 65 kD and its spectrum is typical for a flavin enzyme [Henriksson et al., 1991; Samejima and Eriksson, 1992].

Like cellulases, CDH_{PC} binds to cellulose, and the estimated dissociation constants for binding to crystalline cellulose at pH 5 are in the sub-micromolar range [Henriksson et al., 1997; Samejima et al., 1997], which are among the lowest

measured for cellulolytic enzymes. While CDH strongly binds to cellulose between pH 4 and 7, the binding affinity decreases with increasing pH and only 20% is bound at pH 9 [Renganathan et al., 1990]. However, once CDH binds to cellulose, it is very difficult to elute CDH from the cellulose matrix. The binding of CDH to crystalline cellulose has been visualized by immunochemical spectroscopy studies, which show that CDH has a preference for the amorphous regions of the substrate [Igarashi et al., 1997; Samejima et al., 1997]. In contrast to most cellulases, the affinity for cellulose is located on one of the catalytic domains, the flavin domain, and not on a distinct CBD [Henriksson et al., 1991].

1.3.2 Reactions Catalyzed by Cellobiose Dehydrogenase

CDH oxidizes various small oligosaccharides, cellodextrins, lactose, and mannobiose in addition to cellobiose [Westermark and Eriksson, 1975; Ayers et al., 1978; Bao et al., 1993; Henriksson et al., 1998]; however, cellobiose is the preferred substrate [Bao et al., 1993; Henriksson et al., 1998] and the product cellobionolactone is hydrolyzed spontaneously to cellobionic acid (Fig. 1.4A). ^{1}H-NMR studies showed that CDH is stereospecific towards the anomeric hydroxyl, preferring the β-hydroxyl configuration [Higham et al., 1994]. CDH transfers electrons to various one- and two-electron acceptors, including dichlorophenol-indophenol (DCPIP), quinones, cytochrome *c* (cyt *c*), ferricyanide and other ferric complexes [Bao et al., 1993]. Among these, CDH has the highest specificity for the one-electron acceptor cyt *c* and two-electron acceptor DCPIP. Oxygen can function as an electron acceptor, but its reactivity with CDH is poor [Kremer and Wood, 1992a]. In the presence of cellobiose, ferric iron and oxygen, CDH produces Fenton reagents, Fe^{2+} and hydrogen peroxide, which lead to the generation of hydroxyl radicals [Kremer and Wood, 1992b; Henriksson et al., 1995]. The physiological electron acceptor(s) in the natural environment is still unknown.

1.3.3 Catalytic Cycle of Cellobiose Dehydrogenase

The proposed catalytic cycle of CDH is shown in Fig. 1.4B. The flavin domain is the catalytic site for binding and oxidation of cellobiose [Samejima and

A

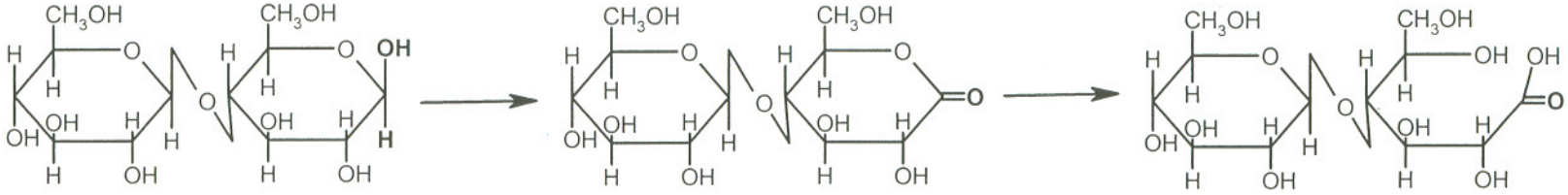

B

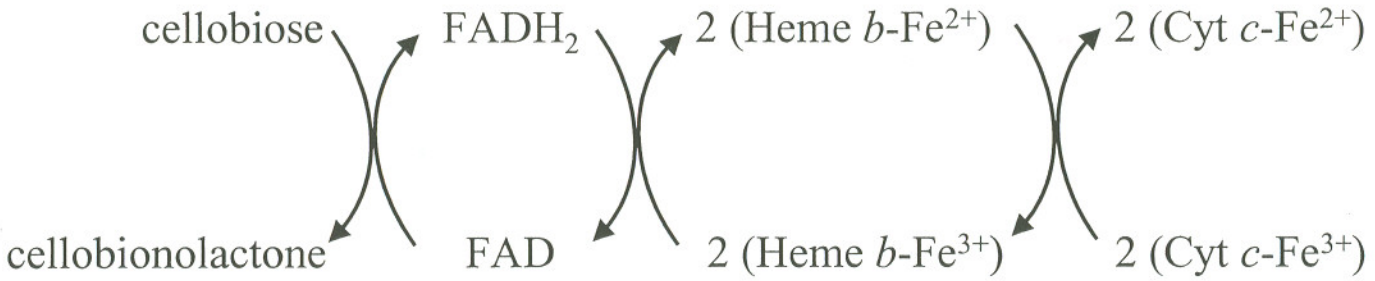

Fig. 1.4 Enzymatic reaction by CDH. (**A**) Cellobiose oxidation, followed by spontaneous hydrolysis of the lactone to a carboxylic acid. (**B**) Catalytic cycle of CDH.

Eriksson, 1992]. The two-electron oxidation of cellobiose yields a reduced flavin, $FADH_2$. One electron can then be transferred to the cytochrome domain, yielding a semiquinone and a reduced heme, both of which have been observed by electron paramagnetic resonance [Morpeth, 1985; Cameron and Aust, 2000] and electronic absorption spectroscopy [Bao et al., 1993], respectively. Under steady-state conditions, the reduced enzyme can be reoxidized by DCPIP in one single two-electron step. This appears to involve only the flavin domain and not the heme-binding domain. The kinetic properties of the two-electron reoxidation of reduced CDH and CBQase are similar [Samejima and Eriksson, 1992]. Both display similar k_{cat} and K_m values and a similar profile for pH dependence. Both enzymes are active between pH 3 and 6.5 with optimum at pH 4.5.

One-electron reduction of acceptors, such as cyt *c*, is facilitated by the presence of the cytochrome domain [Samejima and Eriksson, 1992]. The pH optimum for reduction of cyt *c* by the enzyme is 3.5, and the electron transfer is severly limited above pH 5.5. Pre-steady-state kinetics of CDH [Samejima et al., 1992; Igarashi et al., 2002] indicate that this pH dependence can be attributed to the kinetic properties of inter-domain electron transfer, whereas flavin reduction is pH insensitive at acidic pH. Two mechanisms have been proposed for reduction of the one-electron acceptors. In a traditional scheme, established for flavocytochrome b_2 [Daff et al., 1996], electrons are transferred one by one from FAD to cyt *c* via the heme [Renganathan and Bao, 1994]. Alternatively, the flavin domain itself is the terminal electron donor [Henriksson et al., 1993]. The latter mechanism is supported by the reactivity of CBQase with all one-electron acceptors, including cyt *c*, although all the reduction rates are greatly reduced when compared to holo-CDH.

1.3.4 Biological Function of Cellobiose Dehydrogenase

The physiological role of CDH in the degradation of lignocellulose degradation remains unclear. The many electron acceptors for this enzyme and the many interactions with lignocellulolytic metabolites and enzymes *in vitro* have generated a number of hypotheses regarding the *in vivo* role(s) of CDH [Henriksson et al., 2000]. Establishing of the role(s) of CDH is further complicated by the dynamic nature of

the wood degradation process. In 2001, Archibald and coworkers reported that a cellobiose dehydrogenase-deficient strain of the white-rot fungus *Trametes versicolor* [Dumonceaux et al., 2001] grew poorly on minimal agar plates with crystalline cellulose as sole carbon source, but the strain's ability to biobleach and delignify kraft pulp or depolymerize synthetic lignin remained unchanged. Further, the strain displayed a decreased ability to colonize and degrade white birch wood, suggesting that CDH might be essential to invasion of wood by the fungus.

Reactivity with cellobiose [Bao et al., 1993], the major breakdown product of endoglucanases and cellobiohydrolases (Fig. 1.2) [Beguin and Aubert, 1994], the high affinity for cellulose [Samejima et al., 1997], and the expression of CDH in the presence of cellulose and wood chips [Li et al., 1996; Vallim et al., 1998] support a role for CDH in cellulose degradation. Two main mechanisms for cellulose degradation involving CDH are proposed. CDH enhances cellobiohydrolase activity by relieving competitive inhibition by cellobiose through its oxidation to cellobionolactone [Bao and Renganathan, 1992; Igarashi et al., 1998]. Thus, CDH may act in a synergistic fashion with cellulases in a manner similar to β-glucosidase [Bao and Renganathan, 1992]. However, oxidation instead of hydrolysis of cellobiose is not economical, as extracellular oxidation does not generate intracellular energy units. The second mechanism is based on the reactivity of CDH with ferric iron (and oxygen), leading to the generation of the Fenton reagent ferrous iron and hydrogen peroxide [Kremer and Wood, 1992b]. This is supported by observations such as depolymerization of cellulose by a CDH-cellobiose-Fe^{3+} mixture, the detection of hydroxyl radicals in the reaction medium, and the inhibition of cellulose degradation in the presence of radical scavengers [Henriksson et al., 1995; Mansfield et al., 1997]. However, Renganathan and coworkers showed that the CDH-dependent enhancement of cellulose degradation by a crude mixture of cellulases is not affected by the addition of catalases or iron chelators, which inhibit hydroxyl radical production [Bao and Renganathan, 1992; Subramaniam, 1999].

It has also been proposed that CDH is involved in lignin degradation [Henriksson et al., 2000]. This is based on its *in vitro* interaction with two lignolytic peroxidases, manganese peroxidases (MnPs) and lignin peroxidases (LiPs). These

enzymes generate phenoxy radicals which tend to condense among themselves and with the lignin substrate. CDH can reduce these radicals [Samejima and Eriksson, 1991], preventing repolymerization and thus increase the rate of depolymerization of lignin [Ander et al., 1990; Temp and Eggert, 1999]. MnP oxidizes complexed Mn(II) to the reactive species Mn(III), involved in the one-electron oxidation of lignin. CDH could support this peroxidase in multiple ways [Roy et al., 1994]: by dissolving precipitated $Mn(IV)O_2$ by reduction, by producing cellobionic acid (Fig. 1.4) which could complex the reactive species Mn(III), and by reducing quinones.

1.4 CYTOCHROMES

1.4.1 Classification of Cytochromes

Heme proteins that function as electron carriers between redox groups belong to the family of cytochromes. These proteins are ubiquitous and possess a wide range of properties. They function in a large number of redox processes and appear in many molecular forms: monomeric, membrane-associated, multi-heme, or covalently associated to one or more redox active groups [Chapman et al., 1997]. Cytochromes, however, share some common features: (i) they contain a heme or iron–porphyrin complex (Fig. 1.5), which is covalently or non-covalently bound by the polypeptide, in a hydrophobic pocket; (ii) the heme iron switches between the 2+ (ferrous) and 3+ (ferric) redox states in a physiologically relevant redox reaction; and (iii) the heme iron is chelated by four nitrogens of the pyrrole ring. The fifth heme iron ligand is axially coordinated and is almost always provided by a histidine. The sixth ligand is most often either a histidine or methionine (Fig. 1.5). A well-known exception is chloroplast cytochrome *f*, containing a heme *c* in which the iron is ligated by a histidine and the α-amino group of the protein N-terminus [Martinez et al., 1994].

Cytochromes are classified into groups *a*, *b* and *c*, depending on the porphyrin ring structure and mode of binding of the heme to the protein (Fig. 1.5). Heme *a* (Fig. 1.5) is found in a subunit of cytochrome c oxidase, known as cytochrome aa_3 [Ostermeier et al., 1997]. It is non-covalently bound to the protein and has a His-His

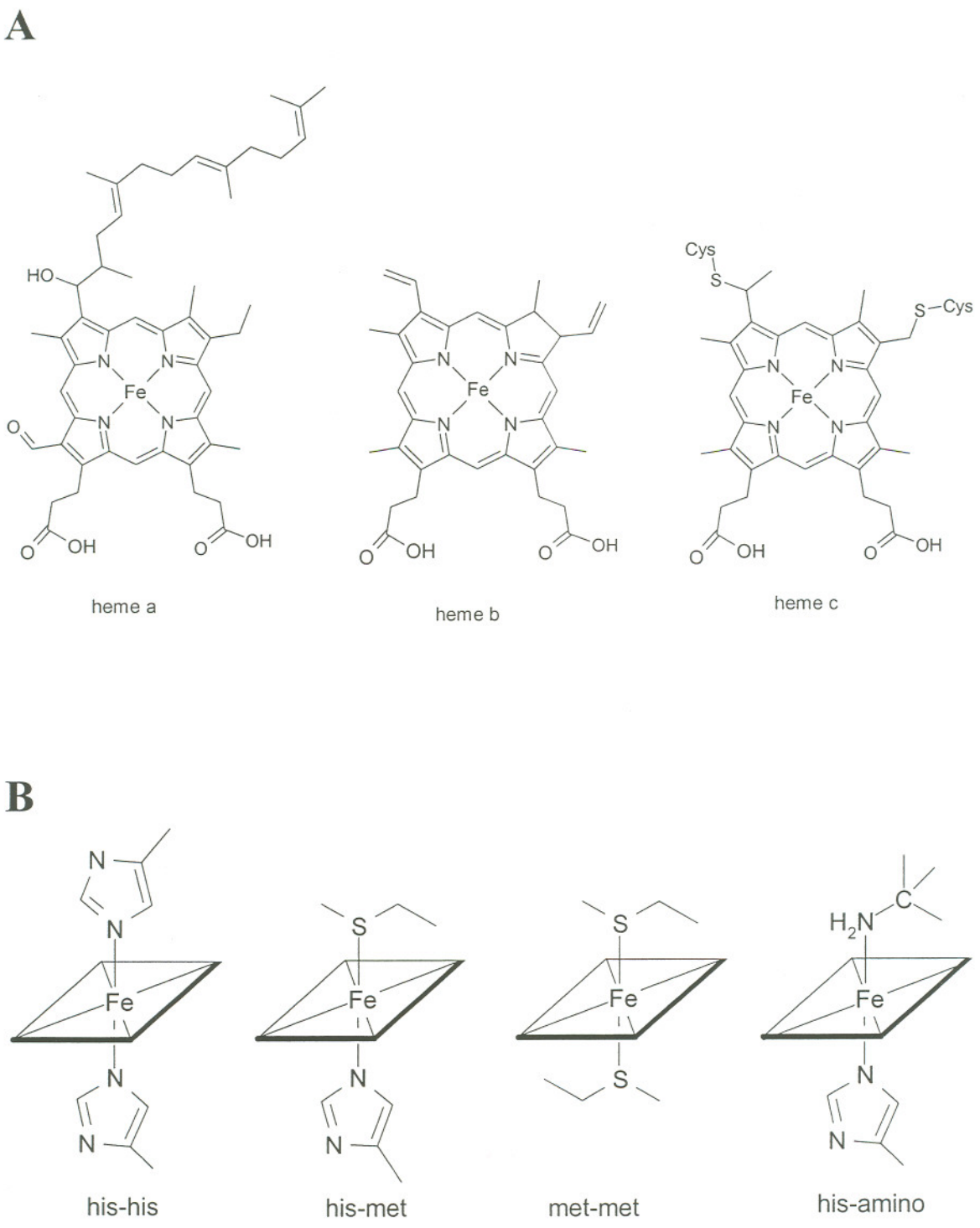

Fig. 1.5 Heme groups found in cytochromes. (**A**) Prosthetic group. (**B**) Axial ligation.

coordination. Heme *b* (Fig. 1.5), also termed protoporphyrin IX, is non-covalently bound, and this prosthetic group is also found in many other heme-containing proteins, e.g. myoglobin, cytochrome P450, catalase and peroxidases. The coordination is predominantly bis-histidyl [von Jagow and Sebald, 1980], and this group includes the ubiquitous electron transfer protein cytochrome b_5. A small subclass displays a His-Met ligation, and it includes soluble cytochrome b_{562} from the periplasm of *E. coli* [Xavier et al., 1978] and the cytochrome domain of CDH [Cox et al., 1992; Hallberg et al., 2000]. The largest group of cytochromes contains heme *c* (Fig. 1.5) [Moore and Pettigrew, 1990]. This prosthetic group is linked to the protein via either one or, most often, two thioethers, involving vinyl group(s) and sulphydryl group(s) of cysteine amino acid residues. The anchoring motif for the heme is in general CxxCH (where x can be any residue) and the His residue forms the fifth ligation to the iron. Based on amino acid sequence and structure, *c*-type cytochromes can be divided into four main classes (I–IV) plus several separate classes with a single member (Cyt c_1, cyt *f*, cyt c_{554} and hydroxylamine oxidoreductase). The axial ligation is predominantly His-Met or His-His.

1.4.2 Functional Roles of Axial Ligands

Structure-function studies, using crystallography and site-directed mutagenesis, have expanded our understanding of the roles axial ligands play in cytochrome function. The coordinating atoms, nitrogen or sulfur, to the iron display an almost invariable geometry. The angles defined by the iron and these atoms are close to 180°, and the Fe-N_{ax}(His) and Fe-S_{ax}(Met) bond lengths are 2.0 and 2.3 Å, respectively, apparently anchoring the porphyrin prosthetic group tightly to the protein [Moore and Pettigrew, 1990]. This geometry is similar to that found in iron-porphyrin model compounds. The strong coordination likely plays an important role in lowering the reorganizational energy, a factor that facilitates long-range electron transfer [Marcus and Sutin, 1985]. Structural data for several cytochromes, including cytochrome *c* [Banci et al., 1997a] and cytochrome b_5 [Banci et al., 1997b], show a practically identical heme axial coordination in the oxidized and reduced state. Structural alterations in the heme-binding pocket are also minimal, which is attributed

to the apolar environment [Gray and Winkler, 1996] and the extended π-system of the porphyrin ring, delocalizing the electrons [Chapman et al., 1997].

Heme ligand substitutions have resulted in cytochrome variants, which are devoid of the heme or in which binding affinity for the heme is very low. Examples are alanine and methionine substitutions in flavocytochrome b_2 [Miles et al., 1993], cytochrome b_{562} [Barker et al., 1996; Kamiya et al., 2001], cytochrome b_5/cytochrome b_5 fusion protein [Davis et al., 2002], iso-1-cytochrome *c* [Hampsey et al., 1988], and cytochrome b_5 [Beck von Bodman et al., 1986]. However, reconstitution with hemin has been successful in variants of cytochrome b_{562} [Barker et al., 1996; Kamiya et al., 2001] and cytochrome b_5 [Rodriguez and Rivera, 1998].

In general, cytochromes display no significant affinity for exogeneous non-reactive ligands, such as cyanide and carbon monoxide, and reactive ligands, such as oxygen and hydrogen peroxide. This can be attributed to the presence of two strong axial ligands that prevent binding of these small compounds. In contrast, axial ligand variants of several *c*-type cytochromes can form a ferrous–CO complex. The M80A cyt *c* binds oxygen in the ferrous state [Wallace and Clark-Lewis, 1992; Lu et al., 1993] and, although an axial ligand variant of cytochrome c_{551} does not form a stable ferrous–oxygen complex, the variant loses its resistance to reoxidation by oxygen [Miller et al., 2000], characteristics of these cytochromes. Besides binding of the exogeneous ligands in many heme enzymes such as peroxidases and heme oxygenases, the heme activates the substrate for the appropriate reaction. For several variants, similar "side-reactions" were observed. Point mutations of the axial ligands in cytochrome b_5 [Sligar and Egeberg, 1987] and cytochrome b_{562} [Kamiya et al., 2001] resulted in variants capable of hydrogen peroxide-dependent oxidation reactions. The H63M variant of cytochrome b_5 performs efficient and regioselective coupled oxidation of the bound heme to produce $>90\%$ of the α-isomer of verdoheme [Rodriguez and Rivera, 1998], a reaction catalyzed by heme oxygenase.

The axial ligation (Fig. 1.5) is obviously an important determinant of the redox properties of heme in cytochromes [Wallace and Clark-Lewis, 1992]. In general, for cytochromes containing a given porphyrin type (heme *b* or heme *c*) (Fig. 1.5), the redox potential of the heme–iron complex with His-His ligation is lower than

that with His-Met ligation. This correlates with redox potential data of the heme model compound [Harbury et al., 1965; Kassner, 1972], and it was estimated that methionine versus histidine ligation should account for a redox potential difference of 160 mV [Moore and Pettigrew, 1990]. Various mutant studies of cytochromes show a similar trend (see Chapter 5).

Early on, it was recognized that other factors around the porphyrin complex, besides the axial ligation (Fig. 1.5), modulate the redox potential: the potential varies over several 100 mVs for each type heme and ligation, and the total range for cytochromes exceeds 1 V (from -475 mV to +640 mV) [Paoli et al., 2002]. Factors such as solvent exposure, surface charges, internal dielectric constant, hydrophobicity, and electrostatic interactions have been considered [Gunner et al., 1997]. Prediction of the redox potential based on the tertiary structure alone is yet not possible, due to the approximation assumed in the theoretical models and due to the lack of high-resolution cytochrome structures in the respective redox states [Mauk and Moore, 1997].

1.5 DEHYDROGENATION REACTIONS BY FLAVIN ENZYMES

1.5.1 Flavins

Flavin-containing proteins are ubiquitous and catalyze a broad spectrum of biochemical redox reactions, including dehydrogenation, hydroxylation and reduction [Bruice, 1980; Walsh, 1980; Ghisla and Massey, 1989]. The most common forms of the flavin prosthetic group are flavin mononucleotide (FMN) and flavin adenine dinucleotide (FAD) (Fig. 1.6). The cofactor is usually non-covalently bound via the ribityl-phosphate (FMN) or ribityl-phosphate-AMP (FAD) to the protein, although covalent attachment to the isoalloxazine ring via a Tyr, His or Cys residue also occurs [Mewies et al., 1998]. The enzymes have been classified based on the sequence and folding topology of the flavin-binding region [Kinoshita et al., 1999; Dym and Eisenberg, 2001], but this does not correlate with enzyme function [Fraaije and Mattevi, 2000].

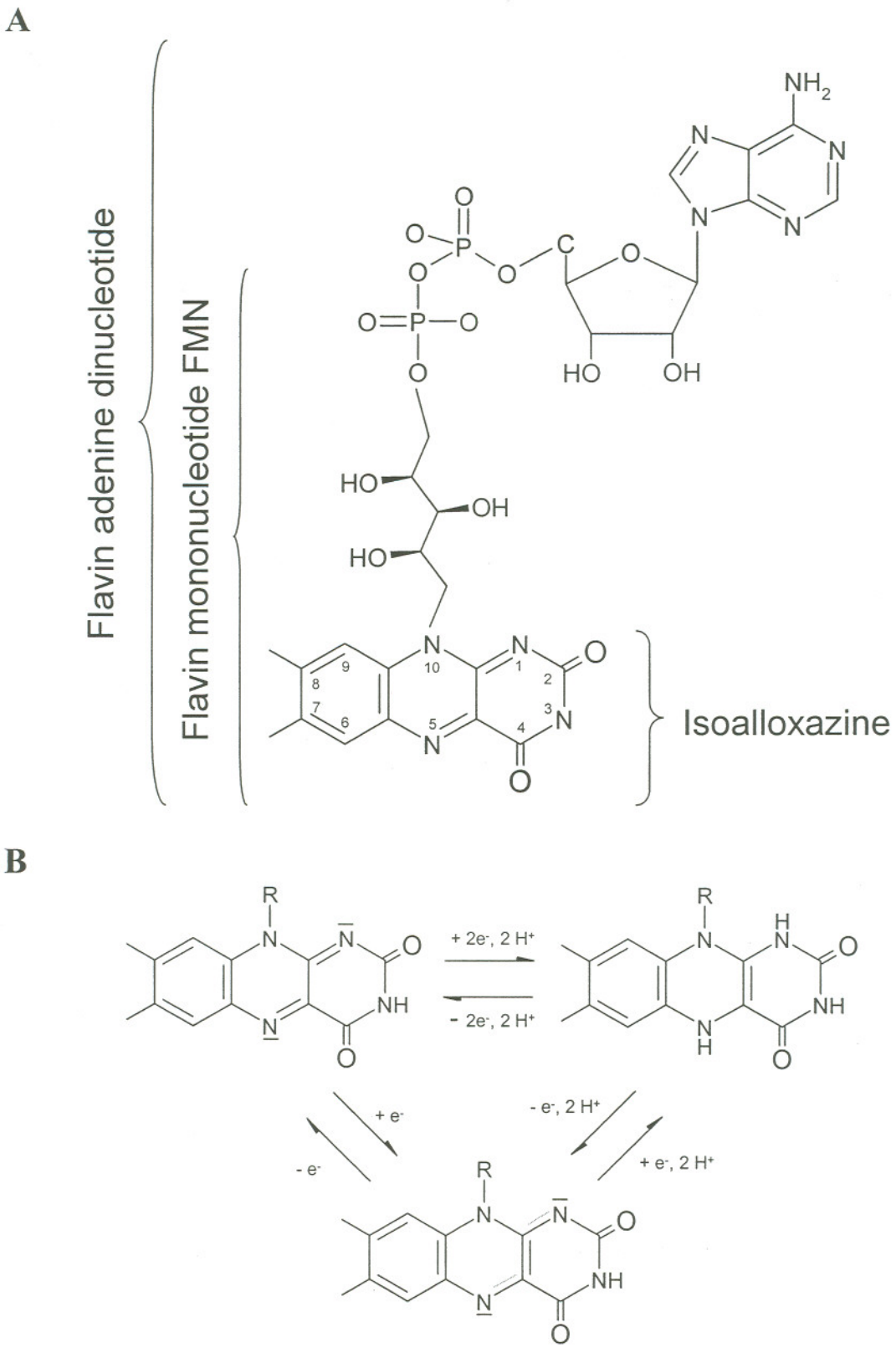

Fig. 1.6 Flavin cofactor. (**A**) Schematic figure of FAD and FMN. (**B**) Three redox states of the isoalloxazine ring.

The versatility of flavoenzymes arises in part from the chemical reactivity of the flavin and its ability to catalyze one– and two-electron redox chemistry (Fig. 1.6) and to react with oxygen. The environment around the cofactor further fine-tunes the enzyme for specific reactions. The redox potential for a free flavin at pH 7 is –207 mV; however, when bound to the enzyme, the potential can range over more than 500 mV (from –495 to +40 mV) [Ghisla and Massey, 1989]. It has been proposed that specific electrostatic, hydrogen bonding and hydrophobic interactions with the flavin modulate its redox properties. Some flavin reactions occur preferentially at a specific locus in the ring. For example, dehydrogenation reactions take place at the N5 locus. Flavin environment has been suggested to influence oxygen reactivity with the reduced flavin; however, this is not well understood. Electrostatic interactions at the active site of lactate monooxygenases [Sun et al., 1996] and glucose oxidase [Su and Klinman, 1999; Roth and Klinman, 2003] have been implicated in the reactivity.

1.5.2 Dehydrogenation Reactions

The FAD- and FMN-dependent enzymes form a major group that catalyzes dehydrogenation reactions (Table 1.1). These reactions involve the rupture of the kinetically stable C–H bond of a substrate, concomitant with the reduction of the flavin. Flavoproteins are among the best-studied enzymes, in part because the oxidation and reduction of flavin can be followed unambiguously using a variety of spectroscopic techniques, in particular electronic absorption spectroscopy [Massey, 1995]. These studies have, in recent years, been augmented by a wealth of structural information from crystallography and site-directed mutagenesis, providing insight into flavin catalysis at the molecular level [Fraaije and Mattevi, 2000].

1.5.2.1 Mechanisms. Three different mechanisms have been proposed for the transfer of redox equivalents from substrate to flavin [Bruice, 1980]. All involve the action of a base that initiates or facilitates the reaction by proton abstraction and polarization of the substrate. In the first mechanism, two electrons are transferred from the α-carbon to the flavin via a hydride anion. In the second mechanism, involving radicals, electrons are transferred in two one-electron steps from the substrate, in conjunction with a proton transfer to the flavin. In the last mechanism, a

Table 1.1

Flavin-Dependent Dehydrogenation Reactions

Enzyme	Substrate	Product	Substrate Activation/ General Base
Dihydroorotate dehydrogenase	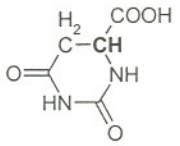	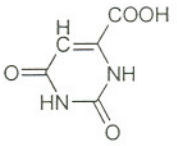	α-Proton abstraction by Cys or Ser
AcylCoA dehydrogenase	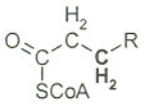	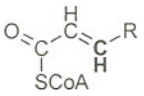	α-Proton abstraction by Glu
α-Hydroxy acid oxidoreductase: - Flavocytochrome b_2 - Lactatate oxidase - (S)-mandelate dehydrogenase	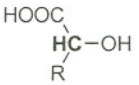	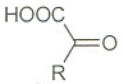	Unresolved: - α-Proton abstraction by His - Hydroxyl deprotonation by His
D-amino acid oxidase	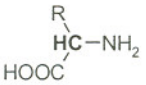	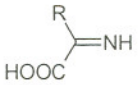	Deprotonated amino group
Vanillyl-alcohol oxidase p-Cresol methylhydroxylase	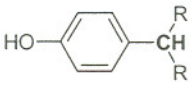	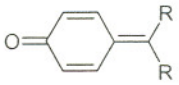	Phenolate anion stabilization
GMC oxidoreductases: - Glucose oxidase - Cholesterol oxidase - Cellobiose dehydrogenase			Hydroxyl deprotonation by His

carbanion is formed by abstraction of a proton from an α-carbon, in conjunction with or followed by the donation of two electrons either directly or via a covalent intermediate. Most enzymes appear to follow one of these mechanisms [Fraaije and Mattevi, 2000], although in some cases, in particular flavocytochrome b_2, the results of extensive kinetic and structural studies were inconclusive with respect to carbanion versus hydride transfer mechanism.

1.5.2.1 Structural Studies. A survey of tertiary structures of flavin enzymes has uncovered similarities in the binding of the isoalloxazine ring to the enzyme [Fraaije and Mattevi, 2000]. An extensive hydrogen bonding network around the isoalloxazine ring has been proposed to modulate the redox properties of the cofactor [Ghisla and Massey, 1989]. In particular, a long-range interaction is observed towards the N5 locus, the site of reduction, and a positively charged entity (Lys or Arg side chain, the N-terminus of an α-helix or a cluster of amide nitrogens) is present in close proximity (<3.5 Å) to the amide (N1–C2=O2) locus. The latter interaction has been proposed to increase the flavin redox potential, thus facilitating the reductive step of the reaction. However, several site-directed mutagenesis studies indicate that this argument may be too simplistic. Arg/Lys variants of dihydroorotate dehydrogenase [Bjornberg et al., 1997] and flavocytochrome b_2 [Reid et al., 1988] were unable to bind FMN. Morphine reductase, a FAD-dependent enzyme with NADH as the electron donor, displayed a positive entity at the amide locus, an Arg. However, substitution (Lys, Met, Glu) of this Arg did not have a significant effect on the redox potential [Craig et al., 2001].

Based on the tertiary structures of flavoenzymes complexed to substrate analogues (product, inhibitor), the position of the site of oxidative attack on substrate should be highly conserved and optimal for electron and proton transfer (Fig. 1.7) [Fraaije and Mattevi, 2000]. The distance between this carbon and the N5 is ~ 3.5 Å, the angle defined by the carbon-N5-N10 atoms ranges between 96 and 117°, and a hydrogen atom at the oxidative site may be orientated towards the N5 (Fig. 1.7). The proposed binding sites and oxidative sites are compatible with predictions from enzymological studies [Ghisla and Massey, 1989]. For example, kinetic studies of the oxidation of dihydroorotate with deuterated analogues suggested that C_6 and not C_5 is

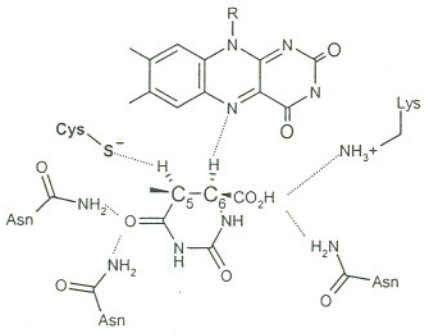

Dihydroorotate dehydrogenase
[Rowland et al, 1997;
Rowland et al, 1998]

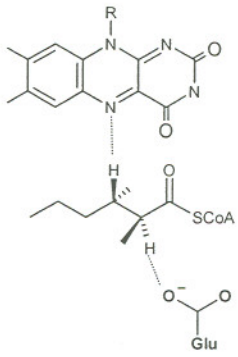

Acyl-CoA dehydrogenase
[Kim et al, 1993;
Bataille et al, 2002]]

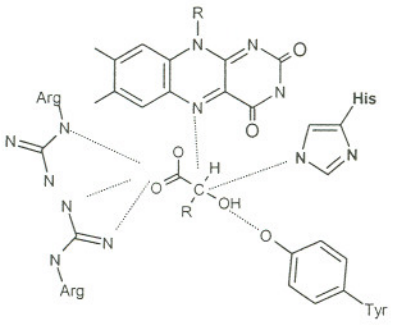

α-hydroxyacid oxidoreductases
[Xia and Matthews, 1990;
Stenberg and Linqvist, 1997;
Sukumar et al, 2001]

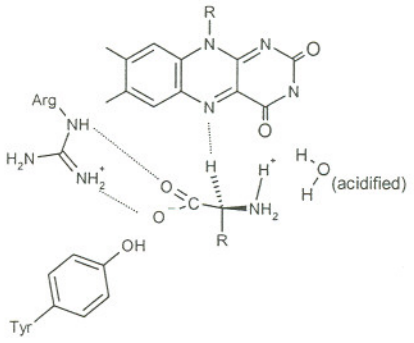

D-amino acid oxidase
[Mattevi et al, 1996;
Umhau et al, 2000]

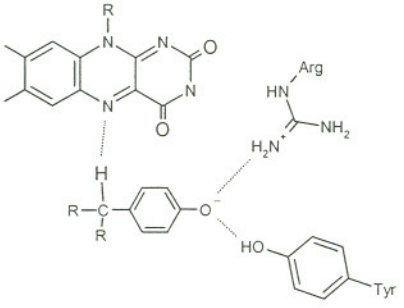

Vanillyl-alcohol oxidase
p-cresol methylhydroxylase
[Mattevi et al, 1997;
Cunane et al, 2000]

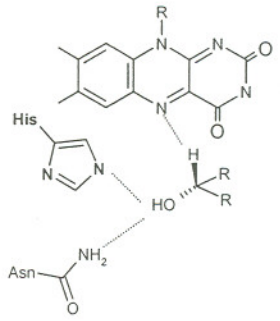

GMC oxidoreductases
[Li et al, 1993;
Hallberg et al, 2002;
Wohlfahrt]

Fig. 1.7 Schematic picture of the active site of flavin-dependent dehydrogenases.

the site of oxidative attack (Fig. 1.7) [Pascal and Walsh, 1984; Keys III and M., 1985; Hines and Johnston, 1989]. The present structural data favors a transfer of redox equivalents from substrate to flavin via a hydride anion, although a radical mechanism cannot be excluded based on structural information alone.

The stereochemically precise coordination of the substrate and thus productive substrate binding is accomplished by a number of interactions between the substrate and protein (Fig. 1.7). These interactions have been proposed to have additional roles in catalysis, including the action of a base that would initiate or facilitate the oxidation reaction by abstracting a proton or polarizing the substrate and stabilizing the negative charge upon proton abstraction or polarization of the substrate. These features have been probed by site-directed mutagenesis and kinetic studies [Fraaije and Mattevi, 2000].

1.5.2.2 GMC Family. The glucose-methanol-choline (GMC) oxidoreductases form a family of FAD-dependent enzymes that carry out the oxidation of non-activated alcoholic substrates, such methanol, cholesterol, β-glucose and cellobiose. These are substrates that do not contain electron-withdrawing groups that could polarize the α-carbon (C–H) or stabilize the formation of a negative charge. Thus, a carbanion mechanism is unlikely to facilitate oxidation. Members of this family have been identified by sequence comparisons and include glucose oxidase, cholesterol oxidase, glucose dehydrogenase, choline dehydrogenase, methanol oxidase, alcohol dehydrogenase and the flavin domain of CDH [Cavener, 1992; Kiess et al.]. Many conserved residues are found in the FAD binding region and are located throughout the sequence. In particular, they all possess a conserved β1-αA-β2 motif at the N-terminus for the binding of the ADP substructure of FAD [Wierenga et al., 1986].

Cholesterol oxidase (CHO) and glucose oxidase (GOX) are the best-studied representatives of the GMC family. In the late 1960s, comprehensive kinetic studies of GOX clarified the individual steps in the GOX reaction [Bright and Appleby, 1969; Weibel and Bright, 1971]. These studies suggest that a basic residue with a pKa of $\sim$5 controls the oxidation of glucose. It was proposed this residue acts as a general base, abstracting the proton of the β-hydroxyl. This may facilitate the transfer of electrons and protons from substrate to flavin. A similar mechanism is proposed for

NAD-dependent alcohol dehydrogenases. These enzymes contain a catalytic zinc that may polarize the oxygen of the substrate, facilitating the direct hydride transfer to NAD. The tertiary structure of the glucose oxidase from *Penicillium amagasakiense* and *Aspergillus niger* [Hecht et al., 1993; Wohlfahrt et al., 1999] identifies two histidines at the C-terminus, positioned near the N5 locus of the flavin. Based on molecular modeling, several binding interactions between glucose and the active site were proposed [Wohlfahrt et al., 1999], and these predictions were supported by site-directed mutagenesis [Witt et al., 2000]. The anomeric β–hydroxyl of the glucose is positioned between the two histidines, hydrogen bonded to the $N^{\epsilon 2}$ and $N^{\delta 1}$ nitrogen atoms (Fig. 1.7, Asn residue is replaced by histidine in GOX). Both histidines could act as a general base in the reductive half of the reaction, and this is supported by mutant studies, showing alanine and valine variants with little residual activity [Witt et al., 2000].

Although both histidines in glucose oxidase are essential for the oxidation of glucose, only one of the histidines is conserved among the other GMC members (Fig. 1.8). The second catalytic residue is instead an asparagine. Comparison of the active site of GOX and CHO shows a conserved geometry for the catalytic residues, with one water molecule between the two residues. The histidine is proposed to act as a base [Li et al., 1993], and this is supported by site-directed mutagenesis studies [Kass and Sampson, 1998]. Mutant studies of the Asn showed that it may modulate the binding of cholesterol as well as the redox properties of the flavin [Yin et al., 2001]. A unique feature of cholesterol oxidase is that it is bifunctional, catalyzing the oxidation of the 3β-hydroxyl of cholesterol, followed by an isomerization reaction, which is assisted by a catalytic base, a glutamate residue [Sampson and Kass, 1997]. The tertiary structure of cholesterol oxidase complexed with a steroid substrate [Li et al., 1993] shows that the 3β-hydroxyl is not directly coordinated to the catalytic residues, His and Asn, but via the active site water. It was suggested that this alternative binding configuration is the result of the dual function of this enzyme [Li et al., 1993]. Based on the sub-atomic resolution structure of cholesterol oxidase [Lario et al., 2003], the same group now suggests that considerable flexibility exists in the active site, and that the 3β-hydroxyl of cholesterol may replace the active site

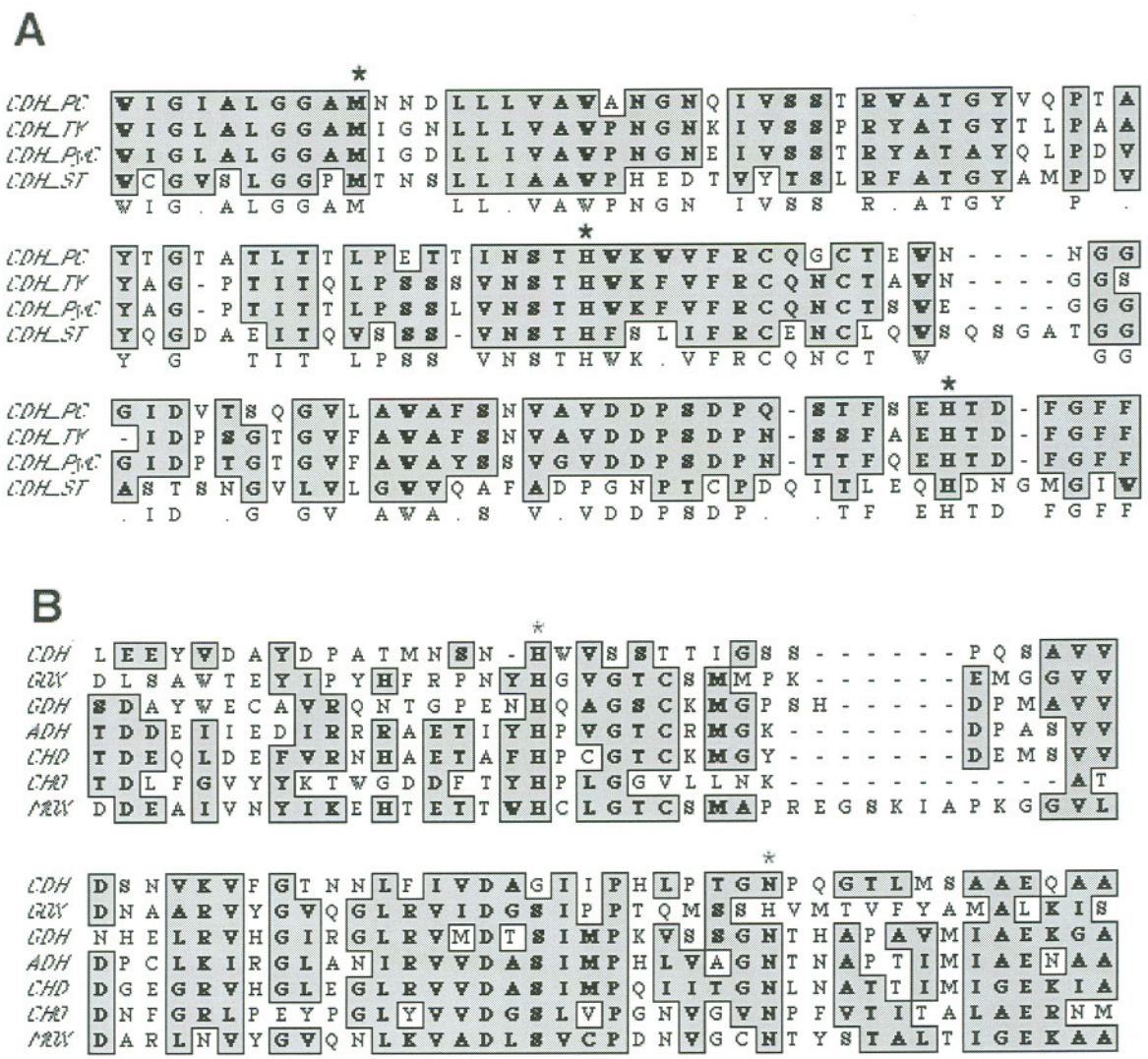

Fig. 1.8 Sequence comparison of the cytochrome domain of four CDHs (**A**) and the C-terminal region of GMC oxidoreductases (**B**). The four CDHs are from *Phanerochaete chrysosporium* (CDH_PC), *Trametes versicolor* (CDH_TV), *Pycnoporrus cinnabarinus* (CDH_PyC), and *Sporotrichum thermophile* (CDH_ST). The GMC oxidoreductases are CDHPC, glucose oxidase (GOX), cholesterol oxidase (CHO), glucose dehydrogenase (GDH), choline dehydorgenase (CHD), methanol oxidase (MOX) and alcohol dehydrogenase (ADH). Residues marked with an asterisk (*) are predicted to be involved in the axial coordination to the heme iron (A) or in enzyme catalysis (B).

water, thus the hydroxyl would be positioned between the two catalytic residues as is suggested for GOX and CDH (see below).

1.6 STRUCTURAL STUDIES OF CELLOBIOSE DEHYDROGENASE

1.6.1 cDNA Cloning and Analysis

cDNAs encoding CDH have been cloned and sequenced from six different organisms: white-rot fungi *P. chrysosporium* [Raices et al., 1995; Li et al., 1996], *P. cinnabarinus* [Moukha et al., 1999], *T. versicolor* [Dumonceaux et al., 1998] and *Grifola frondosa* [Yoshida et al., 2002], as well as the soft-rot fungi *H. insolens* [Xu et al., 2001] and *S. thermophile* (*T. heterothalica)* [Subramaniam et al., 1999]. All genes code for a signal peptide (18–22 amino acids) and a mature protein (749–782 amino acids). Mature CDH from *P. chrysosporium* (CDH_{PC}) consists of 755 amino acids with a predicted mass of 80,115 Da [Li et al., 1996]. The cDNA sequence confirms the two-domain structure of CDH as predicted from biochemical studies: an N-terminal cytochrome domain and a C-terminal flavin domain. The two domains are joined by a linker, enriched with Thr and Ser, typical for linker peptides of cellulolytic enzymes [Gilkes et al., 1991]. This two-module organization is also observed for CDH from the other organisms, with the exception of *S. thermophile*. Its cDNA indicates the presence of an extra peptide stretch at the C-terminus, comprising residue 774-805 [Subramaniam et al., 1999]. This domain shows high sequence similarity to the CBD from *T. reesei* cellobiohydrolase I [Fagerstam et al., 1984].

Based on the amino acid sequence derived from the cDNA, several structural predictions were made for CDH_{PC}. The cytochrome domain does not share sequence similarity with any heme protein or enzyme. Spectroscopic studies indicated that a methionine and a histidine are coordinated to the heme iron of CDH_{PC} [Cox et al., 1992]. Prior to 2001, sequence alignment of four CDH cDNAs indicated that one methionine and two histidines were conserved in the cytochrome domain (Fig. 1.8). In CDH_{PC}, these were methionine 65, histidine 114 or histidine 163. Of the two conserved His, only the sequence surrounding His 114 was conserved. Based on this

rationale, His 114 was proposed to function as the axial ligand [Dumonceaux et al., 1998; Subramaniam et al., 1999].

The flavin-binding domain of CDH exhibits extensive sequence similarity to the GMC oxidoreductases [Raices et al., 1995; Li et al., 1996]. The overall sequence similarity of CDH_{PC} with the other members is approximately 50% [Raices et al., 1995; Li et al., 1996; Subramaniam et al., 1999]. The main consensus is observed in regions predicted to be involved in the binding of the flavin cofactor, including the β1-αA-β2 motif for the binding of the ADP portion of FAD [Wierenga et al., 1986] at the N-terminus (CDH_{PC} residues 217–248). The conserved active site residues for CDH_{PC} are His 689 and Asn 732, located near the C-terminus (Fig. 1.8). Proteolytic studies of CDH_{PC} suggest that a cellulose-binding region resides within the flavin domain [Henriksson et al., 1991; Habu et al., 1993] and the amino acid sequence of CDH_{PC} lacks a distinct CBD. A stretch of 50 amino acid residues (residue 252–301 in CDH_{PC}) was proposed to contain a potential cellulose-binding site [Henriksson et al., 1997]. This sequence constitutes nine aromatic residues, which are proposed to be involved in cellulose binding [Lindner and Teeri, 1997].

1.6.2 Genomic DNA

CDH is encoded by a single gene in *P. chrysosporium* OGC101 [Li et al., 1996; Li et al., 1997] and *Trametes versicolor* [Dumonceaux et al., 2001]. Two alleles were sequenced from *P. chrysosporium*, *cdh-1 and cdh-2* [Li et al., 1997]. Both alleles consist of 14 exons, and the 13 introns are located at exactly the same position in both alleles. Exons 2–5 encode the cytochrome domain and exons 6–14 the flavin domain. The nucleotide similarity of *cdh-1* and *cdh-2* is 97%, with point mutations in both the exon and intron regions; nevertheless, the translated product is identical for both alleles, since the nucleotide changes are found in "silent" positions. The isolation of several cDNA *cdh-1* and *cdh-2* clones during cellulose degradation indicates that both alleles are expressed. A protein-nucleotide Blast search with the sequence of the flavin domain against the complete genome of a homokaryon of *P. chrysosporium* (strain BKM-F-1767) [White-Rot Genome Project, 2002] came up with one unique gene. It codes for the complete *cdh* gene and shows 97% nucleotide

similarity with *cdh-1* and *cdh-2* alleles; the introns are located at exactly the same positions, and the translation products are identical.

1.6.3 Regulation and Expression

The expression of cellulases by wood-rot fungi is regulated at the transcriptional level [Bisaria and Mishra, 1989]. In general, expression is enhanced in the presence of cellulose and repressed by easily metabolized carbon sources, such as glucose. Northern (RNA) blot analysis of total RNA from *P. chrysosporium* cultures indicated that CDH_{PC} mRNA is only produced in the presence of cellulose and not in the presence of glucose or cellobiose [Li et al., 1996]. This suggested that CDH expression by *P. chrysosporium* is also regulated at the transcriptional level by cellulose or its degradation product(s). cDNA transcripts were also detected from *P. chrysosporium*-colonized wood chips [Vallim et al., 1998]. Expression of CDH by *T. versicolor* [Dumonceaux et al., 1998], *P. cinnabarinus* [Moukha et al., 1999] and *S. thermophile* [Subramaniam et al., 1999] also is regulated at the transcriptional level. Besides cellulose, the presence of cellobiose induces the formation of *cdh* mRNA in *S. thermophile*, which is consistent with earlier findings that the CDH protein is secreted in cultures with cellobiose as sole carbon source [Canevascini et al., 1991]. For *P. cinnabarinus*, a small amount of *cdh* transcript was observed in the presence of cellobiose and glucose, but transcription was greatly enhanced with cellulose as sole carbon source [Moukha et al., 1999].

1.6.4 Expression of Recombinant Cellobiose Dehydrogenase

Structure-function studies of CDH using the site-directed mutagenesis methodology require an expression system for the production of recombinant enzyme. At the start of my thesis work, our group had developed a homologous expression system for CDH_{PC} [Li et al., 2000], based on a similar expression system constructed for the homologous expression of two lignin-degrading enzymes, manganese peroxidase (MnP) [Mayfield et al., 1994] and lignin peroxidase (LiP) [Sollewijn Gelpke et al., 1999], as well as the heterologous expression of MnP from *Dichomitus*

squalens [Li et al., 2001]. The *cdh-1* gene was placed under the control of the D-glyceraldehyde-3-phosphate dehydrogenase (*gpd*) promoter (1.1 kb). The *gpd-cdh* construct was inserted into the multiple cloning site of the expression vector pOGI18 [Mayfield et al., 1994], which contained the *Schizophyllum commune ade5* as a selectable marker [Alic et al., 1989], yielding the pAGC1 construct [Li et al., 2000]. The *P. chrysosporium* auxotrophic strain OGC107-1 [Alic et al., 1990; Alic et al., 1991] was transformed with pAGC1. Recombinant wild-type CDH (rCDH) is expressed in transformant cultures supplemented with glucose as sole carbon source when no endogenous wild-type CDH is expressed [Li et al., 1996]. The transformant produced high levels of rCDH (500–600 U/L, ~25% of total extracellular proteins). These levels were significantly higher than was observed for the expression of rLiP or rMnP, and this is attributed to the stability of CDH [Li et al., 2000]. The physical, spectral and kinetic characteristics of the purified rCDH were similar to CDH from the *P. chrysosporium* wild-type strain OGC101. Our group also demonstrated the successful expression of the first mutant of CDH, the heme variant Met65Ala [Li, 1999], allowing use of this homologous expression system for site-directed mutagenesis studies.

Three heterologous expression systems are reported for CDH, two for CDH from *H. insolens* (CDH_{HI}) [Xu et al., 2001] and one for CDH_{PC} [Yoshida et al., 2001]. Recombinant CDH_{PC} is expressed in the methylotrophic yeast *Pichia pastoris*, and the homogeneous, purified recombinant protein exhibits the same physical, spectral, cellulose binding and catalytic properties of the wild-type enzyme. The recombinant CDH_{HI} is expressed in *Fusarium venenaum* and *Aspergillus oryzae* hosts. A homogenous pure flavocytochrome was purified; however, the dehydrogenase activity [Xu et al., 2001] is ~10% of what is observed for the wild-type enzyme [Schou et al., 1998].

1.6.5 Crystal Structure of Cellobiose Dehydrogenase Cytochrome Domain

The topology of the truncated cytochrome domain (residues 1–190; CDH_{CYT}) is unusual for heme-containing proteins [Hallberg et al., 2000]. The polypeptide is folded into a β-sandwich, consisting of one five-stranded and one six-stranded β-sheet

(Fig. 1.9). This structure is stabilized by hydrophobic interactions at the interface of the two sheets. In addition, there are two α-helix turns at the C-terminus. While no sequence similarity is observed, the topology is very similar to the immunoglobulin fold of the heavy chain of the variable domain (V_H domain) of the Fab antibody. In the heme structure, an N-linked carbohydrate chain with two N-acetyl glucosamines and one mannose residue is attached to Asn111. The only other cytochrome structure that consists mainly of β-sheets is the lumen-side domain of cytochrome *f*, containing a heme with an unusual axial coordination, a histidine and an N-terminal amino group [Martinez et al., 1994]. The heme group is located on one face of the β-sandwich, close to the surface. The heme propionates are highly exposed to the solvent, in a position suitable to act in electron transfer between the flavin and cytochrome domains. The heme is bound in a hydrophobic pocket and includes a number of apolar residues, of which most are conserved among the six CDHs. The packing of the pocket is tight, leaving little or no space for entry of additional molecules. Met65 and His163 form the axial ligands to the heme iron (Fig. 1.9). The iron lies almost perfectly in the plane defined by the four pyrrole nitrogen atoms, and the distance to the heme iron for His163-N^{δ} and Met65-S^{γ} is approximately 2.0 and 2.3 Å, respectively. EPR studies suggested an unusual perpendicular orientation of the two axial ligands [Cox et al., 1992], and indeed the planes defined by the methionine side-chain (CH_2-S-CH_3) and the histidine imidazole ring forms an $\sim 80°$ angle.

1.6.6 Crystal Structure of the Cellobiose Dehydrogenase Flavin Domain

Previous studies indicated that CDHs contain predominantly one unmodified FAD, non-covalently bound to a structurally distinct domain [Henriksson et al., 1991; Bao et al., 1993], although in several preparations of CDH from *P.chrysosporium* [Morpeth and Jones, 1986] and *H. insolens* [Igarashi et al., 1999], a modified FAD, likely hydroxylated at the 6′ position (FAD-6OH), is present. This modification reduces the reactivity of the flavin domain for cellobiose oxidation [Igarashi et al., 1999]. The crystal structure of the flavin domain of CDH (CDH_{DH}) from *P. chrysosporium* has been solved for the hydroxylated variant [Hallberg et al., 2002], and confirmed the presence of FAD-6OH. The overall structure (Fig. 1.10) is similar

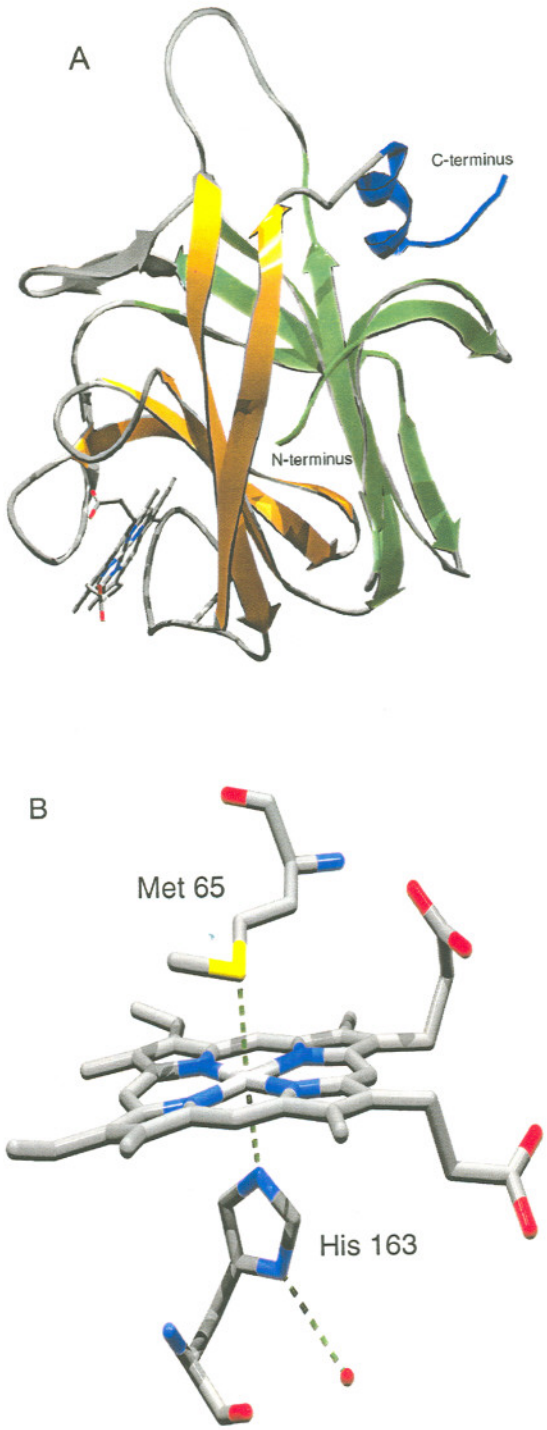

Fig. 1.9 Cytochrome domain of CDH from *P. chrysosporium*. (**A**) Ribbon drawing of the cytochrome domain. (**B**) Axial ligation.

to two members of the GMC oxidoreductase family: glucose oxidase [Hecht et al., 1993; Wohlfahrt et al., 1999] and cholesterol oxidase [Vrielink et al., 1991; Li et al., 1993; Yue et al., 1999]. All three structures are arranged into two structural and functional sub-domains, a flavin-binding (F, purple) and a substrate-binding (S, yellow) domain. The F sub-domain of CDH_{DH} comprises 205 residues (216–249, 404–511 and 693–755), and its structure is of the α/β type, featuring a six-stranded β-pleated sheet, sandwiched between three-stranded β-sheets and three α-helices. As predicted from the amino acid sequence, the F sub-domain exhibits high structural similarity to the domains of the other two members of the GMC family (rmsd-Cα = 1.2–1.5 Å). The substrate-binding (S) sub-domain consists of 335 residues (250–403 and 512–692). The main structural feature is a central twisted, seven-stranded β-sheet with three α-helices at one side of the sheet with the active site on the other side.

Prior to the elucidation of the CDH_{DH} crystal structure, two residues (His 689 and Asn 732) located at the C-terminus were implicated in the catalytic activity on the basis of the multiple sequence alignment of CDH and GMC members (Fig. 1.8) [Subramaniam et al., 1999]. These residues are located at the end of a 12-Å tunnel from the surface of the molecule and near the isollaxozine ring (flavin *re*-face). A water molecule (Wat1214) is located between these residues, hydrogen bonded to His689-N^{ϵ} and Asn732-$N^{\delta 2}$. In conjunction with these residues, the active-site water and the flavin cofactor from CDH_{DH}, GOX and CHO form a highly conserved site [Hallberg et al., 2002].

Based on molecular modeling, possible protein interactions of cellobiose in the active site of CDH_{DH} have been proposed [Hallberg et al., 2002]. Upon entry of the substrate, the water molecule (Wat1214) is expelled from the active site. The anomeric β-hydroxyl (Glc1-O1) of cellobiose is positioned between His689 and Asn732, whereas the α-hydrogen (Glc1-H1) is oriented towards the FAD-N5 locus (Fig. 1.7). This may allow His689 to act as a general base, facilitating oxidation of the substrate via a radical or hydride transfer mechanism. In addition to the hydrogen bond interactions between the β-hydroxyl of Glc1 and His689-$N^{\epsilon 2}$ and Asn732-$N^{\delta 2}$, Arg586 and Glu279 form a hydrogen bond network with cellobiose. A planar

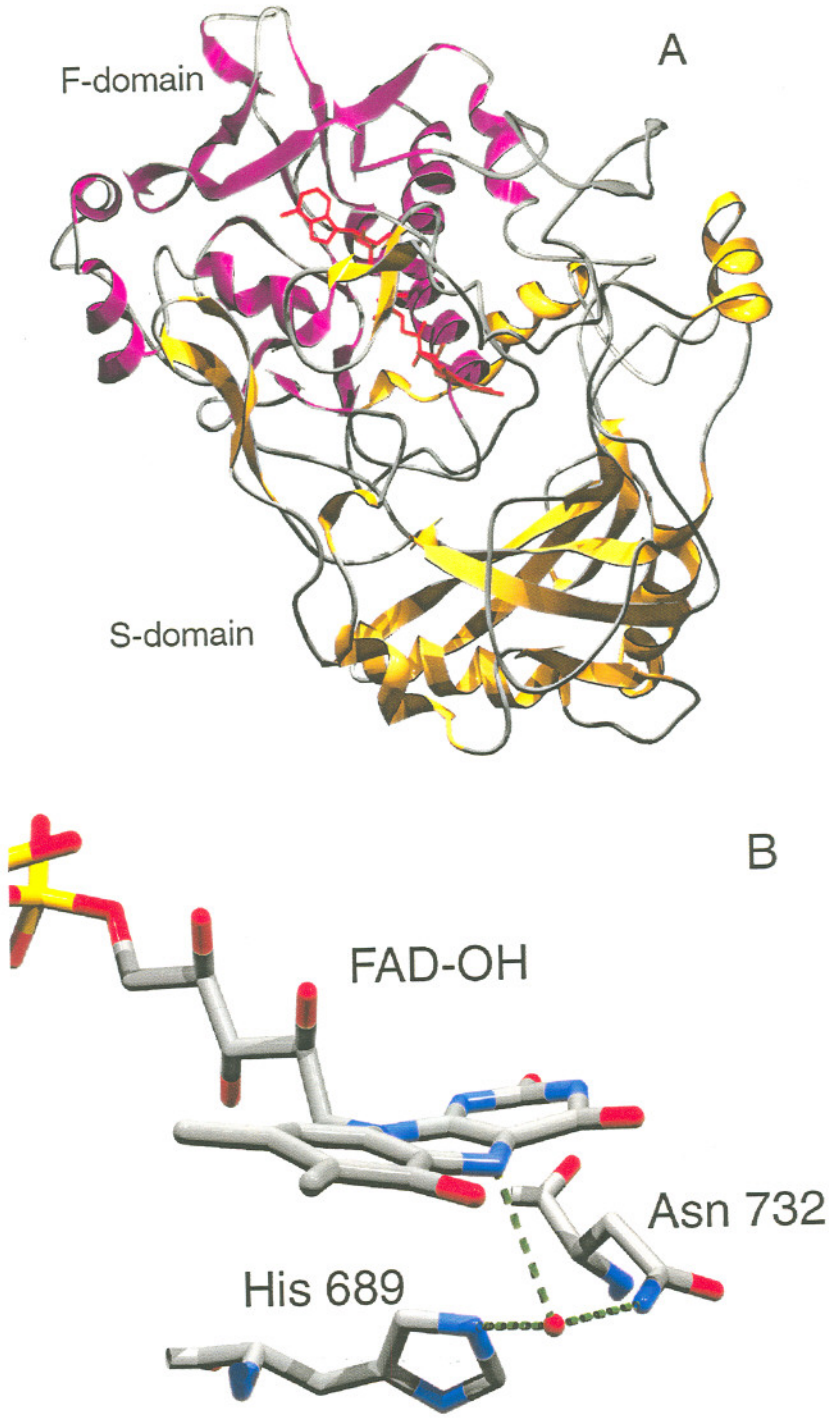

Fig. 1.10 Flavin domain of CDH from *P. chrysosporium*. (**A**) Ribbon drawing of the flavin domain. (**B**) Active site.

hydrophobic stacking interaction between the aromatic ring of Phe282 and the α-face of Glc2 is also likely.

1.6.7 Model for the Flavocytochrome Cellobiose Dehydrogenase

The apparent inability to obtain crystals of intact modular cellulolytic enzymes, such as cellulases and CDH, is attributed to the flexible peptide linker between the two domains [Gilkes et al., 1991]. Small angle X-ray scattering studies of CDH_{PC} [Lehner et al., 1996] and cellulase Cel45 from *H. insolens* [Receveur et al., 2002] suggest an extended and co-linear arrangement of the two modules. However, the flexible spacer would make different spatial organizations of the two modules possible, which is essential for electron transfer between the flavin and cytochrome domains in CDH.

The crystal structures of four flavocytochromes are now known: flavocytochrome b_2 (lactate dehydrogenase of *Saccharomyces cerevisiae* [Xia and Mathews, 1990]; sulfide dehydrogenase of *Chromatium vinosum* [Chen et al., 1994]; *p*-cresol methylhydroxylase of *Pseudomonas putida* [Mathews et al., 1991; Cunane et al., 2000]) and flavocytochrome *c* (fumerate reductase of *Shewanella putrefaciens* MR-1 [Leys et al., 1999]). They all have different topologies for the heme and flavin domains, but share the two-domain structure and the presence of a linker peptide connecting the two domains. The heme cofactor is near the surface, allowing for close positioning of the two cofactors with an edge-to-edge distance smaller than 10 Å. For example, in flavocytochrome b_2, the propionates are highly exposed and are pointed towards the FMN. An electron transfer pathway that involves protein-mediated bonds is proposed [Xia and Mathews, 1990]. The interacting surfaces of the two domains of CDH are highly complementary and are mainly non-ionic in character [Hallberg et al., 2002]. The entrance to the active site in CDH_{DH} is partly covered by a 38 amino acid lid, but it would allow for transient movement to the entrance by the CDH_{CYT} for efficient electron transfer between the two domains [Hallberg et al., 2002].

1.7 RESEARCH SUMMARY

Cellobiose dehydrogenase (CDH) is the only extracellular flavocytochrome reported to date, and it has been proposed to be involved in cellulose as well as lignin degradation. At the start of the research described in this thesis, through the effort of a number of laboratories, CDH from *Phanerochaete chrysosporium* had been biochemically well characterized [Henriksson et al., 2000]. The cDNA of CDH from three different wood-rot fungi—*P. chrysosporium* [Raices et al., 1995; Li et al., 1996], *T. versicolor* [Dumonceaux et al., 1998] and *S. thermophile* [Subramaniam et al., 1999]—had been cloned and sequenced, a homologous expression system for CDH in *P. chrysosporium* had been developed [Li et al., 2000], and a point-mutant of CDH had been expressed [Li, 1999]. Based on the amino acid sequence alignment of CDH from the three wood-rot fungi, as well as sequence comparison of the flavin domain of CDH with a group of FAD-dependent oxidoreductases, members of the glucose-methanol-choline (GMC) family (Fig. 1.8), several predictions were made regarding the axial ligation to the heme iron, the catalytic residues in the flavin domain, flavin binding motifs and residues involved in the binding of CDH to cellulose [Raices et al., 1995; Li et al., 1996; Dumonceaux et al., 1998; Subramaniam et al., 1999]. Using site-directed mutagenesis methodology, the validities of the first two predictions were addressed in this thesis. The flavin and heme variants of recombinant CDH were kinetically, spectroscopically and/or electrochemically characterized and these properties were compared to the recombinant wild-type enzyme. This research has expanded the knowledge of the roles that these critical residues play in CDH. In a broader context, the outcomes contribute to a better understanding of axial ligation in cytochromes and the specific roles that the catalytic residues His and Asn play in GMC oxidoreductases.

Recombinant wild-type CDH (rCDH) was initially purified to homogeneity in three steps (ammonium sulfate precipitation, gel filtration and anionic exchange chromatography) with an overall yield of 30% and only required a four-fold purification, i.e., rCDH constituted approximately 25% of the total protein in the extracellular media [Li et al., 2000]. In Chapter 2, we describe an alternative

purification protocol for rCDH, using a cellulose-affinity step and gel-filtration chromatography. This allowed for a more rapid purification and a higher yield (50%).

Previously, spectroscopic studies suggested that a methionine and histidine form the axial ligation to the heme iron [Cox et al., 1992]. Comparison of the amino acid sequence of CDH from three wood-rot fungi showed that one methionine, Met 65, and two histidines, His 114 and His 163, are conserved in the cytochrome domain of CDH from *P. chrysosporium* [Dumonceaux et al., 1998; Subramaniam et al., 1999]. In Chapter 3, to correctly identify the axially coordinating residues, the corresponding alanine variants were produced using our homologous CDH expression system, and biochemical and spectral characteristics of the variants were studied in detail. We identify Met65 and His163 as the axial ligands, and show that they are critical for the reactivity and integrity of the cytochrome domain. This research complements the crystal structure of the truncated cytochrome domain of CDH [Hallberg et al., 2000] and identifies the functional roles of Met65 and His163.

The methionine–histidine coordination to a *b*-type heme as in CDH is rare; usually both ligands are histidines. To probe the importance of this axial ligation in CDH, methionine 65 was substituted by a histidine. In Chapter 4, we discuss the kinetic, spectral (electronic absorption and resonance Raman) and electrochemical characteristics of the M65H variant, together with the tertiary structure of the truncated cytochrome domain. The M65H variant displays a novel bis-histidine $N^{\epsilon 2}/N^{\delta 1}$ coordination for a heme *b*.

Multiple sequence alignment between CDH and the GMC family suggested that histidine 689 and asparagine 732 are the catalytic residues for the oxidation of cellobiose. To examine the functional, steric and electrostatic constraints of each residue for binding and oxidation of the substrate, each residue was substituted with either Gln, Asn, Glu, Asp, Val, Ala and/or His. The variants were compared to rCDH using steady-state kinetic measurements, and the effect of each mutation on the electronic properties of the flavin cofactor was studied. These results are discussed in Chapter 5 and form a functional complement to the tertiary structure of the flavin domain of CDH [Hallberg et al., 2002].

CHAPTER 2

SIMPLIFIED PROTOCOL FOR THE PURIFICATION OF RECOMBINANT CELLOBIOSE DEHYDROGENASE FROM *PHANEROCHAETE CHRYSOSPORIUM*

2.1 INTRODUCTION

Cellulose-degrading cultures of the white-rot fungus *Phanerochaete chrysosporium* produce cellulases, which are hydrolytic enzymes, as well as an oxidoreductase, the flavocytochrome cellobiose dehydrogenase (CDH), formerly called cellobiose oxidase. This extracellular enzyme has been purified by a number of groups [Ayers et al., 1978; Morpeth, 1985; Henriksson et al., 1991; Samejima et al., 1992; Bao et al., 1993], from a number of different strains of *P. chrysosporium*, using a variety of cultivation conditions (stationary and shaking cultures, and fermentation) and purification protocols. The procedures, typically consisting of 6–8 steps, provided a 60- to ~150-fold purified and homogeneous enzyme, exhibiting a molecular mass of 90 kDa, as determined by SDS-PAGE analysis. The purified enzymes contained one heme *b* and one flavin cofactor. The yields varied between 5% for the first reported purification of CDH by Ayers et al. [Ayers et al., 1978] and ~45% from more recent purification procedures [Bao et al., 1993; Henriksson et al., 1998]. A number of different assays were employed to measure CDH activity. They vary in the nature of substrates (electron donor and electron acceptor), the pH, the reaction temperature and the value of the extinction coefficient for the electron acceptor [Henriksson et al., 2000].

A unique property of cellulolytic enzymes is their binding affinity to cellulose, using a structurally distinct cellulose-binding domain [Lindner and Teeri, 1997]. This affinity is required for the degradation of crystalline cellulose [Klyosov, 1990].

However, for CDH from *P. chrysosporium* (CDH_{PC}), the flavin domain appears to harbor an internal cellulose-binding site [Renganathan et al., 1990; Raices et al., 1995; Li et al., 1996; Henriksson et al., 1997]. CDH displays higher binding affinity for crystalline cellulose than for amorphous cellulose [Samejima et al., 1997], but it binds preferentially to the amorphous regions attached to the crystalline microfibrils [Henriksson et al., 1997; Samejima et al., 1997]. Renganathan and coworkers [Renganathan et al., 1990] showed that CDH tightly binds to microcrystalline cellulose at acidic and neutral pH, but in pH 9 Tris buffer held only 20% of CDH activity. However, once CDH was bound to cellulose at pH 6, only 30% could be eluted by washing with pH 9 buffer. Thus, it appeared that once CDH was bound to cellulose, it was very difficult to be removed.

In 1998, we succeeded in the homologous expression of CDH in *P. chrysosporium* [Li et al., 2000]. The transformation cultures produced high levels of CDH and the flavocytochrome comprised of ~20% of total proteins in the extracellular medium. The recombinant wild-type CDH (rCDH) could be purified to homogeneity in three steps, ammonium sulfate precipitation, gel filtration chromatography and fast protein liquid chromatography (FPLC) using a MonoQ 5/5 anionic exchanger. The physical, spectral, and kinetic characteristics of rCDH were similar to those of the wild-type enzyme. These results indicated that this expression system would allow for site-directed mutagenesis studies, to be carried out on CDH. The first variant that was created was M65A [Li, 1999], to identify methionine 65 as one of the axial ligands to the heme iron [Raices et al., 1995; Li et al., 2000]. The variant is secreted as a 90 kDa (Chapter 3), but using the purification protocol for rCDH, only a 70 kDa, cellobiose-oxidizing flavoenzyme [Li, 1999] was obtained. In an attempt to purify the 90 kDa protein an alternative purification protocol was developed, employing the cellulose binding properties of CDH. In this chapter, we describe a two-step procedure, comprising of cellulose binding and gel-filtration chromatography, to obtain homogenous pure rCDH. The yield is significantly higher (50%, compared to the 30% of the original procedure), and the recombinant protein exhibits similar biochemical properties as the wild-type CDH.

2.2 MATERIALS AND METHODS

2.2.1 Organism

Growth and maintenance of *P. chrysosporium* wild-type strain OGC101 and rCDH transformant strain pAGC1 were as described [Akileswaran et al., 1993; Li et al., 2000]. Briefly, strains were grown and maintained on slants of Vogels medium N [Vogels, 1964], supplemented with 1% glucose (GV slants) or supplemented with 3% maltose extract and 0.15% yeast extract (MYV slants) [Gold and Cheng, 1979].

2.2.2 Production and Purification of rCDH in Stationary Cultures

The rCDH transformant pAGC1 was grown from conidial inocula at 37°C in 30-ml stationary cultures in 250 ml Erlenmeyer flasks. The culture medium contained 2% glucose, 0.2% tryptone, Kirk salts [Kirk et al., 1978], 12 mM ammonium tartrate and 20 mM Na-2,2-dimethyl succinate, and its initial pH was adjusted to 6 [Li et al., 2000].

rCDH was purified from the extracellular medium of 7-day-old stationary cultures. The medium (200 ml) was filtered through Miracloth (Calbiochem, La Jolla, CA), concentrated and dialyzed against 20 mM K-phosphate pH 6. The dialyzed fluid (200 ml, cytochrome *c* activity ~500 U/L) was incubated for 60 min at 4°C with 2 g/100 ml Sigmacell® (type 50), a form of microcrystalline cellulose. The CDH–cellulose complex was separated from the supernatant by centrifugation (16,000 *g*) and washed twice with 20 mM K-phosphate pH 6. CDH was eluted from the cellulose by incubation in 20 mM Tris pH 9 at 4°C for 60 min. The pH of the eluent was then adjusted to 8 and concentrated. Homogeneous CDH was obtained by gel filtration using Sephacryl S200 HR column, equilibrated with 50 mM K-phosphate, pH 6.

2.2.3 SDS-PAGE and Immuno (Western) Blotting Analysis

Sodium dodecyl sulfate-polyacrylamide gel electrophoresis (SDS-PAGE) was performed using a 12% Tris-glycine system in a Miniprotean II apparatus (Bio-Rad, Hercules, CA). The gels were stained with 0.1% Coomassie brilliant blue R-250

(Bio-Rad) in 40% methanol–10% acetic acid solution. Following SDS-PAGE, proteins were transferred electrophoretically to a polyvinylidene (PVDF) membrane (Immobilon-P, Millipore, Billerica, MA) using a Bio-Rad apparatus. Immuno-detection was performed following the protocol Western-Light chemiluminescent detection system (Tropix, Bedford, MA), using polyclonal antibodies raised against *P. chrysosporium* CDH [Li et al., 1996].

2.2.4 Spectroscopic Procedures and Enzyme Assays

Electronic absorption spectra of rCDH were recorded at room temperature with a Cary 100 spectrophotometer (Varian, Mulgrave, Victoria, Australia). Spectra were obtained in 20 mM Na-succinate pH 4.5. The enzymes were reduced by addition of cellobiose (400 μM). CDH activity in culture medium and during purification was measured using the cytochrome *c* (cyt *c*) assay. Assay solution contained 400 μM cellobiose and 12.5 μM ferric cyt *c* in 20 mM Na-succinate, pH 4.5. Cyt *c* reduction was monitored at 550 nm (ϵ = 28 mM^{-1} cm^{-1}).

2.2.5 Kinetic Procedure

The steady-state kinetic parameters for cellobiose oxidation were determined by monitoring ferrous cyt *c* formation (ϵ_{550} = 28 mM^{-1} cm^{-1}) or DCPIP reduction (ϵ_{515} = 6.8 mM^{-1} cm^{-1}). The assays contained a fixed level of ferric cyt *c* (12.5 μM) or DCPIP (40 μM) and varying levels of cellobiose (5–200 μM) in 20 mM Na-succinate, pH 4.5. The steady-state kinetics of cyt *c* and DCPIP reduction were determined with a fixed cellobiose concentration (200 μM) and variable levels of cyt *c* or DCPIP (0.2 to 40 μM).

2.2.6 Flavin Cofactor Extraction

The flavin cofactor was extracted from rCDH by the cold trichloroacetic acid (TCA) method [Morpeth, 1985; Igarashi et al., 1999]. To 20–50 μM rCDH (100 μl) was added 20% TCA solution (100 μl) and the mixture was incubated on ice for 10 min. The precipitate formed was removed by centrifugation and the supernatant was

neutralized by the addition of 600 μl Tris-HCl (1 M), pH 8.0. The amount of extractable flavin was calculated from a standard curve constructed with commercially available FAD. Stoichiometry of FAD in rCDH was calculated from the CDH concentration.

2.2.7 Chemicals

Cellobiose, horse heart cyt *c* (Grade IV), Sephacryl S200 (HR), FAD and Sigmacell® 50 were obtained from Sigma (St. Louis, MO). All other chemicals were reagent grade. Solutions for biochemical characterization of the enzymes were prepared with water from MilliQ-50 system (> 18 MΩ cm) (Millipore Corp., Bedford, MA).

2.3 RESULTS AND DISCUSSION

The original purification protocol for rCDH [Li et al., 2000] was based on the purification of wild-type CDH from the wild-type strain OGC101 [Bao et al., 1993]. It included an ammonium sulfate precipitation step, gel filtration (Sephacryl S200 HR) and anionic exchange chromatography (MonoQ 5/5). A homogeneous 90 kDa rCDH enzyme was obtained in a mere 4-fold purification, with a yield of 30%. Application of this protocol to the purification of the first CDH variant, M65A, however yielded a 70 kDa, cellobiose oxidizing flavin protein [Li, 1999]. One speculation was that in the absence of the axial ligand, the binding of the heme group to the protein is weakened. This might make the CDH variant a target for intracellular processing [Raices et al., 2002], leading to the cleavage of the cytochrome domain and the secretion of the truncated flavin domain. Western blot analysis of the extracellular medium from M65A cultures however showed that a 90 kDa protein appears initially, followed by the appearance of a ~70-kDa protein in later stages (see Chapter 3). This suggested that the 90 kDa M65A variant undergoes degradation of the heme-binding domain during the culture period. In addition, the ammonium sulfate precipitation step appeared to result in complete loss of the holoenzyme. Though the earlier protocol was efficient, a faster and better purification method was needed to

quickly purify unstable variant proteins, possibly obtained from our protein engineering studies. The new protocol took advantage of the cellulose-binding properties of CDH [Renganathan et al., 1990].

rCDH was produced in 250 ml flasks, containing 30 ml media under stationary conditions at 37°C. Western blot analysis of the extracellular fluids, using polyclonal antibodies raised against CDH [Li et al., 1996] showed, over a 10-day culture period, exclusively the presence of one protein band with a molecular mass similar to homogeneous rCDH (Fig. 2.1). This indicated that rCDH did not undergo degradation. rCDH was purified from 7-day-old culture medium [Li et al., 2000].

CDH is a stable enzyme over a broad pH range and 100% CDH activity is retained, after incubation of wild-type CDH (wtCDH) at room temperature in buffers with a pH between 3 to 10.5, over a 12 h period [Bao et al., 1993]. Renganathan and coworkers showed that wtCDH was tightly bound to microcrystalline cellulose at acidic and neutral pH, but binding reduced rapidly above neutral pH, only holding 20% above pH 9 [Renganathan et al., 1990]. Based on these observations a purification protocol involving selective absorption of CDH to cellulose at pH 6 and elution at pH 9 was devised. First, rCDH extracellular fluid was concentrated and dialyzed against 20 mM K-phosphate, pH 6. An added advantage of pH 6 is that the reactivity of CDH towards oxygen and one-electron acceptors is significantly reduced, minimizing the formation of reactive oxygen species [Subramaniam, 1999]. Observance of a strong Soret absorbance at 421 nm from the concentrate indicated high levels of heme proteins. When dialyzate was incubated with microcrystalline cellulose, 90% of rCDH (~500 U/L) was bound to cellulose within 1 h, based on the cyt *c* activity remaining in the supernatant. Washing cellulose suspension with 20 mM K-phosphate pH 6 resulted in loss of ~5% rCDH. Approximately 70% of the bound CDH was eluted by incubation of the cellulose suspension in 20 mM Tris pH 9. At this stage of the purification the rCDH was nearly homogeneous, exhibiting an R_z (A_{421}/A_{280}) value of 0.57, and a specific activity of 7.6 U/mg (Table 2.1). The pH of the eluent was adjusted to pH 8, concentrated, and the rCDH solution was further purified by gel filtration chromatography. Those fractions exhibiting an R_z value = 0.6 were pooled. The total yield, based on initial CDH activity, was ~50%, the R_z

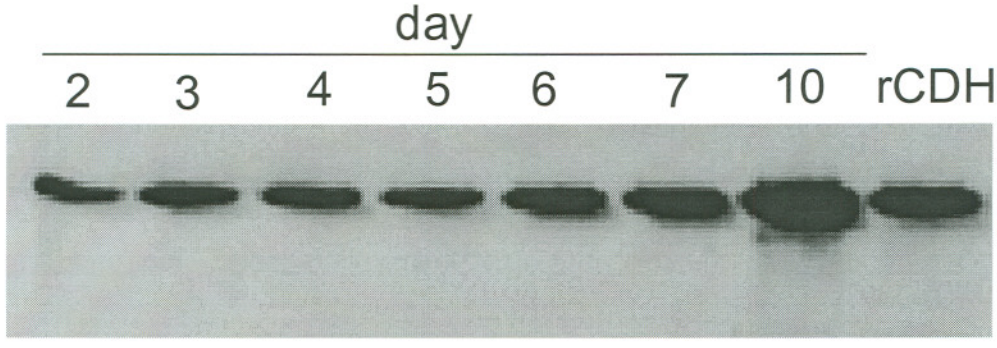

Fig. 2.1 Immunoscreening of 2–10-day-old culture medium for rCDH from pAGC1 transformants.

Table 2.1

Purification of Recombinant Wild-type CDH

Step	Total protein (mg)	Total activity (U)[a]	Specific activity (U/mg)	Yield (%)	Fold purification
Extracellular media[b]	48	81.2	1.7	100	1
Cellulose affinity step	6.7	49.8	7.6	61	4.4
Gel filtration	5	39.9	8.1	49	4.7

[a] Cyt *c* activity;
[b] After concentration and dialysis against 20 mM K-phosphate, pH 6.

value is ~0.62 and the specific activity was 8.1 U/mg (Table 2.1). The latter value is practically identical to the specific activity of rCDH obtained by the original purification method [Li et al., 2000] and similar to wtCDH [Bao et al., 1993]. The steady state kinetic parameters (k_{cat} and K_m) for cellobiose oxidation and DCPIP and cyt *c* were similar to those of wtCDH and rCDH, purified following earlier reported procedures (Table 2.2).

The native (oxidized) rCDH exhibits a Soret maximum at 421 nm, a shoulder at 450 nm, attributed to the flavin cofactor, and two visible bands at 530 and 570 nm. Upon addition of cellobiose, the flavin absorbance bleaches, the Soret absorbance shifts to 429 nm, and two α,β-bands appear at 562 and 532 nm, respectively. The extinction coefficients of oxidized and reduced rCDH at various wavelengths are listed in Table 2.3. The shape and intensities of the absorption bands are very similar to the values determined for wtCDH [Li et al., 2000]. The prosthetic group of the flavin domain of rCDH, extracted by treatment with trichloroacetic acid, displayed a spectrum typical of a flavin chromophore with maxima at 450 and 380 nm (Fig. 2.2), which is very similar to authentic FAD, with the exception of a small blue-shifted shoulder near 450 nm. Earlier studies [Morpeth and Jones, 1986; Hallberg et al., 2002] attributed the shoulder to a 6-hydroxy-FAD, a modified flavin. Based on the extinction coefficients extinction coefficients of the FAD and 6-hydroxy-FAD (Fig. 2.2, insert), it is estimated that rCDH contains more than 95% FAD. This estimation further suggests that approximately 95% of the flavin in rCDH could be extracted.

In conclusion, a simplified purification protocol is developed for rCDH. The CDH enzyme obtained through this protocol exhibit similar biochemical, spectral, and kinetic properties as the wtCDH and rCDH, purified following the original protocols. The modified method required only two steps to obtain a homogeneous CDH and the yield is significantly higher than what previously was obtained. This procedure was successfully adopted in the rapid purification of several variants reported in this thesis.

Table 2.2

Steady-State Kinetic Parameters for rCDH and wtCDH[a]

Enzyme	Cellobiose oxidation (DCPIP)		DCPIP reduction	
	k_{cat} (s^{-1})	K_m (μM)	k_{cat} (s^{-1})	K_m (μM)
rCDH[b]	25.7	40	27.0	6.4
rCDH[c]	ND[d]	ND	24	2.3
wtCDH[c]	ND	ND	23.1	3.8
Enzyme	ellobiose oxidation (cyt *c*)		Cyt *c* reduction	
	k_{cat} (s^{-1})	K_m (μM)	k_{cat} (s^{-1})	K_m (μM)
rCDH[b]	10.5	18	10.8	0.8
rCDH[c]	11.1	22	11.7	0.7
wtCDH[c]	12.0	25	12	0.7

[a] Reactions were performed in 20 mM Na-succinate, pH 4.5. K_m and k_{cat} for cellobiose were determined using 12.5 μM cytochrome *c* or 40 μM DCPIP. K_m and k_{cat} for DCPIP and cyt *c* were determined using 400 μM cellobiose.

[b] This work.

[c] From Li et al., 2000.

[d] ND = not determined.

Table 2.3

Extinction Coefficients of Oxidized and Reduced rCDH[a]

λ (nm)	ϵ (mM^{-1} cm^{-1})	
	Oxidized	Reduced
421	100	88
429	73	132
562	7.5	24

[a] Extinction coefficients were calculated based on absorbance of oxidized and cellobiose reduced rCDH in 20 mM Na-succinate, pH 4.5, and the heme content, estimated with the pyridine hemochromogen method [Berry and Trumpower, 1987].

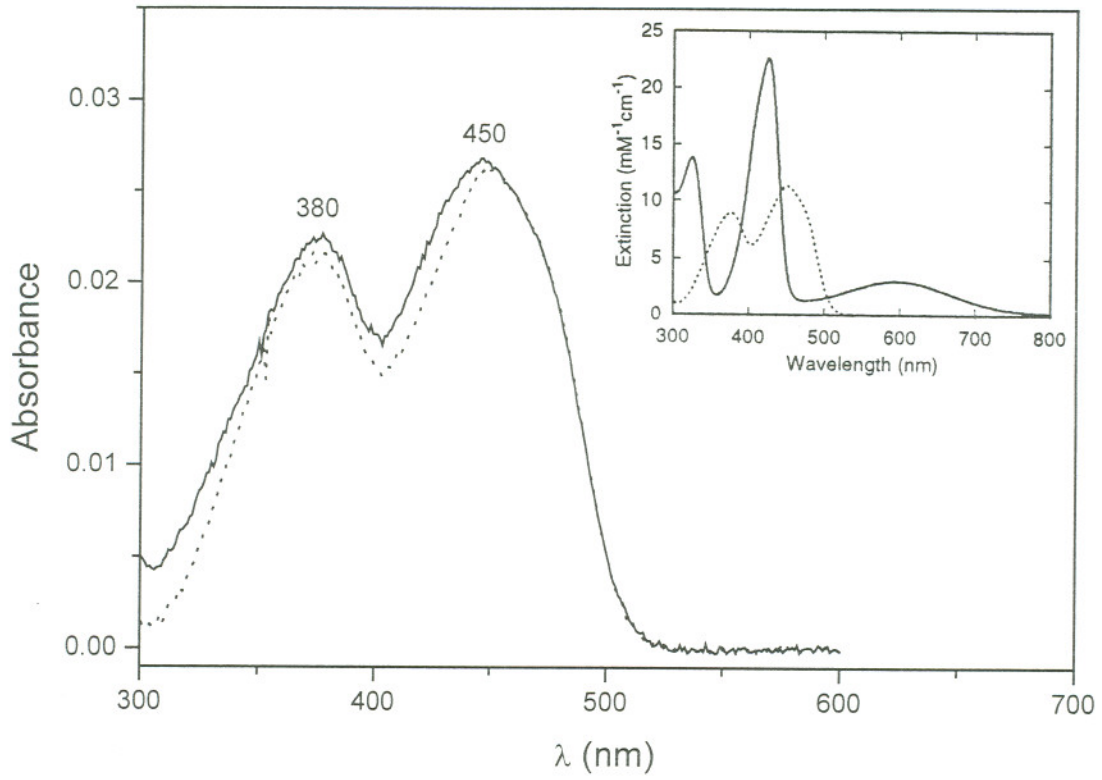

Fig. 2.2 Comparison of absorption spectrum of flavin cofactor extracted from rCDH (—) with spectrum of authentic FAD (---). **Inset*** shows spectra of authentic FAD (---) and 6-hydroxy-FAD (—).

* Originally published as Fig. 7 inset in:

Igarashi, K., Verhagen, M. F., Samejima, M., Schulein, M., Eriksson, K. E., and Nishino, T. (1999) Cellobiose dehydrogenase from the fungi *Phanerochaete chrysosporium* and *Humicola insolens*. A flavohemoprotein from *Humicola insolens* contains 6-hydroxy-FAD as the dominant active cofactor. *J. Biol. Chem.* **274**, 3338-3344.

CHAPTER 3
SITE-DIRECTED MUTAGENESIS OF THE HEME AXIAL LIGANDS IN CELLOBIOSE DEHYDROGENASE FROM *PHANEROCHAETE CHRYSOSPORIUM*[*]

3.1 INTRODUCTION

Cellulolytic fungi secrete an arsenal of hydrolytic enzymes, including several isozymes of cellobiohydrolases, endoglucanases and β-glucosidases, for the degradation of cellulose [Beguin and Aubert, 1994]. In addition, several fungi produce an oxidoreductase, cellobiose dehydrogenase (CDH). This enzyme is the only extracellular flavocytochrome reported to date, catalyzing the oxidation of cellobiose to cellobionolactone in the presence of various one- and two-electron acceptors. However, the physiological electron acceptor has not been identified.

CDH has been purified from several wood-rot fungi [Henriksson et al., 2000] and all CDHs have similar biochemical characteristics. The best-studied example is CDH from *P. chrysosporium* (CDH_{PC}) [Ayers et al., 1978; Bao et al., 1993]. It contains a single flavin adenine dinucleotide (FAD) and a single heme *b* [Ayers et al., 1978; Bao et al., 1993], non-covalently bound to two distinct domains. A protease sensitive linker region connects the two domains [Henriksson et al., 1991; Habu et al., 1993]. During the catalytic cycle of CDH, the flavin domain oxidizes cellobiose, concomitant with the reduction of FAD to $FADH_2$. The $FADH_2$ can be reoxidized by

---

* This material has been published in this or similar form in *Archives of Biochemistry and Biophysics* and is used here with permission of Elsevier Science/Academic Press:

Rotsaert, F. A. J., Li, B., Renganathan, V., and Gold, M. H. (2001) Site-directed mutagenesis of the heme axial ligands in the hemoflavoenzyme cellobiose dehydrogenase. *Arch. Biochem. Biophys.* **390,** 206–214.

transferring the two electrons to two-electron acceptors such as quinones and dichlorophenol-indophenol (DCPIP), without the apparent mediation of the cytochrome domain. However, for the efficient reoxidation of the flavin in two one-electron steps by reduction of one-electron acceptors, such as cytochrome *c* (cyt *c*), a covalent linked heme-binding domain is required.

Spectroscopic studies first suggested that the axial ligands are a methionine and histidine [Cox et al., 1992], an unusual coordination for *b*-type cytochromes. The amino acid sequence of CDH_{PC}, deduced from cDNA sequence [Raices et al., 1995; Li et al., 1996a], identified four histidines and one methionine in the cytochrome domain. Two histidines, His 114 and His 163, and Met65 were predicted to function as axial ligand, based on the conserved position in the CDH sequence from *P. chrysosporium*, *Trametes versicolor* [Dumonceaux et al., 1998] and *Sporotrichum thermophile* [Subramaniam et al., 1999]. Because the surrounding of the His114 was most conserved, this residue was suggested as the most probable histidine ligand [Subramaniam et al., 1999].

At the start of this thesis, our group had achieved homologous expression of recombinant wild-type CDH (rCDH) in *P. chrysosporium* [Li et al., 2000]. Normally, CDH is produced by *P. chrysosporium*, only when cellulose is provided as the sole carbon source [Li et al., 1996a]. By placing CDH under the control of the D-glyceraldehyde-3-phosphate dehydrogenase (*gpd*) promoter, homologous expression of recombinant CDH (rCDH) occurs in cultures supplemented with glucose as the sole carbon source. In this chapter, we identify Met65 and His163 as the heme ligands, using site-directed mutagenesis, and further we propose functional roles for these residues in CDH. While this investigation was in progress, Hallberg et al. reported the crystal structure of the reduced cytochrome domain (residues 1–190) of wild-type CDH_{PC}. The structure also showed that His163 and Met65 are the heme axial ligands [Hallberg et al., 2000].

3.2 MATERIALS AND METHODS

3.2.1 Organisms

Growth and maintenance of *P. chrysosporium* wild-type strain OGC101, prototrophic transformants and auxotrophic strains OGC107-1 (Ade11) and OGC316-7 (Ura11) were described previously [Alic et al., 1990; Akileswaran et al., 1993]. *Escherichia coli* XL1-Blue was used for subcloning.

3.2.2 Construction of *cdh* Transformation Plasmid pUGC1

pUGC1 (Fig. 3.1) was constructed by ligating a 4.4 kb *gpd–cdh* fragment at the multiple cloning site in pUB1.7, a *P. chrysosporium* transformation plasmid containing the *Schizophyllum commune* orotidylate decarboxylase (*Ura11*) gene as a selectable marker [Sollewijn Gelpke et al., 1999]. The *gpd–cdh* fragment, containing the *P. chrysosporium gpd* promoter fused to the *P. chrysosporium cdh-1* gene at the translation start site, was prepared by restriction digestion of pAGC1 [Li et al., 2000] with *EcoR*I, *Xba*I, and *Sph*I. This digestion yielded the *gpd–cdh* fragment (4.4 kb) and two smaller fragments (0.03 and 0.42 kb). pUB1.7 was digested with *Xba*I and *EcoR*I (located in the multiple cloning site). The digested plasmid pUB1.7 and the *gpd–cdh* fragment were purified using the Qiaprep® Miniprep column (Qiagen Inc., Valencia, CA). The *gpd–cdh* fragment was subsequently incorporated in the multiple cloning site of pUB1.7 by ligation of the two digested plasmid samples, using T4 DNA ligase. The correct incorporation of the *gpd–cdh* fragment in pUB1.7 vector was confirmed by comparing the HindIII restriction pattern of pUGC1 with the pattern predicted from sequence (Fig. 3.1).

3.2.3 Construction of Mutant Plasmids pM65A, pH114A and pH163A

The M65A site-directed mutation was introduced into pAGC1 [Li et al., 2000] as described [Li, 1999]. H114A, and H163A site-directed mutations were introduced into pUGC1 using the Transformer™ site-directed mutagenesis kit (BD Biosciences, Clontech., Palo Alto, CA). A single strand of pUGC1 was amplified using two

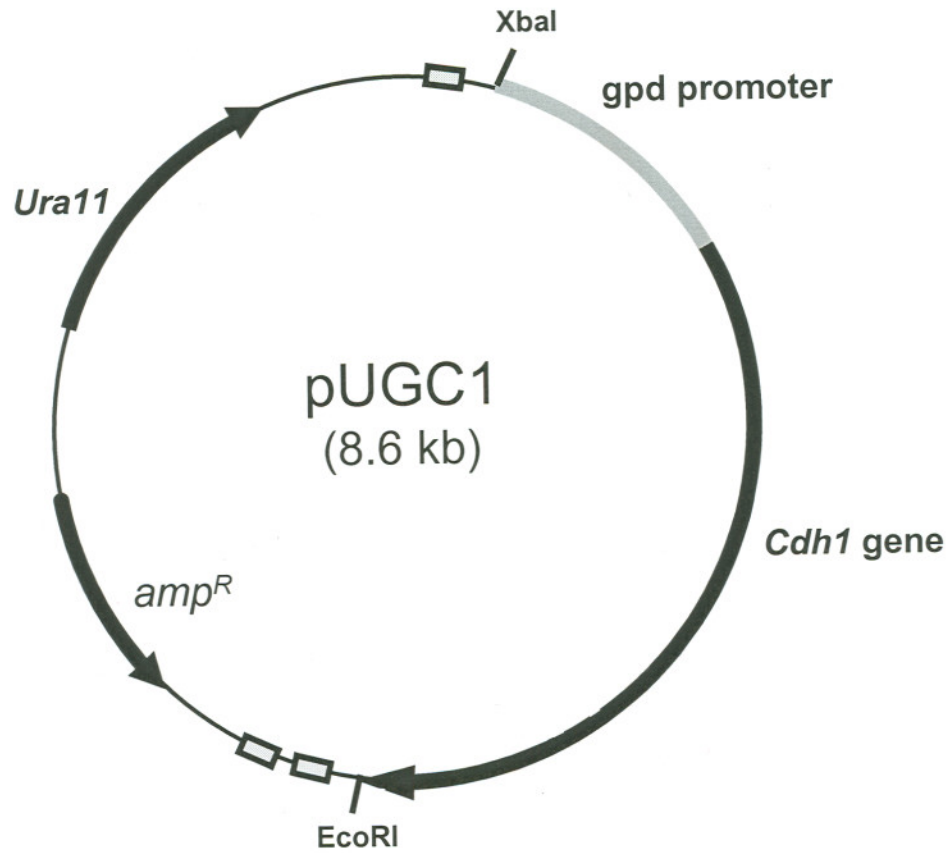

Fig. 3.1 Restriction map of the CDH expression vector pUGC1, containing the *ura1* gene and the *gpd* promoter fused to the *cdh-1* gene.

oligonucleotide primers, a mutagenic primer and a selection primer. The first primer introduced the desired mutation and the second primer mutated the unique *Xba*I restriction site, TCTAGA, to a non-restriction site TCTGGA. Mutagenic primers in the coding region were designed to change the CAC codon (His) to GCC (Ala). The mutant plasmids, pH114A and pH163A, were isolated after the mutagenesis reactions and mutations were confirmed by sequencing.

3.2.4 Transformation of *P. chrysosporium*

Protoplasts of *P. chrysosporium* OGC107-1, an adenine auxotroph, and of *P. chrysosporium* OGC316-7, an uracil auxotroph, were prepared as described [Alic et al., 1990; Sollewijn Gelpke et al., 1999]. The adenine auxotroph was transformed with *Eco*RI-linearized pM65A (5 μg) and the uracil auxotroph separately with *Eco*RI-linearized pH114A or pH163A (2 μg). Transformants were transferred to minimal medium slants (GV-slants, cf. 2.2.1) to screen for adenine or uracil prototrophy [Alic et al., 1987; Alic et al., 1990]. Conidia from prototrophs were then cultured in 250-ml Erlenmeyer flasks containing 20 ml of a high-carbon high-nitrogen (HCHN) medium as described [Kirk et al., 1978], supplemented with 2% glucose, 12 mM ammonium tartrate, 0.2% tryptone, and 20 mM Na-2,2-dimethyl succinate [Li et al., 2000]. The pH of the medium was adjusted to 6.0. The cultures were incubated without shaking at 37°C. Periodically 50–100 μl of extracellular medium was monitored for CDH activity using the cyt *c* and DCPIP assay. The transformant exhibiting the highest DCPIP activity was purified by isolating single basidiospores, as described [Alic et al., 1987; Alic et al., 1990], and was subsequently used for protein production.

3.2.5 Production and Purification of CDH Variant Proteins

The H114A, H163A and M65A CDH variants were grown from conidial inocula at 37°C in 20 ml stationary cultures in 250 ml Erlenmeyer flasks as described above. The extracellular medium (day 6 or 7) was concentrated and dialyzed against 20 mM potassium phosphate, pH 6. The dialyzed and concentrated medium (DCPIP reduction activity $\sim$1000 U L^{-1}.) was incubated for 60 minutes at 4°C with 2 g/100

ml Sigmacell® 50. The cellulose–CDH complex with 85–90% of the initial DCPIP activity, was separated from the supernatant by centrifugation (16,000 x g) and washed twice with 20 mM potassium phosphate (pH 6). CDH was partially eluted from cellulose (70–75%) by incubation in 20 mM Tris pH 9.0 at 4°C for 45 minutes. The eluent was concentrated and further purified by gel filtration using a Sephacryl S200 HR column (Sigma) equilibrated with 50 mM K-phosphate, pH 6. Finally, proteins were purified by fast protein liquid chromatography (FPLC) using a MonoQ HR 5/5 column (Amersham Biosciences, Piscataway, NJ). Separations were performed in 10 mM Tris-HCl, pH 8, and proteins were eluted with a 0–0.3 M gradient.

3.2.6 SDS-PAGE and Immuno (Western) Blot Analysis

Sodium dodecyl sulfate-polyacrylamide gel electrophoresis (SDS-PAGE) and western blot analysis were performed as described in Chapter 2.

3.2.7 Spectroscopic and Kinetic Procedures

Electronic absorption spectra of rCDH and its variants were recorded at room temperature with a Shimadzu UV-260 spectrophotometer (Shimadzu Biotech, Pleasanton, CA). CDH variants were reduced either with cellobiose (400 μM) or a grain of dithionite. CDH activity during culturing and purification were monitored using the cyt *c* and/or DCPIP assays. The reaction mixture contained 400 μM cellobiose and 12.5 μM cyt *c* or 40 μM DCPIP in 20 mM Na-succinate, pH 4.5. Reduction of cyt *c* and DCPIP were monitored at 550 nm (ϵ_{550} = 28 mM^{-1} cm^{-1}) and 515 nm (ϵ_{515} = 6.8 mM^{-1} cm^{-1}), respectively. The steady-state kinetics of cellobiose oxidation were determined by monitoring ferrocytochrome *c* formation or DCPIP reduction. The assays contained a fixed level of ferricytochrome *c* (12.5 μM) or DCPIP (40 μM) and varying levels of cellobiose (5–200 μM) in 20 mM Na-succinate, pH 4.5. The steady-state kinetics of cyt *c* and DCPIP reduction were determined in a similar fashion, with a fixed cellobiose concentration (200 μM) and variable cyt *c* and DCPIP concentrations (0.2 to 40.0 μM).

3.2.8 Chemicals

Cellobiose, horse heart cyt *c* (Grade IV), Sephacryl S200 (HR) and Sigmacell® (type 50) were obtained from Sigma (St. Louis, MO). Molecular biology reagents were obtained from New England Biolabs (Beverly, MA) or Stratagene (La Jolla, CA). All other chemicals were reagent grade. Solutions used in biochemical characterization of the enzymes were prepared in Millipore Q-50 (Millipore Corp., Bedford, MA) purified water (> 18 MΩ cm).

3.3 RESULTS

3.3.1 Expression of Alanine Variants

The alanine mutations in the transformation plasmids pM65A, pH114A and pH163A were verified by DNA sequencing. The transformation of the adenine or uracil auxotrophic strains with *Eco*RI-linearized mutant plasmids resulted in the isolation of 15 to 20 transformants for each construct. Each transformant was individually grown in 20-ml stationary cultures, supplemented with glucose as sole carbon source. Extracellular CDH activity was monitored periodically using cyt *c* and DCPIP reduction assays. For each mutant, several transformants rapidly reduced DCPIP, but only the pH114A transformants showed significant cyt *c* reduction. The transformants exhibiting the highest DCPIP activity were further purified by fruiting as described previously [Alic et al., 1987; Alic et al., 1990], and used for the expression and study of the CDH variants.

The amount of mutant protein, secreted by the pM65A, pH114A and pH163A transformants was similar to rCDH transformant [Li et al., 2000], based on DCPIP activities in the extracellular media. Western-blot analysis of total extracellular proteins from M65A and H163A cultures using CDH polyclonal antibodies indicated the presence of a major 90 kDa protein band on days 2 to 3 (Fig. 3.2). In the latter stages a second protein band with 70 kDa molecular weight appeared and the intensity of the 90 kDa band decreased (Fig. 3.2). Analysis of the extracellular proteins from the H114A cultures indicated only the presence of the 90 kDa protein over a 10-day culture period, as was observed for rCDH (Fig. 2.1).

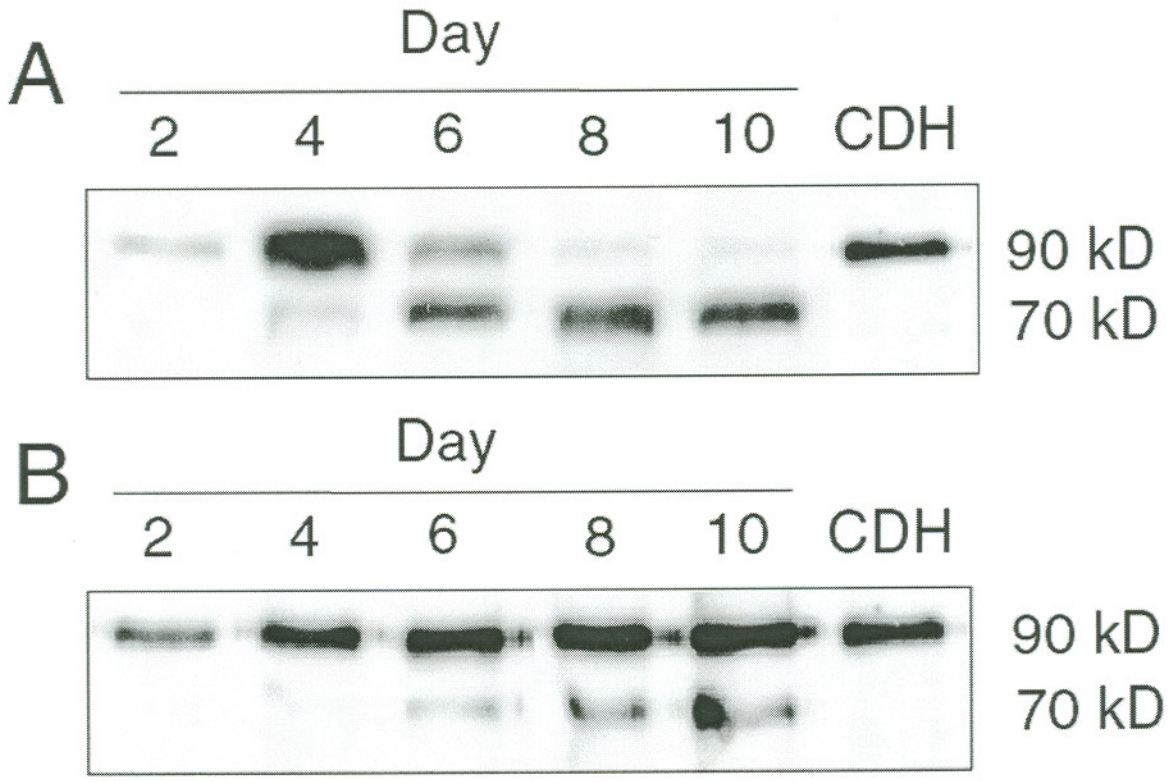

Fig. 3.2 Immuno-screening of culture medium from the transformants M65A (**A**) and H163A (**B**) CDH variants. An aliquot of extracellular medium (1 μl) was taken at regular intervals, electrophoresed, and proteins were electrophoretically transferred to a PVDF membrane. CDH variants were detected using polyclonal antibodies raised against *P. chrysosporium* CDH and Western-Light chemiluminescent detection system (Tropix Inc., Bedford, MA). Lanes 1–5, CDH variants from aliquots of extracellular medium, taken on days 2, 3, 5, 6, and 10; lane 6, purified rCDH.

3.3.2 Purification and Characterization of the H114A Variant

A conserved feature of enzymes involved in the degradation of cellulose, such as CDH and cellulases, is their affinity for cellulose. CDH binds strongly to microcrystalline cellulose under mildly acidic and neutral pH conditions, and can be eluted under basic pH conditions [Renganathan et al., 1990]. Thus, a cellulose-affinity purification step was used to quickly separate CDH variants from other extracellular proteins. The H114A was then purified to homogeneity using gel filtration and anion exchange chromatography. The last step did not improve the R_z value (A_{421}/A_{280} = 0.61) and thus this step has been removed in the other studies (Chapters 4 and 5). The molecular weight of the H114A variant was 90 kDa, identical to rCDH (Fig. 3.3). The absorption spectra of both proteins were essentially identical: the native ferric enzymes exhibited absorbance bands at 421, 530 and 570 nm, attributable to the heme, and an absorbance band around 450 nm, attributable to the flavin (Fig. 3.4, Table 3.1) [Bao et al., 1993; Li et al., 2000]. Cellobiose addition shifted the heme absorbances of both enzymes to 429, 532 and 562 nm, and bleached the flavin absorbance. The steady-state kinetic parameters k_{cat} and K_m for cellobiose, cyt *c* and DCPIP are comparable for the two proteins (Table 3.2).

3.3.3 Purification and Characterization of the M65A and H163A Variants

Western-blot analysis indicated the presence of two proteins with molecular masses of 70 kDa and 90 kDa in 7-day old cultures from the pM65A and pH163A transformants (Fig. 3.2). Fractions from the Sephacryl S-200 column were analyzed for DCPIP activity and heme absorbance. Fractions, containing DCPIP activity, were separated into two pools, one exhibiting a strong heme absorbance and one exhibiting a weak or no heme absorbance. The latter was further purified by FPLC. For both the pM65A and pH163A transformants, a pure 70 kDa protein was obtained (Fig. 3.3). UV-Visible spectra of the 70 kDa proteins exhibited absorbances at 386 and 458 nm indicating the presence of a flavin (Fig. 3.5, Table 3.1). Addition of cellobiose led to more than 80% bleaching of absorption band at 458 nm. The steady-state kinetic parameters, K_m and k_{cat}, for cellobiose oxidation by the 70 kDa M65A variant were 37 μM and 24.1 sec^{-1}, respectively (Table 3.2). The

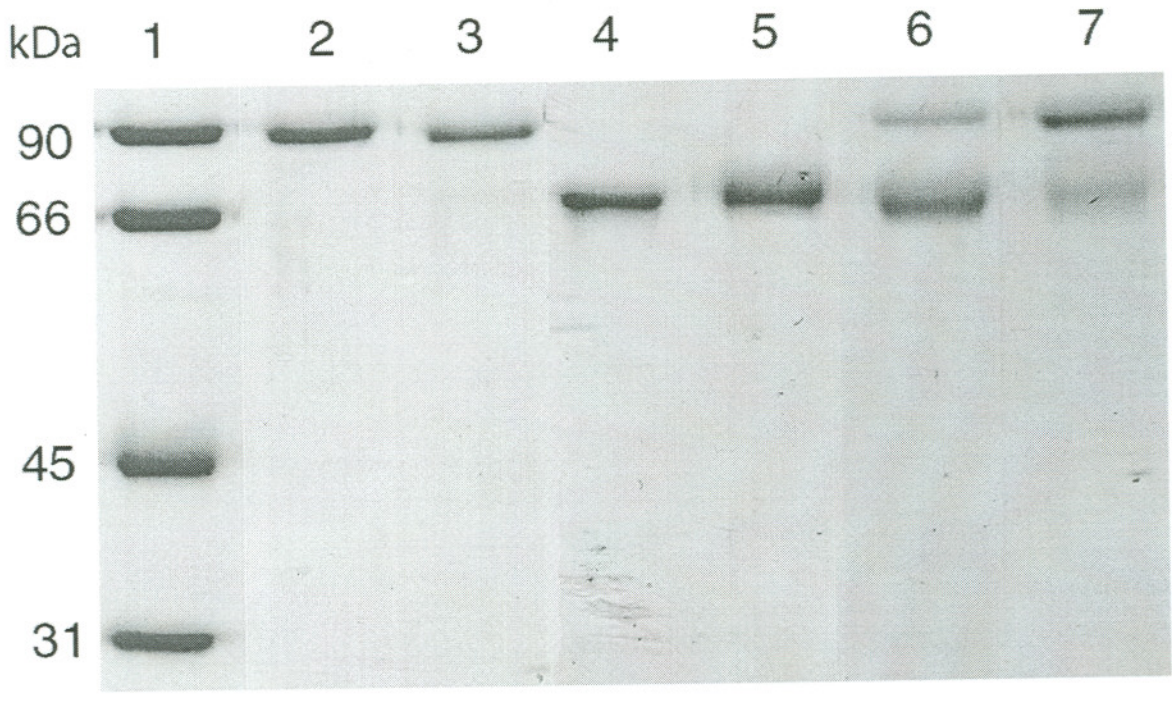

Fig. 3.3 SDS-PAGE analysis of purified CDH variants. Lane 1, molecular weight markers; lane 2, recombinant wild-type CDH; lane 3, H114A variant; lane 4, 70-kDa flavoprotein from M65A variant; lane 5, 70-kDa flavoprotein from H163A variant; lane 6, partially purified 90-kDa protein from M65A variant; and lane 7, partially purified 90-kDa protein from H163A variant.

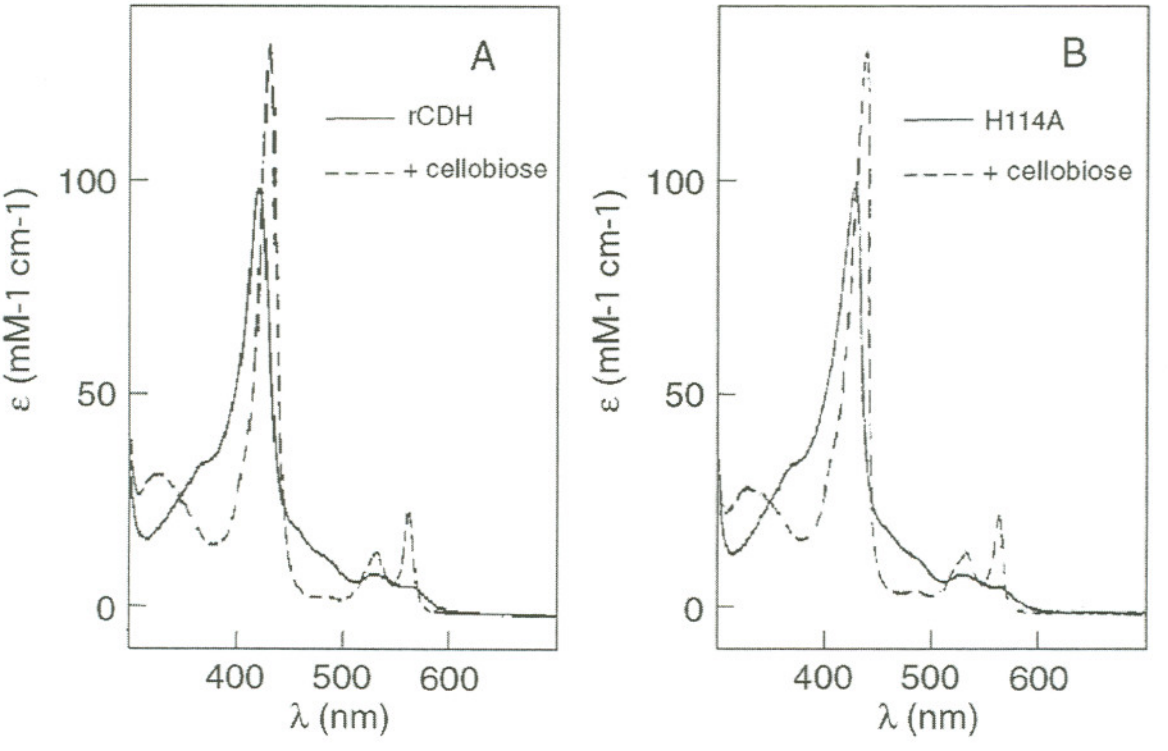

Fig. 3.4 Absorption spectra of H114A CDH variant (**A**) and rCDH (**B**). Oxidized (—), reduced with cellobiose (---).

Table 3.1

UV-Visible Spectral Characteristics of rCDH and CDH Variants

Protein sample	Oxidized	Cellobiose reduction[a]	Dithionite reduction[b]
rCDH	421 530 570	429 532 562	429 532 562
H114A	421 530 570	429 532 562	429 532 562
M65A (90 kD)	408 (sh) 423 533 569	408 (sh) 423 533 569	428 533 569
M65A (70 kD)	384 458	352 470	ND[c]
H163A (90kD)	360 437 544 573	360 413 438 544 573	360 414 (sh) 437 544 573
H163A (70 kD)	384 458	352 468	ND[c]

[a] Addition of 400 μM cellobiose.

[b] Addition of a grain of dithionite.

[c] ND = Not determined.

Table 3.2

Steady-State Parameters for rCDH and CDH Variants[a]

Enzyme	Cellobiose oxidation (DCPIP)		DCPIP reduction	
	k_{cat} (s^{-1})	K_m (μM)	k_{cat} (s^{-1})	K_m (μM)
rCDH	25.7	40	27.0	6.4
H114A	27.0	40	25.5	6.2
M65A (70 kDa)	24.1	37	25.0	7.6
H163A (70 kDa)	26.8	44	28.5	7.9
Enzyme	Cellobiose oxidation (cyt *c*)		Cyt *c* reduction	
	k_{cat} (s^{-1})	K_m (μM)	k_{cat} (s^{-1})	K_m (μM)
rCDH	12.1	18	14.2	0.7
H114A	14.2	16	15.1	0.7

[a] Reactions were performed in 20 mM Na-succinate, pH 4.5. K_m and k_{cat} for cellobiose were determined using 12.5 μM cytochrome *c* or 40 μM DCPIP. K_m and k_{cat} for DCPIP and cytochrome *c* were determined using 200 μM cellobiose.

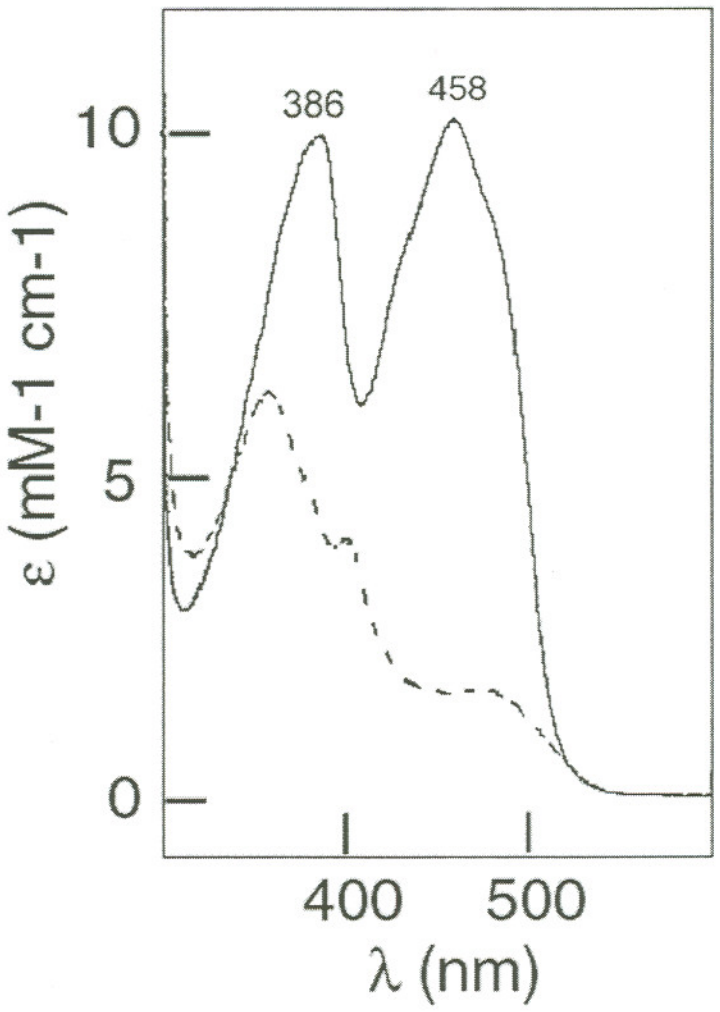

Fig. 3.5 Absorption spectra of the 70-kDa protein from the M65A variant. Oxidized (—), reduced with cellobiose (---).

corresponding values for the 70 kDa H163A variant were 44 μM and 26.8 sec^{-1}. These kinetic values for these variants were comparable to that of the flavocytochrome rCDH (Table 3.2).

The yield of the pooled chromatographic fractions, which exhibited DCPIP activity and a strong heme absorbance, was low. SDS-PAGE analysis also indicated that these fractions were only partially purified, containing both the 90 kDa and 70 kDa proteins (Fig. 3.3). Further purification by FPLC resulted in complete loss of the 90 kDa proteins and for this reason, the 90 kDa proteins were not purified to homogeneity. The 90 kDa protein from the M65A variant exhibited absorbances at 423, 533, and 569 nm, which indicated the presence of a heme (Fig. 3.6, Table 3.1). The shoulder around 450 nm was attributed to the flavin. Upon addition of cellobiose the UV-visible spectrum remained substantially unchanged except for a decrease in the 380 and 450 nm bands attributable to the bleaching of flavin absorption. The addition of dithionite shifted the Soret absorption of the M65A heme protein to 428 nm; nevertheless the features in the visible region (500 –600 nm) did not change. The UV-visible spectrum of the partially purified 90 kDa protein from the H163A variant exhibited absorbances at 360, 437, 544, and 573 nm (Fig. 3.7, Table 3.1). Upon addition of cellobiose or dithionite, the 360 and 440 nm absorbances decreased and a new absorbance at 415 nm emerged. The absorbances at 544 and 575 nm remained essentially unchanged.

3.4 DISCUSSION

CDH belongs to the class of flavocytochromes, which also includes flavocytochrome b_2 (lactate dehydrogenase) from *Saccharomyces cerevisiae* [Appelby and Morton, 1959; Jacq and Lederer, 1974], L(+)-mandelate dehydrogenase from *Rhodatorula graminis* [Yasin and Fewson, 1993; Illias et al., 1998] and glyoxylate dehydrogenase from *Tyromyces palustris* [Tokimatsu et al., 1998]. The commonality among these enzymes is that they contain a heme and a flavin cofactor, bound to two structurally distinct domains, which are connected by a peptide linker. The flavin domain catalyzes substrate oxidation, whereas the cytochrome domain facilitates the

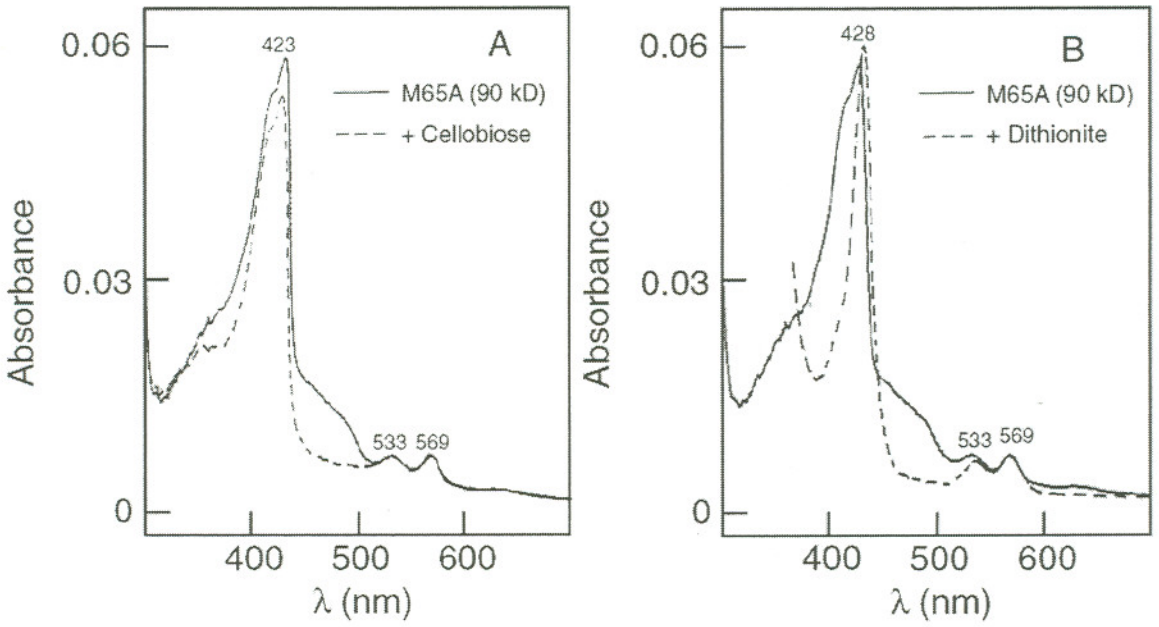

Fig. 3.6 Absorption spectra of M65A CDH variant (90 kDa). (**A**) Oxidized (—); reduced with cellobiose (400 μM) (---). (**B**) Oxidized (—); reduced with dithionite (---).

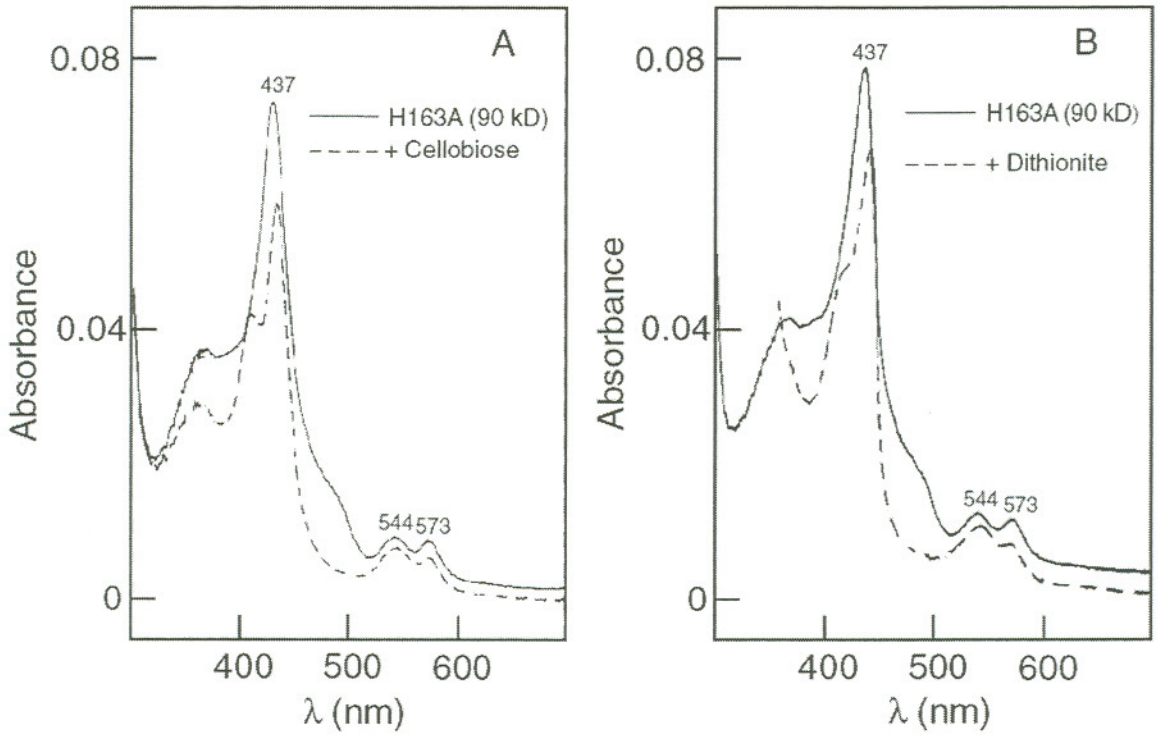

Fig. 3.7 Absorption spectra of H163A CDH variant (90 kDa). (**A**) Oxidized (—); reduced with cellobiose (---). (**B**) Oxidized (—); reduced with dithionite (---).

electron transfer to one-electron acceptors, such as cyt *c*. Although CDH shows high affinity for this substrate, the extracellular location of CDH rules out that cyt *c* is the physiological electron acceptor.

Spectroscopic studies first suggested that a methionine and histidine form the axial coordination to the heme iron [Cox et al., 1992]. This is unusual for *b*-type cytochromes, which more commonly possess *bis*-histidyl ligations. Comparison of the CDH sequences available at the beginning of our research, from *P. chrysosporium* [Raices et al., 1995; Li et al., 1996a], *Trametes versicolor* [Dumonceaux et al., 1998] and *Sporotrichum thermophile* [Subramaniam et al., 1999] identified one conserved methionine, Met65, and two conserved histidines, His114 and His163, in CDHPC [Subramaniam et al., 1999]. Using a homologous expression system for recombinant CDH (rCDH), we have expressed three alanine mutants to identify the axial ligands to the heme iron and to probe the functional importance of these residues for the enzyme.

Cyt *c* activity in the extracellular medium of H114A transformation cultures was a first indication that His 114 is not involved in the binding of the heme. Indeed, the biochemical, spectral and kinetic properties of the H114A mutant protein are essentially identical to those of rCDH (Tables 3.1 and 3.2; Fig. 3.2), indicating that this residue is not essential for binding or reactivity of the heme. This excludes histidine 114 as a heme iron axial ligand. In addition, comparison of the six now available amino acid CDH sequences suggests that this position is not completely conserved and that the CDH from the soft-rot fungus *Humicola insolens* [Xu et al., 2001] contains a serine residue.

It was anticipated that point mutations of the axial ligands would preserve the oxidation of cellobiose by the flavin domain, but that electron transfer (ET) to acceptors such as cyt *c* would be diminished. This was previously observed for two axial ligand variants of flavocytochrome b_2, H43M [Miles et al., 1993] and H66C [Mowat et al., 2000]. Substitution of His 66 by Cys decreased the redox midpoint potential of the heme and thus lowered the thermodynamic driving force for ET between the two domains. CDH activity in the extracellular medium during the 7 day

culture period showed the expected reactivities: the two electron acceptor DCPIP was still rapidly reduced in the presence of cellobiose and DCPIP activity peaked around day 7, similar to what is observed for rCDH [Li et al., 2000]. However, over the 7-day period no significant cyt *c* reduction was observed in the culture media of the M65A and H163A transformants.

It also was anticipated that the point mutation of an axial ligand would result in the purification of a 90 kDa CDH variant, which is either devoid of heme or containing a loosely bound heme. Western-blot analyses of the extracellular medium from the M65A and H163A transformants with CDH polyclonal antibodies show the presence of a 90 kDa protein early in the culture growth (Fig. 3.2). DCPIP activity was also detected during this time for both mutants. In later stages, a second protein band appeared with a molecular weight of 70 kDa, concomitant with the decrease in the 90 kDa band intensity for the M65A variant. The 70 kDa protein when purified to homogeneity (Fig. 3.3) has the spectral characteristics of a flavin protein (Fig. 3.5), similar to the truncated flavin domain of CDH purified from *P. chrysosporium* wild-type cultures, grown under cellulolytic conditions [Samejima and Eriksson, 1992]. The steady-state kinetic parameters K_m and k_{cat} for oxidation of cellobiose in the presence of DCPIP are similar to rCDH (Table 3.2). These properties strongly suggest that this protein is the flavin domain of the M65A and H163A variant.

The 90 kDa proteins from the M65A and H163A transformants rapidly degraded during purification. Attempts to purify the 90 kDa proteins from 4-day old cultures was futile and it was contaminated with the flavin domain. However, the electronic absorption spectra of the unpurified preps suggested the presence of a heme cofactor (Figs. 3.6 and 3.7). The low yield and instability did not allow for a detailed study of the 90 kDa CDH variants. The Soret absorptions suggested the presence of multiple heme species. The addition of exogeneous ligands imidazole and cyanide resulted in small changes in the Soret of M65A and H163A 90 kDa variant (data not shown), possibly indicating the presence of a penta- or hexa-coordinate heme *b* with a displaceable ligand. Addition of cellobiose to the variant proteins resulted in the reduction of the FAD cofactor, based on the bleaching of the absorbance around 450 nm. For the M65A mutant, no heme spectral changes are

observed, indicating the absence of electron transfer from the reduced flavin to the heme. Features in the visible region were unaffected by a strong reductant as dithionite, which might indicate the presence of inert heme species.

The axial ligands in cytochromes play an important role in anchoring the prosthetic group to the polypeptide. For most *b*-type cytochromes with a non-covalently bound heme group, substitution of the axial ligand with a methionine or alanine has resulted in the production of the apo-form, during protein synthesis, purification and/or storage. This has been observed for heme ligand variants of flavocytochrome b_2 [Miles et al., 1993], cytochrome b_5/cytochrome b_5 reductase fusion protein [Davis et al., 2002], cytochrome b_5 [Beck von Bodman et al., 1986; Barker et al., 1996] and cytochrome b_{562} [Rodriguez and Rivera, 1998]. In several cases the apo-form could be reconstituted with hemin [Barker et al., 1996; Rodriguez and Rivera, 1998]. However, a thermal stability analysis of an axial ligand variant of cyt b_{562} showed that the holo (heme-reconstituted) form of the M7A variant is not more stable than the apo-form of the wild-type or the M7A variant [Kamiya et al., 2001], thus emphasizing the critical role of the axial coordination for binding of the heme to the protein and the stability of the protein. The 90 kDa alanine variants of CDH could not be purified in significant amount, which can be attributed to cleavage in the peptide linker between the two domains, and/or degradation of the heme binding domain. rCDH is significantly more stable during the same culture and purification conditions (Chapter 2). However, autocatalytic cleavage within the peptide linker, during storage and thawing of recombinant and wild type protein can occur (not published results). Apparently, the absence of one axial ligand makes the cytochrome domain more susceptible to degradation.

3.5 CONCLUSION

This study shows that Met65 and His163 are the axial ligands to the heme iron of the CDH, in agreement with the crystal structure of the cytochrome domain of wild-type CDH [Hallberg et al., 2000]. We further demonstrate that the His-Met ligation is required for electron transfer between flavin and cytochrome domain and

provide stability to this domain. Alanine mutations have lead to the generation of the 70 kDa flavin domain of CDH. N-Terminal amino acid analysis of the flavoproteins indicates the presence of multiple protein species indicating that cleavage occurs at several locations, including the linker region, which has been previously reported [Li et al., 1996a].

CHAPTER 4

BIOPHYSICAL AND STRUCTURAL ANALYSIS OF A NOVEL HEME-*B* IRON LIGATION IN THE FLAVOCYTOCHROME CELLOBIOSE DEHYDROGENASE*

4.1 INTRODUCTION

Cellobiose dehydrogenases (CDHs) are extracellular fungal flavocytochromes with a role in the biodegradation of lignocellulose [Henriksson et al., 2000]. The CDH gene from the white-rot fungus *Phanerochaete chrysosporium* has been cloned and sequenced [Raices et al., 1995; Li et al., 1996], revealing a full-length protein of 755 amino acids, partitioned into a cytochrome domain (residues 1–190) and a flavin domain (residues 216–755) connected by a ~30-residue peptide linker. A flavin adenine dinucleotide (FAD) cofactor is bound to the flavoprotein domain, while the cytochrome domain contains a 6-coordinated low-spin (6cLS) Fe–protoporphyrin IX [Cox et al., 1992; Cohen et al., 1997]. In the reductive half reaction, the flavin domain catalyzes the oxidation of cellobiose to yield cellobiono-1,5-lactone [Higham et al., 1994], with the concomitant reduction of FAD. During the ensuing oxidative half reaction, the flavin is re-oxidized to FAD by an electron acceptor, either directly for two-electron acceptors such as DCPIP, or via the cytochrome domain for one-electron acceptors, such as cytochrome *c* (cyt *c*).

Rotsaert, F. A. J., Hallberg, B. M., de Vries S., Moënne-Loccoz, P., Divne, C., Renganathan, V., and Gold, M. H. (2003) Biophysical and structural analysis of a novel heme b iron ligation in the flavocytochrome cellobiose dehydrogenase. *J. Biol. Chem.*, in press.

The 1.9 Å resolution crystal structure of the wild-type *P. chrysosporium* CDH cytochrome domain has been reported elsewhere [Hallberg et al., 2000]. The heme-binding module features an unusual fold among cytochromes: an immunoglobulin-like β-sandwich consisting of a five-stranded and a six-stranded β-sheet. The protoheme group is bound in a hydrophobic pocket at one face of the β-core, with one heme edge exposed to solvent. Three loops protrude from the β-sheet and wedge the *b*-type heme. The packing of the heme pocket formed by various non-polar residues is tight, leaving little space for exogeneous molecules. The crystal structure [Hallberg et al., 2000] confirmed earlier spectroscopic predictions [Cox et al., 1992], that the heme-iron ligation is ligated by a methionine and histidine with an unusual, near-perpendicular arrangement ($\sim 100°$) of the two planes defined by the methionine thioether group and the His163 imidazole ring. The distances of the Fe–N and Fe–S bonds, 2.0 Å and 2.3 Å, respectively, are typical of those observed in *c*-type cytochromes with Met-His iron ligation.

Results from site-directed mutagenesis of the two protoheme-iron ligands confirmed their importance (Chapter 3). Substitution of either residue with an alanine demonstrated that the Met-His coordination is essential for heme reactivity, i.e., the electron transfer (ET) to one-electron acceptors. In addition, the loss of an axial protein ligand rendered the cytochrome domain highly susceptible to degradation. Indeed, similar mutant studies in other *b*-type cytochromes reveal a weaker binding [Miles et al., 1993] or non-incorporation of the heme [Beck von Bodman et al., 1986; Hampsey et al., 1988; Davis et al., 2002]. Loss of the protoheme in the alanine variants of CDH may lead to unfolding of the cytochrome domain, rendering it more susceptible to proteolytic cleavage. In contrast, in *c*-type cytochromes, replacing the axially ligated methionine with a histidine produced a stable protein with some properties similar to the wild-type [Raphael and Gray, 1989; Darrouzet et al., 1999; Miller et al., 2000; Aubert et al., 2001]. Speculation about the coordination geometry to the protoheme in these variants has been advanced [Raphael and Gray, 1989; Darrouzet et al., 1999], but no structural studies have been reported. Herein, we report the results from site-directed mutagenesis, kinetic, electrochemical,

spectroscopic and crystallographic studies on the M65H variant of *P. chrysosporium* CDH.

4.2 MATERIALS AND METHODS

4.2.1 Organisms

Growth and maintenance of the auxotrophic strain OGC316-7 (Ura 11) and prototrophic transformants were as described previously [Alic et al., 1990; Akileswaran et al., 1993]. *Escherichia coli* DH5α was used for subcloning plasmids.

4.2.2 Construction of the Mutant Plasmid pM65H

The M65H site-directed mutation was introduced into pUGC1 (Fig. 3.1) using the Transform™ site-directed mutagenesis kit (BD Biosciences, Palo Alto, CA) (chapter 3). The mutant primer changed the ATG codon (Met) to the CAC codon (His). The mutant plasmid pM65H was isolated and the mutation was confirmed by sequencing.

4.2.3 Transformation of *P. chrysosporium* with pM65H

Protoplasts of *P. chrysosporium* OGC316-7 (Ura11), a uracil auxotroph, were prepared as described previously [Sollewijn Gelpke et al., 1999; Li et al., 2000], transformed with *Eco*RI-linearized pM65H (2 μg), and potential transformants were screened for uracil prototrophy [Sollewijn Gelpke et al., 1999; Li et al., 2000]. Conidia from prototrophs were then cultured in high-carbon high-nitrogen (HCHN) stationary liquid cultures with glucose as the sole carbon source [Li et al., 2000] and assayed for extracellular CDH activity using both the cyt *c* and 2,6-dichlorophenol-indophenol (DCPIP) assays (see Chapter 3, [Li et al., 2000]). The transformant exhibiting the highest activity was purified by isolating single basidiospores as described elsewhere [Alic et al., 1989; Alic et al., 1991], and progeny were re-screened for CDH activity in liquid cultures.

4.2.4 Production and Purification of the M65H Variant

The M65H strain was grown for 7 days at 37°C from conidial inocula in HCHN stationary liquid cultures with glucose as the sole carbon source. The extracellular fluid from 7 day-old cultures was concentrated and dialyzed against 20 mM potassium phosphate (pH 6). Subsequently, the variant protein was purified by cellulose-affinity chromatography and Sephacryl S200 gel filtration (Sigma, St. Louis, MO), as described in Chapter 2.

4.2.5 Preparation of Cytochrome Domains

The cytochrome domains of recombinant wild-type CDH (rCDH) and M65H (CYT_{M65H}) were obtained by limited proteolysis with papain [Henriksson et al., 1991; Cohen et al., 1997], and purified by FPLC using a MonoQ HR 5/5 anion exchanger (Amersham Bioscience, Piscataway, NJ) with a 0 to 1 M NaCl gradient in 10 mM Tris-HCl, pH 8.

4.2.6 SDS-PAGE and Western Blot Analysis

Sodium dodecyl sulfate-polyacrylamide gel electrophoresis (SDS-PAGE) was performed using a 12% Tris-glycine system [Laemmli, 1970] in a Miniprotean II apparatus (Bio-Rad, Hercules, CA), and gels were stained with Coomassie blue. Western blot-analysis was performed as described in Chapter 2.

4.2.7 Estimation of Protein and Heme Content

Protein concentration was determined by the bicinchoninic acid method [Smith et al., 1985]. Heme content was estimated by the pyridine hemochromogen procedure [Berry and Trumpower, 1987].

4.2.8 Spectroscopic Procedures

Electronic absorption spectra of rCDH and the M65H variant were recorded at room temperature with a Cary 100 spectrophotometer (Varian, Mulgrave, Victoria Australia). Spectra were obtained in 20 mM Na-succinate, pH 4.5. The enzymes were reduced under aerobic or anaerobic conditions by addition of cellobiose (200

μM) or excess dithionite. The CO adduct of the reduced form of the M65H variant was obtained by briefly bubbling CO gas through a cellobiose or dithionite reduced enzyme solution, under anaerobic conditions. To measure the association rate of CO, native M65H variant ($\sim$1.5 μM) was added to an anaerobic solution of 20 mM Na-succinate, pH 4.5, containing 60–240 μM CO and $>$100 μM dithionite. Ligand association was followed by the change in the absorbance at 431 nm.

4.2.9 Resonance Raman Spectroscopy

Resonance Raman spectra were measured on 15 μL of each sample sealed in a glass melting-point capillary tube, using a custom McPherson 2061/207 spectrograph (Chelmsford, MA) equipped with a Princeton Instruments LN1100PB liquid-N_2-cooled CCD detector and Kaiser Optical Systems holographic notch filter (Ann Harbor, MI). Excitation light was provided by an Innova 302 krypton laser (413 nm) (Laser Innovations, Moorpark, CA). The laser power at the sample was $\sim$40 mW. Plasma emission lines were removed by an Applied Photophysics prism monochromator (Surrey, UK). Data at room temperature and 90 K were collected in a back-scattering geometry with the sample capillary placed in a copper cold finger. For the 90 K experiments, the capillary was cooled by liquid nitrogen. Spectral data were processed using GRAMS/386 (Thermo-Galactic, Salem, NH) and Origin (Microcal, Northhampton, MA) data analysis programs. Spectra were calibrated against indene as an external standard. Frequencies are estimated to be accurate to $\pm$ 1 cm^{-1}.

4.2.10 Enzyme Assays and Kinetic Procedure

CDH activity was measured using the cyt *c* and DCPIP assay (Chapter 3). The steady-state kinetic parameters for cellobiose oxidation were determined by monitoring ferrocytochrome *c* formation (ϵ_{550} = 28 mM^{-1} cm^{-1}) or DCPIP reduction (ϵ_{515} = 6.8 mM^{-1} cm^{-1}). The assays contained a fixed level of ferricytochrome *c* (12.5 μM) or DCPIP (35 μM) and varying levels of cellobiose (5–200 μM) in 20 mM Na-succinate, pH 4.5. The steady-state kinetics for cyt *c* and DCPIP reduction were determined with a fixed cellobiose concentration (200 μM) and variable cyt *c* and DCPIP concentrations (0.2 to 40 μM).

4.2.11 Potentiometric Titration

Potentiometric titrations were carried out at room temperature in a borosilicate glass cell, similar to that described previously [Dutton, 1978]. The potential was measured with a platinum electrode versus a REF401 calomel electrode (Radiometer analytical, France). All values are expressed with respect to the standard hydrogen electrode (NHE). The electrodes were calibrated against a pH 7 standard solution of quinhydrone (E_m = +293 mV vs. NHE) with a Metrohm 632 pH meter (Metrohm Ltd., Switzerland). The redox midpoint potential was determined in 50 mM Na-succinate, pH 4.5. Redox equilibration between the protein and the electrode was achieved by the use of a mixture of dyes: phenazine methosulfate, phenazine ethosulfate, Fe^{3+}-EDTA, 2-hydoxy-1,4-naphthoquinone, anthraquinone-1,5-disulfonate, anthraquinone-2,6-disulfonate, and/or anthraquinone-2-sulfonate. The redox titration was carried out with stirring of the buffered solution (5.5 ml) containing 5 μM enzyme and the mediator dyes (each 20 μM, except Fe^{3+}-EDTA, 50 μM). Prior to the reductive titration, the solution of enzyme and mediators was flushed with argon. The solution was then allowed to reach equilibrium and the first UV-vis spectrum was recorded on a HP 8353 Diode Array spectrophotometer (Hewlett Packard, Palo Alto, CA). The redox potential of the system was adjusted by the addition of a small volume of 10 or 100 mM dithionite via a Hamilton syringe. After equilibration (constant reading of absorbance and potential), a spectrum was recorded, the potential noted and an additional small volume of dithionite was added. This process was repeated until the enzyme was completely reduced. The oxidative titration was carried out by the addition of small amounts of air to the cell, followed by flushing with argon. The system was allowed to equilibrate, a spectrum was recorded, and the potential noted. This procedure was repeated until the enzyme was completely oxidized. The redox state of the heme in CDH was determined from the α band of the heme *b*: 562 nm for rCDH and 560 nm for M65H variant. The absorbance at this wavelength, corrected for the absorbance at 800 nm, was plotted against the potential of the system. The graph was fitted against the Nernst equation to obtain the redox midpoint potential E_m. The Nernst plot for both oxidative and reductive titration showed no hysteresis, implying that the system was at equilibrium.

4.2.12 Protein Preparation for Crystallization

The M65H variant was cleaved proteolytically with papain to yield distinct cytochrome and flavin fragments as described previously [Henriksson et al., 1991; Cohen et al., 1997]. The fragments were fractionated on a MonoQ HR 5/5 anion exchanger in 20 mM Tris-HCl, pH 8.0, using a linear NaCl gradient (0 to 1 M), followed by re-fractionation of the samples containing CYT_{M65H} at pH 4.2, using a linear Na-acetate gradient (50 mM to 1 M). Crystals of CYT_{M65H} were grown at room temperature using the hanging-drop vapor-diffusion method [McPherson, 1982]. Hanging drops were prepared by mixing equal volumes of protein solution (3 mg/ml) and reservoir. The reservoir contained 30% (w/v) polyethylene glycol 4000, 5% (v/v) 2-methyl 2,4-pentanediol, 100 mM HEPES, pH 7.5 and 10 mM $CaCl_2$. Crystals appeared as red hexagonal rods of space group $P6_5$ with cell constants $a = b = 139.0$ Å and $c = 52.67$ Å and with two molecules in the asymmetric unit.

4.2.13 X-ray Crystallographic Data Collection and Refinement

Data were collected at 100 K using synchrotron radiation (source ID14-EH4, ESRF, Grenoble, France, $\lambda = 0.9763$ Å). Data reduction and scaling were carried out using MOSFLM [Powell, 1999] and SCALA [Evans, 1993], respectively. The previously reported structure of the *P. chrysosporium* CDH cytochrome domain at 1.9 Å resolution (PDB ID code 1D7C) [Hallberg et al., 2000] was used as a starting model for crystallographic refinement against CYT_{M65H} amplitudes. Initial refinement and manual model building were performed with the programs CNS [Brunger et al., 1998] and O [Jones et al., 1991], respectively. Final refinement was done with REFMAC5 [Murshudov et al., 1997] at 1.9 Å resolution, using anisotropic scaling, hydrogens in their riding positions, and atomic displacement parameter refinement, using the "translation, libration, screw-rotation" (TLS) model. The two non-crystallographically related molecules were defined as rigid bodies during TLS refinement. All least-squares planes and angles between normals and least-squares planes were calculated, using the program MOLEMAN2 [Kleywegt, 2000].

4.3 RESULTS

4.3.1 Expression and Purification of the M65H Variant

The M65H mutation was verified by DNA sequencing. Transformation of the Ura$^-$ strain (Ura11) with linearized pM65H resulted in the isolation of several prototrophic transformants. Each was grown in liquid, HCHN cultures, conditions under which endogenous wild-type CDH is not expressed [Li et al., 1996; Li et al., 2000]. The extracellular medium was monitored for CDH activity, using the cyt *c* and DCPIP reduction assays. Several transformants exhibited significant DCPIP reduction activity, but none efficiently reduced cyt *c*. The transformant exhibiting the highest DCPIP activity was purified by fruiting and isolating single basidiospore derived colonies [Alic et al., 1989; Alic et al., 1991]. The purified transformant was incubated at 37°C in HCHN medium for 7 days. The amount of protein secreted was ~50% of rCDH cultures, based on the DCPIP reduction assay. Western-blot analysis of the extracellular medium over the 7-day-old culture period indicated the presence of 90 kDa CDH-like protein. The M65H protein was purified to homogeneity by cellulose affinity chromatography and gel-filtration. The R_z value (A_{411}/A_{280}) was 0.77 and the extinction coefficient of the Soret maximum at 411 nm was 133 mM^{-1} cm^{-1}.

4.3.2 Steady-State Kinetics

Measuring CDH activity in the extracellular medium of M65H transformants suggested that the cytochrome variant efficiently reduced DCPIP, but its ability to reduce cyt *c* was impaired significantly. Under steady-state conditions, linear double-reciprocal plots were obtained in 20 mM Na-succinate, pH 4.5, for the purified variant and the rCDH protein. The apparent K_m values for cellobiose and DCPIP and k_{cat} values for cellobiose oxidation and DCPIP reduction were similar for both CDH proteins (Table 4.1). However, the specific activity for cyt *c* reduction by the M65H variant was approximately 100-fold lower (Table 4.1).

Table 4.1

Steady-State Parameters for rCDH and M65H Variant at pH 4.5[a]

Enzyme	Cellobiose oxidation (DCPIP)			DCPIP reduction		
	k_{cat} (s^{-1})	K_m (μM)	k_{cat}/K_m (M^{-1} s^{-1})	k_{cat} (s^{-1})	K_m (μM)	k_{cat}/K_m (M^{-1} s^{-1})
rCDH	25.7	40	$6.4 \cdot 10^5$	27.0	6.4	$4.2 \cdot 10^6$
M65H	26.0	35	$7.6 \cdot 10^5$	25.0	7.4	$3.4 \cdot 10^6$
Enzyme	Cellobiose oxidation (cyt *c*)			Cyt *c* reduction		
	k_{cat} (s^{-1})	K_m (μM)	k_{cat}/K_m (M^{-1} s^{-1})	k_{cat} (s^{-1})	K_m (μM)	k_{cat}/K_m (M^{-1} s^{-1})
rCDH	10.5	18	$5.8 \cdot 10^5$	10.8	0.8	$1.4 \cdot 10^7$
M65H	0.1	NA[b]	NA	0.1	NA	NA

[a] Reactions were performed in 20 mM Na-succinate, pH 4.5. K_m and k_{cat} for cellobiose were determined using 40 μM DCPIP or 10 μM cyt *c*. K_m and k_{cat} for DCPIP and cyt *c* were determined using 200 μM cellobiose.

[b] NA = not applicable.

4.3.3 UV-Vis Spectrocopy of rCDH and the M65H Variant

The electronic absorption spectra for both rCDH and the M65H variant were dominated by the heme *b* spectrum, with a weak absorbance near 450 nm from the flavin. The ferric heme spectrum of rCDH was typical for a low spin (LS) heme iron, with a Soret maximum at 421 nm and visible bands at 530 and 570 nm (Fig. 4.1A, Table 4.2). The M65H substitution altered the optical properties of the ferric heme, giving rise to a spectrum that contained a mixture of LS and high-spin (HS) protoheme iron signals (Fig. 4.1A, Table 4.2). Moreover, the Soret band was blue-shifted to 411 nm in the variant, and the band at 730 nm, characteristic of a Met-Fe ligation [Moore and Pettigrew, 1990], disappeared. A weak band indicative of a HS species in the ferric state was introduced at 630 nm. The analysis of possible heme absorbances near 500 nm was compromised by the flavin absorbance. Therefore, the truncated cytochrome domain was obtained by limited proteolysis, and the resulting electronic absorption spectrum showed a maximum at 495 and shoulders at 530 and 560 nm (Fig. 4.1A). As was observed with rCDH, the ferric heme in M65H was unreactive with both cyanide and imidazole (50 mM).

The optical properties of the dithionite-reduced recombinant wild-type and variant CDHs were similar and were typical of a LS ferrous heme. The main differences were (i) the intensity of the absorptions, and (ii) small blue-shifted α and β bands in the variant (Fig. 4.1B and Table 4.2). Cellobiose rapidly reduced both the flavin and heme in the wild-type enzyme. Addition of a large excess of cellobiose to M65H variant appeared to reduce the flavin completely, whereas the heme iron was only partially reduced (Fig. 4.2A). The extent of reduction of the heme was approximately 20% (Fig. 4.1B). Under anaerobic conditions, a 90% reduction of the heme was observed within 45 min. The ferrous wild-type *b*-heme did not bind CO, whereas the variant forms a ferrous-CO complex, exhibiting a Soret maximum at 425 nm, and α and β bands at 540 and 572 nm, respectively (Fig. 4.2A). However, Fe^{2+}-CO complex formation was slow and could be monitored on a conventional spectrophotometer. The observed time courses were dominated by a single-exponential process (Fig. 4.2B) and were linearly dependent on the ligand

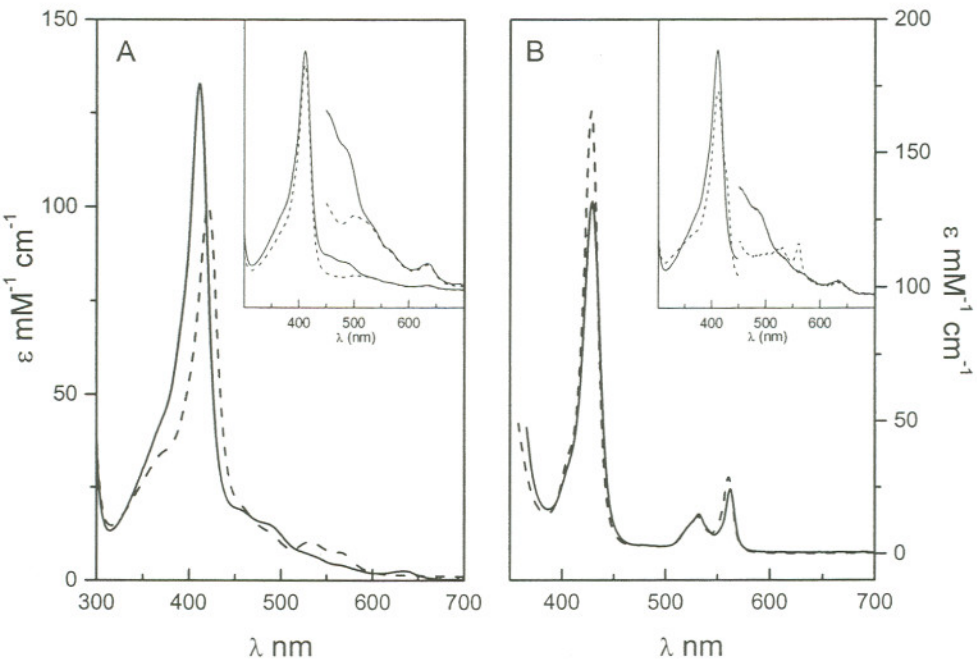

Fig. 4.1 Electronic absorption spectra of wild-type rCDH (---) and the M65H variant (—) in 20 mM Na-succinate, pH 4.5. (**A**) Oxidized and (**B**) reduced with dithionite. *Insert A:* Oxidized M65H variant, flavocytochrome (—), cytochrome domain (---); *Insert B:* M65H variant, oxidized (—), reduced with 200 μM cellobiose under aerobic conditions (---).

Table 4.2

Spectral Features and Heme Redox Midpoint Potentials for rCDH, Its M65H Variant and Selected Heme Proteins with Histidine Ligation

Protein	Oxidized	Reduced	E_m
rCDH	421 530 570	429 532 562[a]	+164
rCDH (cyt domain)	421 530 570	429 532 562[a]	+161
M65H	411 530560 630	428 530 560[a]	-53
M65H (cyt domain)	411 495 530 560 630	428 530 560[a]	ND[b]
cytochrome b_5[c]	413 532 560	423 526 556	+4
cytochrome b_{562}[d]	418 529 558	427 531 562	+167
HRP[e]	403 500 641	437 556	
MetMb[f]	410 505 635	434 556	+61

[a] Addition of 400 μM cellobiose (rCDH) or grain of dithionite (rCDH, M65H, cytochrome domains).

[b] ND = not determined.

[c] UV-vis from Ozols and Strittmatter [1964]; redox potential from Reid et al. [1982].

[d] UV-vis from Itagaki and Hager [1966]; redox potential from Moore et al. [1985].

[e] UV-vis from Tamura et al. [1972].

[f] UV-vis from Antonini and Brunori [1971]; redox potential from Lloyd et al. [1995].

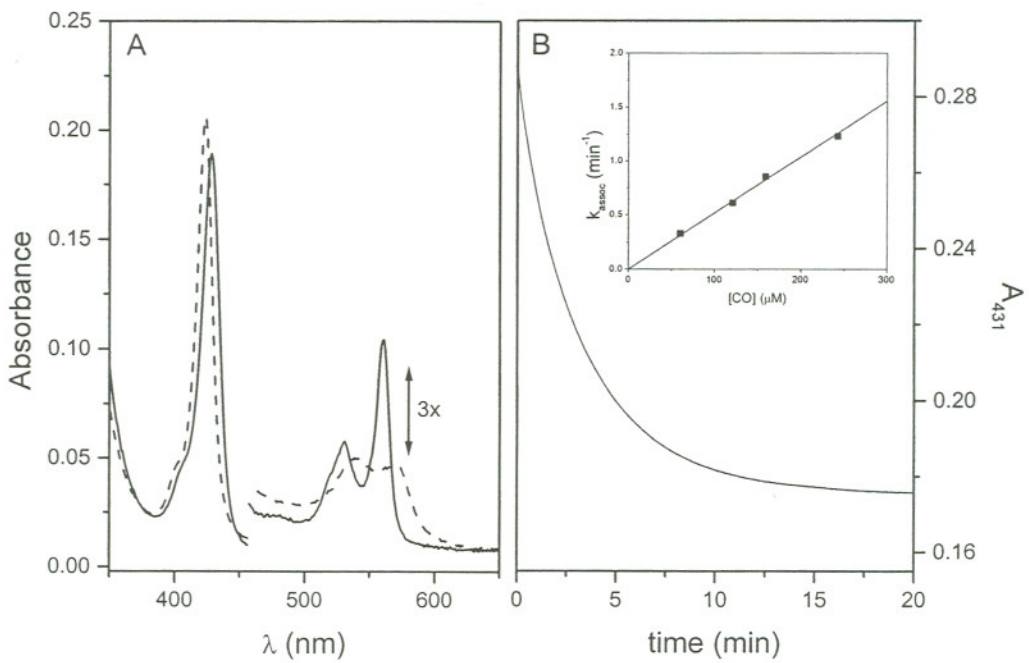

Fig. 4.2 Electronic absorption spectra of M65H variant ($\sim 1.5\ \mu$M) in 20 mM Na-succinate, pH 4.5. (**A**) Reduced with cellobiose (—), Fe^{2+}-CO complex (---) under anaerobic conditions. (**B**) Kinetic trace and fit for conversion of ferrous M65H variant to ferrous-CO complex in the presence of 60 μM CO. *Insert B:* Observed rate of association of CO to the ferrous M65 variant in 20 mM Na-succinate, pH 4.5, at room temperature.

concentration from 60 to 240 μM (insert Fig. 4.2B). The small association rate constant was calculated to be 8.6×10^{-5} μM^{-1} s^{-1}.

4.3.4 Resonance Raman Spectroscopy

To further investigate the coordination and spin states in wild-type CDH and the M65H variant, resonance Raman (RR) high-frequency spectra were obtained, using Soret excitation (Fig. 4.3 and 4.4; Table 4.3). The spectral data of rCDH were similar to those reported for the wild-type CDH [Cohen et al., 1997]. The oxidation marker ν_4 was observed at 1371 cm^{-1} in both enzymes (Fig. 4.3), indicating a ferric heme. In the case of rCDH, the core-size marker bands ν_2 and ν_3 at 1575 and 1505 cm^{-1}, respectively, identified the ferric heme as a 6-coordinated LS (6cLS) heme species [Spiro and Li, 1988]. Essentially identical RR data were obtained with the truncated heme domain with only minor chances, attributed to contribution from the flavin cofactor [Cohen et al., 1997]. In the M65H variant, ν_3 was observed at 1480 cm^{-1}, indicating 6cHS heme species [Spiro and Li, 1988]. Weak shoulders at 1638 (ν_{10}) and at 1505 cm^{-1} (ν_3) reflected the presence of a minor population of 6cLS heme. The LS ν_3 band was obscured by a band at 1515 cm^{-1} assigned as ν38 [Spiro and Li, 1988]. By lowering the temperature to 90 K, both enzymes exhibited similar RR spectra, with ν_2, ν_3 and ν_{10} at 1577, 1507 and 1642 cm^{-1} respectively, characteristic of a 6cLS heme. The electronic absorption spectra of the reduced CDH proteins (Fig. 4.1B) were both indicative of a 6cLS system and the RR spectra supported this conclusion, with ν_2 and ν_3 at 1580 and 1494 cm^{-1} respectively for both CDH proteins (Table 4.3).

4.3.5 Optical Potentiometric Titration

The redox potentials of the heme prosthetic group were obtained by optical potentiometric titration. The extent of reduction of the heme could readily be determined from the α bands, a wavelength where the absorbances of the flavin cofactor and the redox mediators were negligible. The heme in the holo-wild-type enzyme and its truncated heme domain exhibited a similar redox potential at pH 4.5 (+164 mV vs. NHE, Fig. 4.5, Table 4.2). This value was in close agreement with

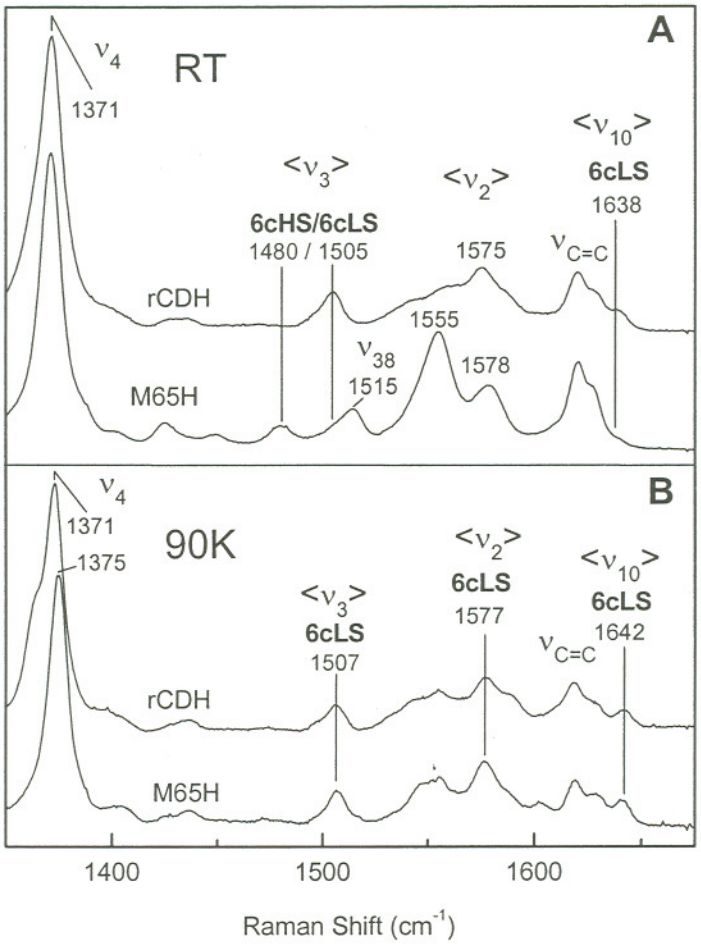

Fig. 4.3 High frequency RR spectra of the oxidized rCDH and the M65H variant, obtained at room temperature (**A**) and 90 K (**B**), with Soret excitation (413 nm) in 20 mM Na-succinate, pH 4.5. HS, high spin; LS, low spin; 6c, 6-coordinate.

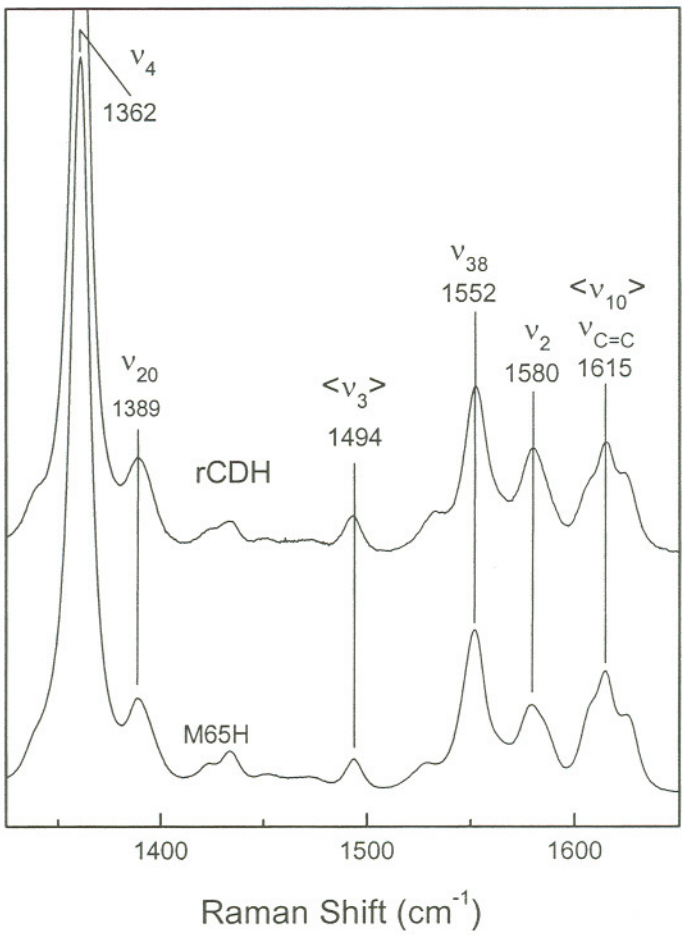

Fig. 4.4 High frequency RR spectra of the reduced CDH and the M65H variant, obtained at room temperature, with Soret excitation (413 nm) in 20 mM Na-succinate, pH 4.5.

Table 4.3

High Frequency Resonance Raman Vibration Modes

Enzyme	T(K)	ν_4	ν_3	ν_2	ν_{10}
Ferric rCDH	295	1371	1505	1575	1638
	90	1371	1507	1577	1642
Ferric M65H	295	1371	1480	1555/1578	1621
	90	1375	1507	1577	1642
Ferric cyt b_5[a]		1373	1502	1579	1640
Myoglobin[b]		1373	1483	1563	1621
Ferrous rCDH	295	1362	1494	1580	1615
Ferrous M65H	90	1362	1494	1580	1615
Ferrous cyt b_5[a]		1359	1493	1584	1615

[a] From Choi et al. [1982].

[b] From Spiro et al. [1979].

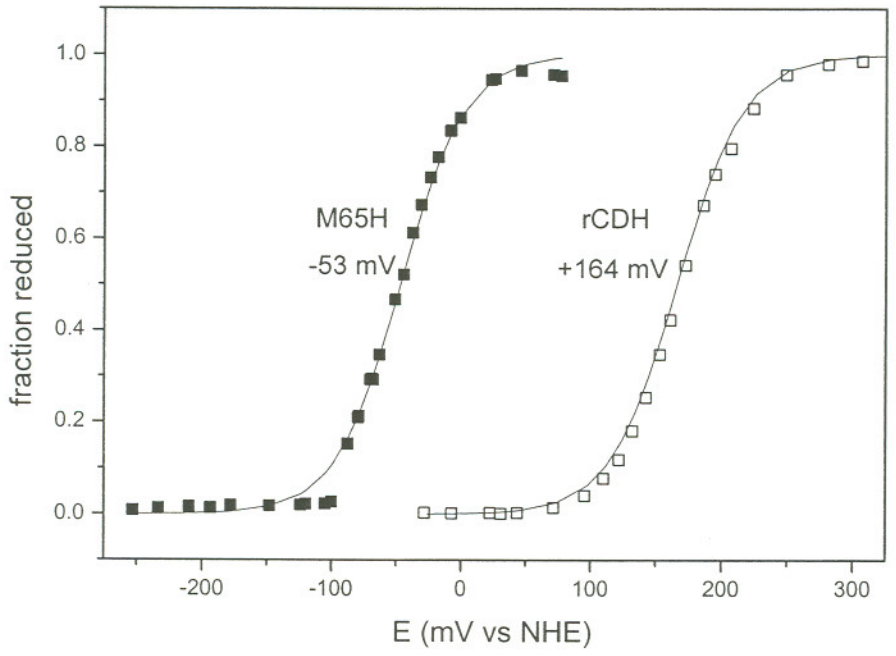

Fig. 4.5 Oxidative redox titrations of rCDH (□) and M65H CDH variant (■). Optical potentiometric titrations were performed at pH 4.5, as described in Section 4.2.

previous electrochemical measurements of native CDH [Kremer and Wood, 1992] and its truncated heme domain [Igarashi et al., 1999] and similar to the value of the heme group in cytochrome b_{562} [Moore et al., 1985], a second example of a *b*-type heme with a Met-His coordination. Substitution of Met 65 by histidine resulted in a 210 mV drop to –53 mV (Fig. 4.5, Table 4.2). This value was in the range for *bis*-histidyl cytochromes, such as cytochrome b_5 [Reid et al., 1982].

4.3.6 Overall Structure of CYT_{M65H}

Data collection and model refinement statistics to 1.9 Å resolution are summarized in Table 4.4. The final model contained two protein molecules (residues 1–186), 336 water molecules, six cadmium ions, two protoheme groups, one polyethylene glycol molecule (modeled as $C_{11}O_6$), and two *N*-linked carbohydrate chains at Asn111, each with two *N*-acetyl glucosamine residues. This model had *R* and R_{free} values of 0.17 and 0.20, respectively. The CYT_{M65H} structure was similar to that of the wild-type (Fig. 1.9) with rmsd values of 0.20 Å for 186 C^{α} atoms, and 0.28 Å for all atoms in the residue zone 1 to 186. The electron density for the CYT_{M65H} molecule was of good quality (Fig. 4.6A), and the only region with less well-ordered electron density was found in a loop, composed of residues 36 to 39 in one of the non-crystallographically related molecules (molecule A). Compared with the wild-type CDH cytochrome (Fig 1.9), differences in the protein occurred, as expected, exclusively in close proximity to the substitution site (Fig. 4.6B). Local protein backbone displacements of 0.5 to 0.6 Å occurred at residues 63 to 65, and of 0.5 to 0.7 Å at residues 87 to 90. In the wild-type cytochrome, Tyr90 was positioned close to the heme-ligating residue Met65, and the Tyr90 hydroxyl group formed a hydrogen bond to the D-propionate side chain of the protoheme. To accommodate the bulkier histidyl imidazole ring at position 65, the backbone of Tyr90 was displaced by 0.6 Å away from the protoporhyrin ring (Fig. 4.6B). At position 87, the backbone was displaced by 0.5 Å due to steric hindrance between the C^{β} atom of Ala87 and the imidazole ring of His65. However, the His65 backbone moved closer to the protoporphyrin ring by 0.7 to 0.8 Å.

Table 4.4

Statistics for X-ray Crystallographic Data Collection and Refinement

Data collection[a]	
Resolution (Å) full range / outer shell	48–1.90 / 2.00–1.90
Observations (measured/unique)	256,083 / 45,850
Multiplicity	5.6 (4.9)
Completeness (%)	99.4 (97.5)
$<I / \sigma(I)>$	5.0 (1.1)
R_{merge}[b] (%)	11.3 (57.5)
Refinement	
Resolution range (Å)	28–1.90
Completeness for range (%)	99.2
R_{factor}[c] / number of reflections (work)	0.173 / 43,870
R_{free} / number of reflections (free)	0.198 / 1,852
Number of non-hydrogen atoms	3,341
Mean B values (Å^2) protein all atoms (A/B)	26.1 / 30.4
Rmsd bond lengths (Å) / angles (°)	0.019 / 1.73
Ramachandran plot outliers[d] (%)	2.1

[a] The outer shell statistics using 5% of the reflections are in soft brackets.

[b] $R_{merge} = [\ \Sigma_{hkl}\ \Sigma_i\ |I-<I>|\ /\Sigma_{hkl}\ \Sigma_i\ |I|\ ] \times 100\%$.

[c] $R_{factor} = \Sigma_{hkl}\ |\ |F_o|-|F_c|\ |\ /\ \Sigma_{hkl}\ |F_o|$

[d] Percentage of residues that fall outside core regions of the Ramachandran plot [Ramakrishnan and Ramachandran, 1965] as defined by Kleywegt and Jones [1996].

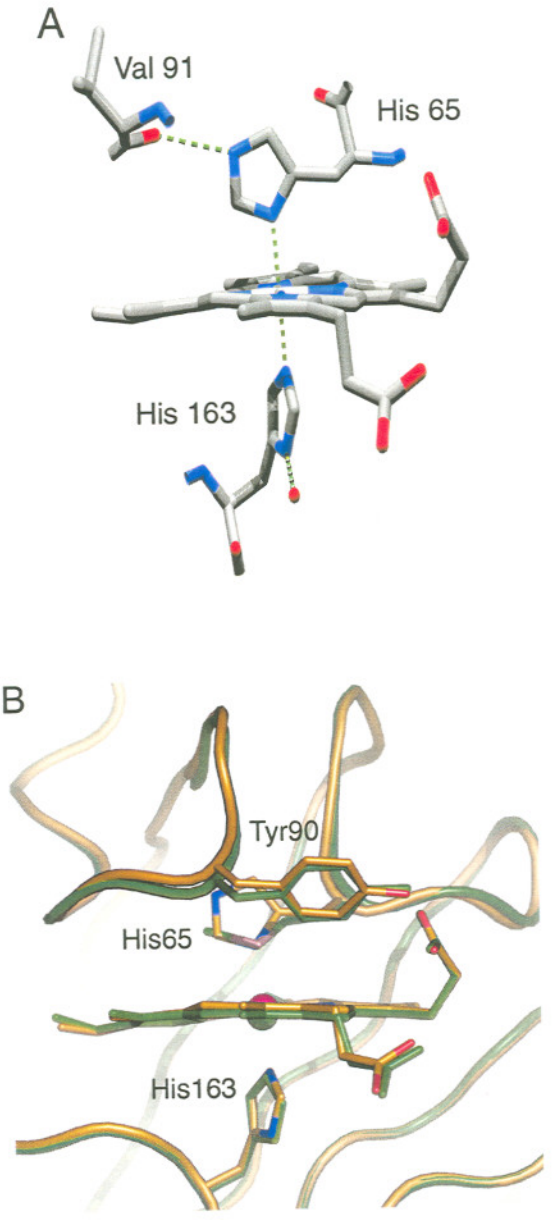

Fig. 4.6 (**A**) The axial ligation in the M65H variant. The 6-coordinated heme iron is ligated by His65 $N^{\delta 1}$ and His163 $N^{\delta 2}$. (**B**) Superposition of the M65H variant (green) and wild-type (golden) heme-binding pocket (PDB ID code 1D7C, Fig. 1.9) [Hallberg et al., 2000]. The drawings were made with the program Pymol (official URL, http://pymol.sourceforge.net) or POV-ray (official URL, http://www.povray.org).

4.3.7 Structural Details of the Heme-Binding Site

Wild-type CDH features an unusual type of protoheme ligation (Fig 1.9): Met65-His163 with the plane defined by the methionine CH_3-S-CH_2 group almost perpendicular (100°) to the plane of the histidyl imidazole ring. Introducing a histidine residue at position 65 in CYT_{M65H}, resulted in a histidine side chain conformation similar to that of the original methionine (Fig. 4.6B). In this conformation, the $N^{\delta 1}$ atom of His65 was suitably positioned to ligate the heme iron. Given the backbone conformation at residue 65, ligation through the histidyl $N^{\epsilon 2}$ was highly unlikely. The Fe-His65 $N^{\delta 1}$ bond (2.1 Å) was shorter than the wild-type Fe-Met65 S^{γ} bond (2.3 Å), whereas the length of the Fe-His163 $N^{\epsilon 2}$ bond remained unchanged (2.1 Å). The His65 χ^1 torsion angle assumed favorable values of 180.0°/181.5° (mol A/B; trans); whereas those of His163 deviated significantly from ideal values: χ^1 of 34.5°/32.6° (mol A/B; gauche$^-$). This unfavorable configuration is however also observed in the wild-type structure (Fig 1.9) [Hallberg et al., 2000]. The χ^2 values were 103°/98° (mol A/B) for His65, and 72°/74° (mol A/B) for His163.

The angle between the normals to the planes of the two histidyl imidazole rings was slightly larger, 114°/118° (mol A/B) than the angle between Met65 CH_3-S-CH_2 and the His163 imidazole ring ($\sim$100°) in the wild-type; thus deviating further from a perpendicular arrangement in the variant. The orientation of the His65 imidazole ring was further stabilized by a hydrogen bond formed between His65 $N^{\epsilon 2}$ and the main-chain carbonyl oxygen of Val91. In both wild-type and variant, the protoporphyrin ring adopted a nearly planar conformation ($\sim$170°; corresponding to the angle between the normals to the two planes defined by pyrrole atoms C2A-C3D-C4A-C1D and C1B-C4C-C3B-C2C, respectively).

4.4 DISCUSSION

4.4.1 Axial Coordination in the M65H Variant

The CYT_{M65H} structure was determined at 100 K, and the coordination of the protoheme Fe^{2+} is stably 6-coordinated by the two His ligands, His65 and His163,

and the four pyrrole nitrogens (Fig. 4.6). The Fe-N(His) distances and the angles defined by N(His)-Fe-N(pyrrole) are typical for *bis*-histidyl ligated cytochromes, 2.1 Å and ~90°, respectively. A unique feature of the axial coordination is the Fe-His65-$N^{\delta 1}$ bond. Although histidyl $N^{\delta 1}$ ligation occur in non-heme iron and copper complexes, it is rarely encountered in heme proteins. Indeed, the only previous example of heme-Fe ligation through a histidyl $N^{\delta 1}$ is that of the *c*-type, LS Heme-1 in the tetra-heme cytochrome c_{554} (cyt c_{554}) from the bacterium *Nitrosomonas europaea* [Iverson et al., 1998]. The structure of cyt c_{554} has been determined in the reduced form at 1.6 Å resolution, and in the oxidized form at 1.8 Å resolution, PDB ID codes 1FT5 and 1FT6, respectively [Iverson et al., 2001], and the structure of the Heme-1 site is essentially identical in the two oxidation states. The cyt c_{554} Heme-1 is coordinated by His102 $N^{\delta 1}$ and His15 $N^{\epsilon 2}$. In addition, on the His $N^{\epsilon 2}$ side of the porphyrin ring, a common C-x-y-C-H motif covalently attaches the heme to the protein through Cys11 and Cys14. The heme-binding sites in CYT_{M65H} and cyt c_{554} (Heme-1) are very similar: the histidine residues have favorable side-chain torsion angles, the length of the Fe-His $N^{\delta 1}$ bonds are identical (2.1 Å), and the angle to the normals of the planes is nearly perpendicular. The orientation of the His102 imidazole ring in cyt c_{554} is stabilized by a hydrogen bond between His102 $N^{\epsilon 2}$ and Gln126 $O^{\epsilon 1}$, equivalent to the hydrogen bond between His65 $N^{\epsilon 2}$ and the main-chain carbonyl oxygen of Val91 in CYT_{M65H}.

The rearrangements in CDH Met65His occur, not unexpectedly, at the His65 site of the heme-binding pocket. This site is formed by two loops: residues 61-69 (loop A) and 87-93 (loop C). In order to accommodate the bulkier histidine side chain at position 65 and to properly orient its $N^{\delta 1}$ atom for ligation ($\angle N^{\epsilon 2}$-Fe-$N^{\delta 1}$ ~180°), minor backbone displacements of 0.5 to 0.7 Å are required in loop A and at Tyr90 in the adjacent C-loop (Fig. 4.6A), indicating that these loops have a degree of conformational freedom. The dense packing around His65 and the hydrogen bond between His65 $N^{\epsilon 2}$ and Val91 O may stabilize this alternative coordination. In addition, an extended hydrogen bonding network is present within the backbone of loop A, and between the Tyr90 hydroxyl group and the D-propionate carboxylic acid group. The displacement of backbone atoms may introduce main-chain strain that

cause the observed thermally induced spin state transition and the binding of carbon monoxide (see below).

4.4.2 Spectroscopic Studies

The electronic absorption and RR spectra of the ferrous M65H variant (Fig. 4.1, Table 4.3) confirm a *bis*-histidyl coordination at room temperature, deduced from the cryogenic tertiary structure of ferrous CYT_{M65H}. The cryogenic RR spectrum of the variant in the ferric state is also indicative of 6cLS heme species (Fig. 4.3), thus it is likely that both histidines are coordinated to the heme iron, as is displayed by the ferrous CYT_{M65H} structure. At ambient temperature, however, the ferric heme undergoes a spin state conversion to a predominantly 6cHS species. This suggests coordination of a water molecule, implying replacement of the histidine ligand upon oxidation, or conversion to a HS histidine residue. Although the room temperature data cannot rule out a His/aquo coordination, considering the *bis*-histidyl coordination in the ferrous state, as well as the slow formation of a Fe^{2+}-CO adduct (see below), we favor a model where both histidines, His65 and His163, coordinate to the heme iron in both ferric and ferrous state. In support, redox state dependent, thermally induced spin state transitions have been previously observed in a variant of myoglobin (Mb), Mb-H64V/V68H [Qin et al., 1994; Dou et al., 1995], which contained an engineered *bis*-histidyl heme. The 30% population of the ferric HS state at ambient temperature was attributed to a weaker ligand field, the result of a tilted His68 [Qin et al., 1994; Dou et al., 1995] and a longer Fe-imidazole $N^{\epsilon 2}$ bond [Dou et al., 1995]. The weakened *bis*-histidyl ligation is not obvious in the tertiary structure of CYT_{M65H}; however, it may arise from a strained backbone, the alteration in the proper axial coordination an/or heme-ring distortion.

4.4.3 Heme Reactivity

The M65H mutation results in a marked decrease in catalytic reactivity, *i.e.*,a significantly reduced rate for inter-domain electron transfer (ET) (Fig. 4.1B), as well as negligible cyt *c* reductase activity (Table 4.1). The drop in the redox potential by 210 mV for the heme in the M65H variant (Fig.4.4, Table 4.3) is a likely

explanation, lowering the thermodynamic driving force for ET between the flavin and cytochrome domain in the M65H variant. On the basis of earlier work [Harbury et al., 1965], it was estimated that histidine versus methionine ligation should account for a redox potential difference of 160–168 mV [Moore and Pettigrew, 1990], close to that we observe. Previous mutant studies in horse heart cyt *c* [Raphael and Gray, 1989], *Rhodobacter capsulatus* cytochrome c_1 heme [Darrouzet et al., 1999], *Pseudomonas* cytochrome c_{551} [Miller et al., 2000] and cytochrome c_{555} from *Aquifex aeolicus* [Aubert et al., 2001] demonstrated that a substitution of an axially ligated methionine by a histidine can lower the heme redox midpoint potential by 200 to 400 mV. Other factors, such as the dielectric constant, the hydrogen bonding network, and electrostatic interactions also modulate the redox properties of a heme group [Gunner et al., 1997]. Thus the range indicates that other modifications can occur in the heme-binding pocket upon a change in ligands.

A second factor, possibly responsible for the low rate of electron transfer to cytochrome *c*, is the difference in spin states for the ferric and ferrous M65H heme iron. To lower the reorganizational energy, thus facilitating ET, cytochromes invariably contain a strongly ligated heme iron that is LS in both redox states. The spin-state conversions of the heme iron during the catalytic cycle of the M65H variant will likely impair electron transfer between the redox groups. The residual cyt *c* activity is also similar to the activity of the truncated flavin domain [Henriksson et al., 1993], possibly suggesting a weak direct flavin-to-cyt *c* electron-transfer pathway, rather than via the heme domain.

With the drop in the redox potential, the reactivity of the heme iron atom with carbon monoxide is an added feature of variants of cytochromes with a substitution of an axially ligated methionine by a histidine. For CO to bind to either side of the iron, significant rotation about the χ^1 of the axial ligands is likely needed as well as backbone shifts. Indeed, the M65H variant exhibits an unusual low CO association rate of 8.6×10^{-5} μM^{-1} s^{-1} (Fig. 4.2B), a value $\sim$10,000-fold lower than that for Mb [Dou et al., 1995] or 20-fold lower than that for the heme based oxygen sensor Dos [Delgado-Nixon et al., 2000]. The sensor protein requires the displacement of the endogenous methionine ligand upon binding of CO and other gaseous molecules

[Gonzalez et al., 2002]. The CO association rate for the M65H variant reflects the displacement of a histidine ligand and possibly the rearrangement of the backbone. Considering the inability of rCDH to bind CO and the absence of any structural changes around His163 due to the M65H substitution (Fig. 4.6), we favor His65 as the CO binding site.

4.5 CONCLUSIONS

The M65H variant of the flavocytochrome CDH displays a novel *bis*-histidyl coordination to heme *b* iron, involving the $N^{\delta 1}$ nitrogen atom of His65 and $N^{\epsilon 2}$ nitrogen atom of His163. As expected, flavin reactivity is retained, but flavin-to-heme ET is essentially abolished, most likely owing to a decrease in the redox potential of the protoheme cofactor. The spin state of the heme iron is dependent on temperature as well as redox state, but both histidines remain coordinated in the absence of exogeneous ligands. In contrast to the wild-type protein, the heme iron binds CO, which apparently replaces His65. Finally, the tertiary structures of the M65H cytochrome and the Heme-1 site in cyt c_{554} indicate that an iron $N^{\epsilon 2}/N^{\delta 1}$ coordination is *a priori* neither sterically nor energetically unfavorable [Moore and Pettigrew, 1990; Zaric et al., 2001]. However, restraints on the heme-ligand orientation and backbone conformation may aggravate fine-tuning of the microenvironment around the heme, constituting a possible bottleneck for heme-iron-$N^{\delta 1}$ ligation. Thus, this may have resulted in a strong preference for ligation through His $N^{\epsilon 2}$, as is observed in almost all heme proteins examined to date.

CHAPTER 5

ROLE OF THE FLAVIN DOMAIN RESIDUES, HIS689 AND ASN732, IN THE CATALYTIC MECHANISM OF CELLOBIOSE DEHYDROGENASE FROM *PHANEROCHAETE CHRYSOSPORIUM*[*]

5.1 INTRODUCTION

Cellobiose dehydrogenase (CDH) is a unique extracellular flavocytochrome, purified from several filamentous fungi [Henriksson et al., 2000] of which the enzyme from *P. chrysosporium* is the best studied [Ayers et al., 1978; Morpeth, 1985; Bao et al., 1993]. Two cofactors, a flavin adenine dinucleotide (FAD) and a protoporphyrin IX, are non-covalently bound to two distinct domains of the single polypeptide chain, and the two domains are connected by a heavily glycosylated, hydroxyamino-rich linker peptide [Henriksson et al., 1991; Habu et al., 1993; Li et al., 1996]. The flavin domain is involved in the oxidation of cellobiose and other soluble oligosaccharides, such as cellotriose, cellotetraose and lactose, to their corresponding lactones [Samejima and Eriksson, 1992]. The 1β-hydroxyl of the reducing end of the substrate is oxidized [Higham et al., 1994] with concomitant reduction of FAD, and the electrons are subsequently transferred directly to two electron acceptors such as 2,6-dichlorophenol-indophenol (DCPIP) or, via the heme domain, to one-electron acceptors such as cytochrome *c* [Henriksson et al., 2000].

Based on gene sequence comparisons, the flavin domain of CDH (CDH_{DH}) was predicted to be a member of the glucose-methanol-choline (GMC) family [Raices et

---

[*] This material has been published in this or similar form in *Biochemistry* and is used here with permission of the American Chemical Society.

Rotsaert, F. A. J., Renganathan, V., and Gold, M. H. (2003) Role of the flavin domain residues, His 689 and Asn732, in the catalytic mechanism of cellobiose dehydrogenase from *Phanerochaete chrysosporium*. *Biochemistry* **42**:4049–4056.

al., 1995; Li et al., 1996], which includes methanol oxidase, cholesterol oxidase (CHO), glucose oxidase (GOX) and choline dehydrogenase [Cavener, 1992; Kiess et al., 1998]. These FAD-dependent oxidoreductases catalyze the oxidation of a diverse group of non-activated alcohols, and their main consensus sequences include the FAD binding domain. The tertiary structures of CDH_{DH} (Fig. 1.10) [Hallberg et al., 2002], GOX [Wohlfahrt et al., 1999] and CHO [Vrielink et al., 1991; Li et al., 1993] reveal a highly conserved catalytic site, containing two conserved residues, a His and an Asn or His, which are located in the structurally conserved C-terminal region. In the CDH_{DH} crystal structure, these residues, His689 and Asn732, are positioned near the isoalloxazine ring (Fig. 1.10). Conservation of the position of these residues in GMC proteins suggests a similar activation mechanism for oxidation of the substrate.

Molecular modeling has identified several possible interactions between cellobiose and the protein, which provide insights into catalysis and substrate binding [Hallberg et al., 2002]. The channel from the surface to the catalytic site accommodates a cellobiose molecule, and an active-site water (Fig. 1.10) is replaced by the anomeric β-hydroxyl CO1. In addition, the anomeric α-hydrogen CH1 of cellobiose is oriented towards the FAD-N5. His689 is the only basic residue near the β-hydroxyl of cellobiose, and the orientation of His689 suggests that it may act as a general base. Hydrogen bonding of Asn732 with the anomeric hydroxyl suggests that this residue may contribute to binding of the substrate.

In this study, we assess the roles of His689 and Asn732 in binding and oxidation of the substrates, cellobiose and lactose, using site-directed mutagenesis and steady-state kinetic measurements. In addition, we investigate the effect of the mutations on the electronic properties of the flavin cofactor.

5.2 MATERIAL AND METHODS

5.2.1 Organisms

Growth and maintenance of the *Phanerochaete chrysosporium* auxotrophic strain OGC316-7 (Ura11) and prototrophic transformants were as described [Akileswaran et al., 1993]. *Escherichia coli* DH5α was used for subcloning plasmids.

5.2.2 Construction of the Mutant Plasmids

The site-directed mutations at the Asn732 position (N732H/Q/A/E/D) were introduced into pUGC1 (Fig. 3.1), which contains 1.1 kb of the *gpd* gene promoter, fused to the *P. chrysosporium cdh-1* coding region (3.1 kb), using the Transform™ site-directed mutagenesis kit (BD Biosciences, Palo Alto, CA). A mutagenic primer introduced the N732 mutations, changing the AAC codon (Asn) to CAC (His), CAG (Gln), GCT (Ala), GTC (Val), GAG (Glu), or GAC (Asp). The mutant plasmids were isolated and the mutation was confirmed by dideoxy sequencing (Oregon National Primate Research Center, Beaverton, OR). A protocol, similar to that described above, was used to create site-directed mutations at the His689 position (H689N/Q/A/E/V).

5.2.3 DNA Transformation of *P. chrysosporium*

Protoplasts of *P. chrysosporium* OGC316-7 (Ura11) were prepared as described [Akileswaran et al., 1993; Sollewijn Gelpke et al., 1999], transformed with *Eco*RI-linearized mutant plasmids (2 μg), and potential transformants were screened for uracil prototrophy [Akileswaran et al., 1993; Sollewijn Gelpke et al., 1999]. Subsequently, conidia from prototrophs were transferred to high carbon-high nitrogen (HCHN) stationary liquid cultures, containing 2% glucose, Kirk's salts, 20 mM Na-2,2-dimethylsuccinate and 12 mM ammonium tartrate as described [Li et al., 2000]. Production of CDH was assayed using the cytochrome *c* and DCPIP assays (Chapter 3) and by western blot analysis of extracellular protein using polyclonal antibodies raised against *P. chrysosporium* CDH [Li et al., 1996]. The transformed strains exhibiting the highest activity and/or highest CDH protein levels were purified by isolating single basidiospores as described [Alic et al., 1989; Alic et al., 1991], and the progeny were rescreened for CDH activity and/or CDH secretion.

5.2.4 Production and Purification of Recombinant Wild-Type and Variant Proteins

Each recombinant strain was grown from a conidial inoculum in 250 ml Erlenmeyer flasks containing 30 ml of a HCHN stationary liquid medium as described

above. The variant proteins were purified from the extracellular medium on day 7 [Li et al., 2000]. The extracellular fluid was concentrated and dialyzed against 20 mM potassium phosphate, pH 6. Subsequently, the variant proteins were purified by cellulose-affinity chromatography and gel filtration (Chapter 2).

5.2.5 Flavin Cofactor Extraction

The free flavin cofactor was obtained by the cold trichloroacetic acid (TCA) method [Morpeth, 1985; Igarashi et al., 1999]. To 20–50 μM recombinant wild-type CDH (rCDH) or flavin domain variants (100 μl) was added 20% ice-cold TCA (100 μl) and the mixture was incubated on ice for 10 min. The precipitate was removed by centrifugation, and the supernatant was neutralized by the addition of 600 μl of Tris-HCl (1 M), pH 8.0. The concentration of extracted FAD was calculated from a standard curve, using the absorbance at 450 nm. The concentrations of the proteins prior to extraction were calculated using a Soret absorbance at 421 nm (ϵ_{421} = 100 mM^{-1} cm^{-1}).

5.2.6 Preparation of Truncated Flavin Domains

The flavin domains of recombinant wild-type and variant proteins were prepared using a limited proteolysis protocol [Henriksson et al., 1991; Cohen et al., 1997]. The flavocytochromes (20 μM), purified to homogeneity or purified through the cellulose affinity step, were incubated with 200 μg/ml of papain in 0.1 M potassium phosphate, pH 7, containing 2 mM EDTA and 2 mM dithiothreitol (DTT), for 2 h at room temperature. This digested protein solution was concentrated and dialyzed against 10 mM Tris-HCl, pH 8, and the flavin domain was purified by FPLC, using a mono-Q 5/5 column with a 0–300 mM NaCl gradient in 10 mM Tris-HCl, pH 8.

5.2.7 SDS-PAGE and Immuno (Western) Blot Analysis

Sodium dodecyl sulfate-polyacrylamide gel electrophoresis (SDS-PAGE) and western blot analysis were performed as described in Chapter 2.

5.2.8 Spectroscopic Procedures

Electronic absorption spectra of rCDH as well as N732 and H689 variants were obtained at room temperature in 20 mM sodium-succinate, pH 4.5, with a Cary 100 spectrophotometer (Varian, Australia). The proteins were reduced with either cellobiose (500 μM) or Na-dithionite.

5.2.9 Enzyme Assays and Kinetic Procedures

CDH activity was measured using either the cytochrome *c* or DCPIP assay (Chapter 3). The specific activity of cellobiose oxidation with DCPIP as electron acceptor was determined with 400 μM cellobiose and 35 μM DCPIP in 20 mM Na-succinate, pH 4.5 [ϵ_{515} = 6.8 mM^{-1} cm^{-1}]. The steady-state kinetic parameters for cellobiose oxidation were also determined by monitoring ferrocytochrome *c* formation [ϵ_{550} = 28 mM^{-1} cm^{-1}]. The assays contained a fixed amount of ferricytochrome *c* (12.5 μM) and varying levels of cellobiose (5–800 μM) or lactose (50 μM–60 mM) in 20 mM Na-succinate, pH 4.5. Stock solutions of cellobiose and lactose were left overnight for equilibration (mutarotation). A non-linear regression algorithm was employed to obtain the Michaelis-Menten kinetic parameters k_{cat} and K_m, using a publicly available software package, LSW-Data analysis Toolbox (MDL Information System Inc.), integrated in Microsoft Excel.

5.2.10 pH Dependence of Cellobiose Oxidation

The effect of pH on CDH activity was monitored in the presence of cellobiose (400 μM) and the electron acceptors cytochrome *c* (12.5 μM) or DCPIP (35 μM). The buffer systems (20 mM) used were Na-succinate (pH 3–5), potassium-phosphate (pH 5.5–7.5), and Tris (pH 8.0–9.0). Cytochrome *c* reduction was measured at 550 nm. The spectral characteristics of DCPIP were dependent on the pH of the reaction medium. The following wavelength and extinction coefficients were used: pH 3.0–4.5, 515 nm (6.8 mM^{-1} cm^{-1}); pH 5.0, 535 nm (6.8 mM^{-1} cm^{-1}); pH 5.5, 585 nm (8.2 mM^{-1} cm^{-1}); pH 6.0, 600 nm (12.7 mM^{-1} cm^{-1}); pH 6.5, 600 nm (15.7 mM^{-1} cm^{-1}); pH 7, 600 nm (16.8 mM^{-1} cm^{-1}); pH 7.5–9.0, 600 nm (17.7 mM^{-1} cm^{-1}).

5.2.11 Chemicals

Cellobiose, horse heart cytochrome c (Grade IV), Sephacryl S200 (HR) and Sigmacell 50 were obtained from Sigma (St. Louis, MO). Papain was purchased from Boehringer-Mannheim GmbH (Germany). Glucose and potassium-phosphate were obtained from J. T. Baker (Phillipsburg, NJ). Molecular biology reagents were obtained from New England Biolabs (Beverly, MA) or Stratagene (La Jolla, CA). All other chemicals were purchased from Sigma. Solutions were prepared in Millipore Q-50 (Millipore Corp., Bedford, MA) purified water (>18 MΩ cm).

5.3 RESULTS

5.3.1 Preparation of Cellobiose Dehydrogenase N732 and H689 Variants

A variety of substitution mutations at the H689 and N732 positions were created in pUGC1 (Fig. 3.1), and the mutations were confirmed by DNA sequencing. The mutant CDH enzymes were homologously expressed in *P. chrysosporium* [Li et al., 2000]. Western blot analyses were utilized to select strains secreting the highest level of mutant protein, because CDH activities in most of these mutant transformation cultures were extremely low. The CDH variants were detected by electronic absorption spectroscopy in the concentrated extracellular fluid. The variant proteins were purified to homogeneity, based on their R_z values ($A_{421}/A_{280} > 0.6$). The expression levels of the flavin variants were 20–100% of that observed for rCDH, based on the amount of CDH protein purified from the extracellular medium. SDS-PAGE analysis indicated a molecular mass of 90 kDa for all the purified flavin variants, similar to wild-type CDH [Li et al., 2000]. FAD cofactors were isolated from rCDH and the variant proteins by the TCA precipitation method [Morpeth, 1985; Igarashi et al., 1999]. Their electronic absorption spectra were similar to authentic FAD, exhibiting maxima at 380 and 450 nm. The flavin occupancy was ~90–95% for rCDH and the flavin variants.

5.3.2 Catalytic Properties of H689 Variants

The CDH activity in the extracellular media of the H689 variants was drastically reduced as measured by the cytochrome *c* and DCPIP assays. Despite the very low residual activities, a combination of a much larger amount of enzyme used in the assays (100–500 nM as compared to 1–20 nM), a more sensitive UV-vis spectrophotometer (Cary 100), and longer recording times allowed us to conduct a steady-state kinetic analysis of the H689 variants with cytochrome *c* as the electron acceptor (Table 5.1). The k_{cat} for cellobiose oxidation ranged from 0.002 to 0.009 s^{-1}, a ~5000-fold decrease from rCDH. However, each variant exhibited a K_m similar to the wild-type enzyme (20 μM). The steady-state kinetic parameters were also determined for a second substrate, lactose (Table 5.1). rCDH and the flavin variants H689A and H689Q exhibited k_{cat} values for lactose oxidation that were similar to that for cellobiose oxidation. However, the K_m values for lactose, with both rCDH and the H689 variants, were 15-fold higher than those for cellobiose.

5.3.3 Catalytic Properties of N732 Variants

Table 5.2 lists the k_{cat} and K_m values for rCDH and the N732 variants (N732H/Q/A/E/D) with cellobiose or lactose as the substrate and cytochrome *c* as the electron acceptor. The k_{cat} values of the variants for cellobiose oxidation were 5- to 4000-fold lower than for rCDH, and the order of decrease was His < Gln < Ala < Glu < Asp. All variants, except N732A, exhibited higher K_m values for cellobiose, which ranged from 2.5- to 15-fold higher than that for rCDH. The k_{cat} values for lactose oxidation with the N732 variants were similar to that for cellobiose oxidation (Table 5.2), as is observed for rCDH and the H689 variants. However, the K_m for lactose was affected in the N732 variants, increasing 5-fold for the N732A variant to 60-fold for N732E. The relative binding strength of the two substrates can be determined by calculating the difference in binding energy. Assuming that oxidation of lactose and cellobiose follows a similar reaction mechanism and the ratio of the configuration at the anomeric carbon (α:β) is similar for the two substrates, the difference in binding energy is similar to the change in activation energy ($\Delta(\Delta G^{\ddagger})$).

Table 5.1

Steady-State Kinetic Parameters for rCDH and H689 Variants[a]

Enzyme	Cellobiose oxidation	
	k_{cat} (s^{-1})	K_m (μM)
rCDH	11.6	16
H689N	0.003	19
H689Q	0.003	21
H689A	0.002	21
H689V	0.001	31
H689E	0.007	22
	Lactose oxidation	
rCDH	10.7	270
H689Q	0.002	290
H689A	0.002	280

[a] Reactions were performed at room temperature in 20 mM Na-succinate, pH 4.5. K_m and k_{cat} for cellobiose and lactose were determined using 12.5 μM cytochrome *c* and varying the substrate concentration between 5 and 400 μM (cellobiose) and between 50 μM and 2 mM (lactose).

Table 5.2

Steady-state Kinetic Parameters for rCDH and the N732 Variant[a]

Enzyme	Cellobiose oxidation		Lactose oxidation		$\Delta(\Delta G^{\ddagger})^{b}$
	k_{cat} (s^{-1})	K_m (μM)	k_{cat} (s^{-1})	K_m (μM)	kJ mol^{-1}
RCDH	11.6	16	10.7	270	7.2
N732H	2.0	40	1.3	2300	11.2
N732Q	0.8	41	0.9	4000	10.9
N732A	0.3	17	0.5	1200	9.0
N732E	0.16	230	0.2	16,600	9.4
N732D	0.003	170	0.004	11,400	9.2

[a] Reactions were performed in 20 mM Na-succinate, pH 4.5, at room temperature. K_m and k_{cat} for cellobiose were determined using 12.5 μM cytochrome *c* and varying the substrate concentration between 5 and 800 μM (cellobiose) and between 50 μM and 60 mM (lactose).

[b] $\Delta(\Delta G^{\ddagger}) = -RT \ln [(k_{cat}/K_m)_{lactose}/(k_{cat}/K_m)_{cellobiose}]$, where T = 298 K and R = 8.314 kJ mol^{-1} K^{-1}. $\Delta(\Delta G^{\ddagger})$ is a measure for the difference in binding energy between cellobiose and lactose.

This change can be calculated using the relationship $\Delta(\Delta G^{\ddagger}) = -RT \ln [(k_{cat}/K_m)_{lactose}/(k_{cat}/K_m)_{cellobiose}]$ [Fersht, 1985]. This shows that for the wild-type enzyme, lactose binding was energetically less favorable by 7.2 kJ mol^{-1}, and that a mutation of N732 weakened the binding of lactose by a further 2–4 kJ mol^{-1} (Table 5.2).

5.3.4 pH Dependence of Activity

Wild-type CDH exhibits an acidic pH optimum with a broad maximum between pH 3 and 5 for the oxidation of cellobiose with DCPIP (Fig. 5.1A) [Samejima and Eriksson, 1992; Igarashi et al., 1999]. Activity gradually decreases above pH 5 with an apparent pKa of 6. Hence, the specific activities for rCDH and the flavin variants were measured at pH 4.5 (Table 5.3). All H689 variants (data not shown) and the N732H/Q/A variants (Fig. 5.1) exhibited a pH dependence similar to the wild-type enzyme. The mutations N732E and N732D introduce a carboxylate group, which may be ionized, and these variants exhibited a neutral pH optimum (6.5–7) with DCPIP as the electron acceptor (Fig. 5.1A). In the presence of the one-electron acceptor cytochrome *c*, all flavin variants, except N732E and N732D, had a similar pH profile to that for rCDH, with the highest activity at pH 3, decreasing as the pH increased (Fig. 5.1B). In contrast, the N732D and N732E variants exhibited optima at pH 6 and 5, respectively (Fig. 5.1B).

5.3.5 Absorption Spectra of the H689 and N732 Variants

The UV-vis spectra of the oxidized and sodium-dithionite reduced H689 and N732 variants are similar to the wild-type protein rCDH (Fig. 5.2 insert) [Li et al., 2000]: the absorption bands at 421, 529 and 570 nm are attributed to a ferric, low spin heme and the bands at 429, 532 and 562 are attributed to a ferrous, low spin heme [Cohen et al., 1997]. The weak absorbance between 450 and 500 nm indicates the presence of a flavin. Under aerobic and anaerobic conditions, cellobiose (500 μM) completely reduced the FAD and heme group in both rCDH and the N732H variant. In contrast, the addition of cellobiose did not reduce either the heme or the flavin in any of the H689 variants or the N732D variant, under aerobic conditions,

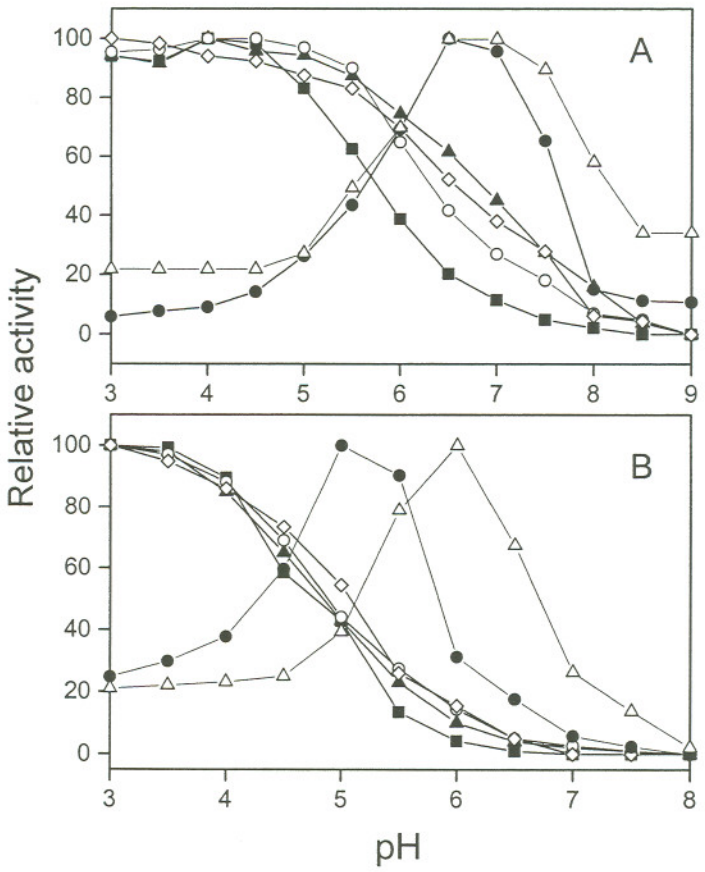

Fig. 5.1 Dependence of cellobiose oxidation on pH by rCDH and N732 variants: rCDH (■) and the N732 variants, N732H (▲), N732Q (○), N732A (◇), N732E (•) and N732D (△), with DCPIP (**A**) and cytochrome *c* (**B**) as electron acceptor. Reaction conditions are as described in the text.

Table 5.3

Specific Activity of rCDH and the H689 and N732 Variants at pH 4.5[a]

Enzyme	Electron acceptor	
	Cytochrome *c*	DCPIP
rCDH	6.8	17
N732H	1.1	3.7
N732Q	0.5	0.7
N732A	0.2	0.2
N732E	0.1	0.08
N732D	0.002	0.003
H689Q	0.002	0.007
H689N	0.002	0.007
H689A	0.002	0.007
H689V	0.001	0.003
H689E	0.004	0.01

[a] Assays were performed in 20 mM Na-succinate, pH 4.5, at room temperature, using 400 μM cellobiose and 12.5 μM cytochrome *c* or 35 μM DCPIP. Specific activity is calculated in μmole/min/mg.

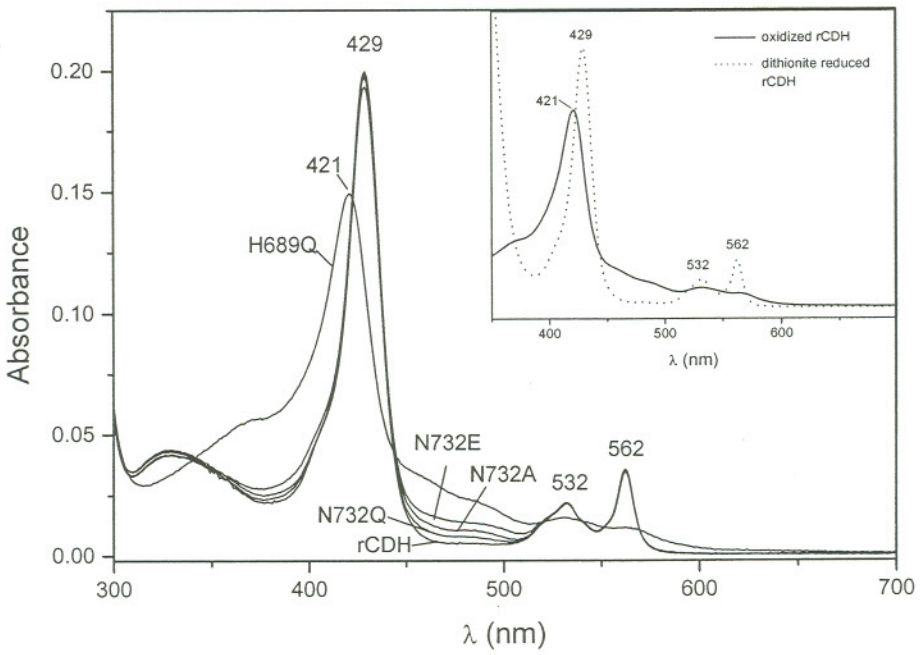

Fig. 5.2 Electronic absorption spectra of cellobiose-reduced CDH holo-enzymes under aerobic conditions. The flavocytochromes rCDH, and the CDH variants N732Q, N732A, N732E and H689Q () were treated with 500 μM cellobiose at pH 4.5 under aerobic conditions and the resulting spectra were stable over at least 15 minutes. **Insert** shows the electronic absorption spectra of rCDH, oxidized (—) and dithionite-reduced (---).

and only the heme appeared to be slowly reduced under anaerobic conditions. Finally, under aerobic conditions the heme domain was completely reduced in the N732Q/A/E variants, whereas the flavin was only partially reduced (Fig. 5.2). Based on the residual absorbance at 458 nm and an absorption coefficient of 10 mM^{-1} cm^{-1} (Chapter 2), the FAD in N732Q, N732A, and N732E was reduced ~75, 50, and 35%, respectively. The addition of cellobiose under anaerobic conditions resulted in the complete reduction of both cofactors in these N732 variants.

5.3.6 The Flavin Domain of rCDH and Variants

Because the heme absorbance dominates the UV-vis spectrum of a flavocytochrome such as CDH, the truncated flavin domains of rCDH and several flavin domain variants (N732H/Q/A/E/D and H689Q/A) were produced by limited proteolysis and anionic exchange chromatography. The molecular mass for the flavin domain of each variant, determined by SDS-PAGE, was approximately 60 kD, as was observed previously [Henriksson et al., 1991]. The specific activities of each of the flavin domains for cellobiose oxidation in the presence of DCPIP were similar to those for the 90 kD enzymes, suggesting that the isolated flavin domains remained intact. The electronic absorption spectra of the flavin domain for most of the H689 and N732 variants were similar to the flavin domain of rCDH, with maxima at 386 and 458 nm (Fig. 5.3A). The N732D variant exhibited blue-shifted maxima at 383 and 452 nm (Fig. 5.3A). The addition of cellobiose to rCDH and the N732H/Q/A/E/D variants under anaerobic conditions resulted in bleaching of the absorbance and it is estimated that >90% of the flavin was reduced (Fig. 5.3B).

5.4 DISCUSSION

Flavoproteins, such as the flavin domain of cellobiose dehydrogenase (CDH_{DH}), glucose oxidase (GOX), cholesterol oxidase (CHO), and monoamine oxidase, catalyze the oxidation of non-activated alcohols and amines, which lack an electron-withdrawing group adjacent to the position of dehydrogenation. Two different mechanisms, a radical mechanism [Silverman et al., 1980; Li et al., 1993]

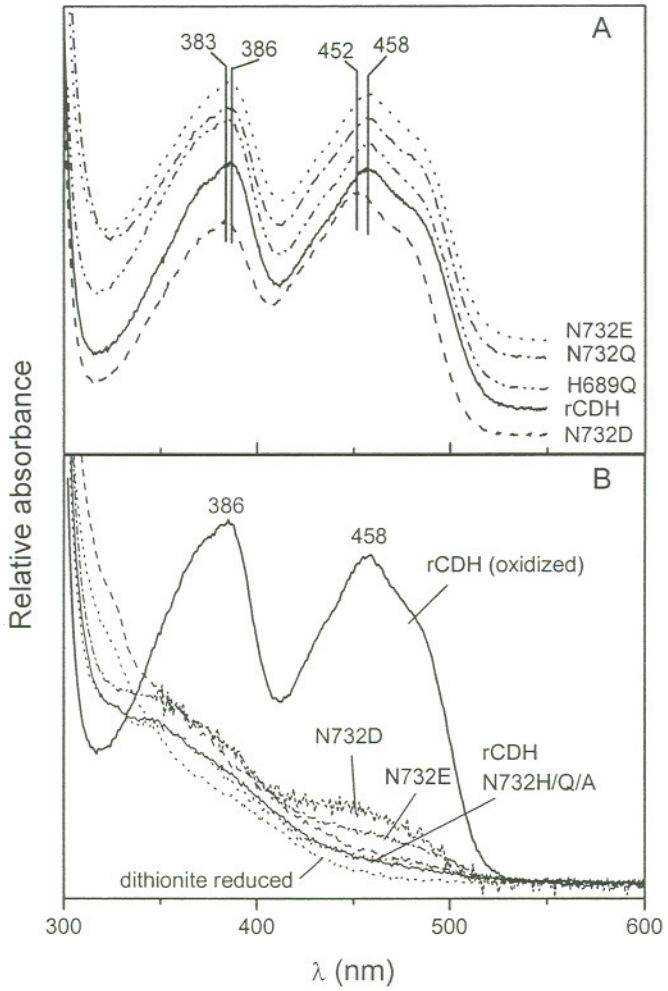

Fig. 5.3 Electronic absorption spectra of the truncated flavin domain of rCDH and the variants N732H/Q/A/E/D and/or H689Q. (**A**) Oxidized; (**B**) reduced with cellobiose (30–300 μM) under anaerobic conditions.

and a hydride transfer mechanism [Ghisla and Massey, 1989; Li et al., 1993], have been proposed to account for the dehydrogenation of these non-activated substrates. In the radical mechanism, electrons are transferred from the substrate, one at a time; whereas in the hydride transfer mechanism, two electrons are transferred in a single step. Despite this difference, both reactions appear to be assisted by the action of a general base [Ghisla and Massey, 1989].

The tertiary structures of three members of the GMC oxidoreductase family, CDHdh [Hallberg et al., 2002], GOX [Hecht et al., 1993; Wohlfahrt et al., 1999] and CHO [Vrielink et al., 1991; Yue et al., 1999], reveal a highly conserved active site, including an active site water and two semi-conserved residues, His and Asn (in GOX, the Asn residue is replaced by a His). In CDH, the active site water, Wat1214, is hydrogen bonded to $N^{\epsilon 2}$-His689 and $N^{\delta 2}$-Asn732. This site is located near the isoalloxazine ring and at the end of a 12 Å channel that can accommodate a cellobiose molecule. Molecular modeling suggests that Wat1214 is expelled from the active site on binding of the substrate, and the anomeric β-hydroxyl CO1 of cellobiose is positioned between His689 and Asn732 (Fig. 5.4). In this model, His689 may act as a general base, activating the substrate for oxidation by deprotonation of the β-hydroxyl (Fig. 5.5). The anomeric α-hydrogen of cellobiose, pointing toward the FAD-N5, is optimally positioned for efficient hydrogen and electron transfer (Figs. 5.4 and 5.5). The productive binding of the anomeric hydrogen is most likely assisted by the interaction between the β-hydroxyl and the two residues, His689 and Asn732. Previous mutant studies in GOX [Witt et al., 2000] and CHO [Kass and Sampson, 1998; Yamashita et al., 1998; Yin et al., 2001] have demonstrated the importance of their active site residues in catalysis. In this report, we have assessed the steric and electrostatic constraints of His689 and Asn732 of CDH from *P. chrysosporium* in binding and oxidation of the substrates cellobiose and lactose. The structural and kinetic properties of variants were assessed by kinetic and spectroscopic studies.

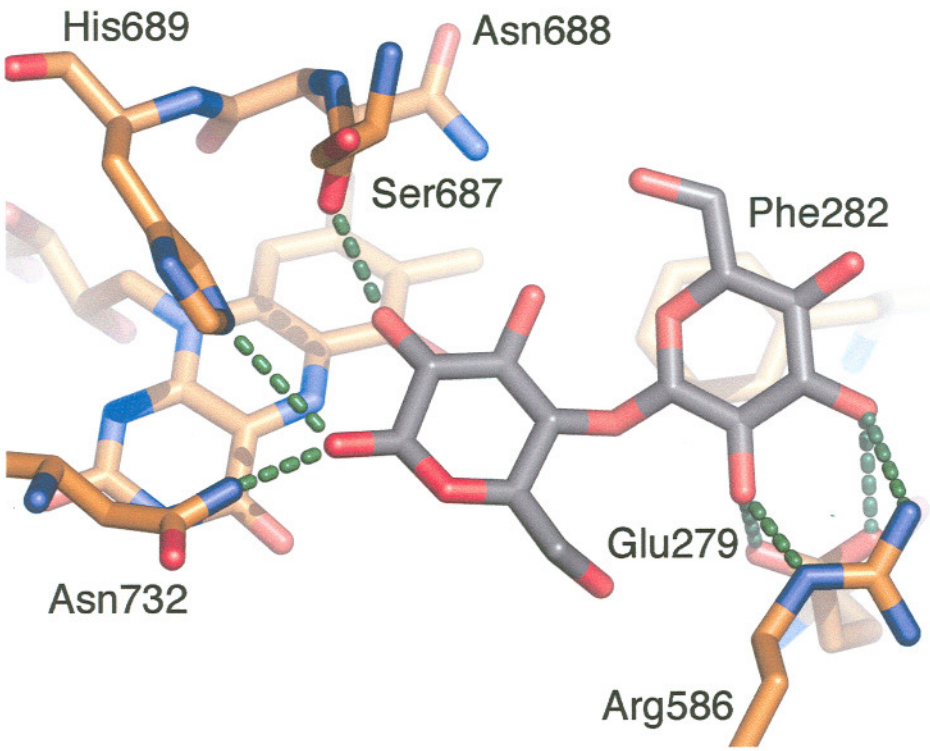

Fig. 5.4 The active site of CDH_{DH} complexed with cellobiose. The binding modes for the substrate were obtained by docking cellobiose in the active site of CDH_{DH} [Hallberg et al., 2002]. Atom colors: carbon, yellow (protein), grey (cellobiose); oxygen, red; nitrogen, blue.

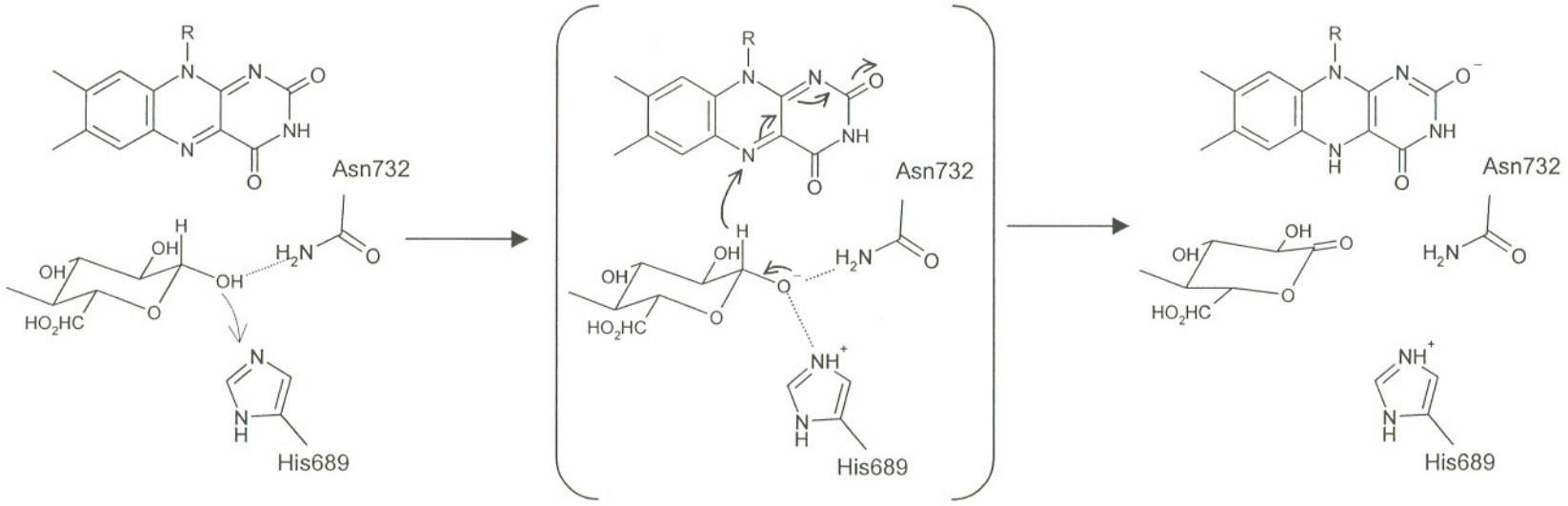

Fig. 5.5 Schematic diagram of cellobiose oxidation by CDH, assisted by the action of the general base His689, and interaction between 1β-hydroxyl of cellobiosethe and active site residues His689 and Asn732.

5.4.1 Role of His689

All the variants containing a substitution at His689 exhibit a significantly reduced oxidation rate for cellobiose (Tables 5.1 and 5.3), implicating this residue in catalysis. This is further supported by the apparent lack of any spectral changes in the heme and flavin cofactor in the presence of cellobiose, i.e., no apparent reduction of the flavin and heme cofactors were observed upon binding of cellobiose (Fig. 5.2). The low residual activity (>1000-fold decrease in k_{cat}) in all H689 variants may be the result of the absence of the base His689 near the β-hydroxyl (Wat1204). The general base His689 deprotonates the 1β-hydroxyl substrate, thus facilitating oxidation of cellobiose (Fig. 5.5). This conclusion agrees with the site-directed mutagenesis studies on the catalytic histidine in CHO from *Streptomyces* sp. [Kass and Sampson, 1998; Yamashita et al., 1998] and GOX from *Penicillium amagasakiense* [Witt et al., 2000]. Practically all substitutions resulted in a more than 10^3-fold decrease in catalytic activity. The significant residual activity for one of the variants of CHO, H447Q with 1% residual activity, was attributed to the presence of a base, Glu361, in the active site [Kass and Sampson, 1998]. Not such a residue is present in CDH or GOX.

An alternative role of the catalytic histidine in CHO has recently been proposed, based on a sub-atomic resolution crystal structure of cholesterol oxidase [Lario et al., 2003]. This structure of the substrate free enzyme suggests that the $N^{\epsilon 2}$ atom of the active site histidine, His447, is protonated and thus may act as hydrogen bond donor, rather than as a general base. An electron-rich patch, composed of the side chain of a second base in the active site, Glu361, and the lone pair electrons on the sulfur atom of M122 and O4 of the FAD, may instead be responsible for lowering the pK_a value of the steroid hydroxyl, thus facilitating the oxidation. The role of His447 would be to assist in optimizing substrate geometry towards this electron-rich patch and the N5 locus of FAD. This mechanism is unlikely to take place in CDH. Indeed, no electron-rich patch can be identified in the active site of CDH_{DH} [Hallberg et al., 2002]. Moreover, while the kinetic data for the N732 variants indicate a change in Km, consistent with its role in H-bond formation with the substrate (see below), substitution of H689 has no effect on the binding constant (Table 5.1).

5.4.2 Role of Asn732

The second catalytic residue, Asn732, would not act as a general base, but it appears optimally positioned to assist in the binding of the anomeric β-hydroxyl of cellobiose (Fig. 5.4) [Hallberg et al., 2002]. All Asn732 variants exhibit a reduced rate for cellobiose oxidation (Tables 5.2 and 5.3), implicating this residue in catalysis. The wide variation in the k_{cat} (0.004–2.7 s^{-1}) and the K_m (16–230 μM) for cellobiose among the N732 variants suggests that each substitution uniquely alters the substrate specificity of the enzyme, i.e., each substitution uniquely changes the active site structure, affecting the binding as well as the positioning of the substrate with respect to the general base, His689, and the flavin, FAD-N5. Thus, the N732A variant exhibits a low K_m, indicating that it easily accommodates cellobiose. However, this variant lacks a hydrogen bond donor to assist in positioning the anomeric carbon. While the residues Gln and His may act as hydrogen bond donors, they are bulkier than Asn. The 6 to 14-fold lower k_{cat} and 2 to 3-fold higher K_m for N732Q and N732H suggest structural changes in the cellobiose–enzyme complex, affecting both binding and oxidation of the substrate. The Glu or Asp substitutions introduce possible hydrogen bond donors or, if ionized, a residue that may assist in the polarization of the β-hydroxyl of cellobiose. For example, in CHO, the residual activity in the H447Q variant is partly attributed to the presence of a second active site base, Glu361, which is hydrogen bonded to the active site water [Kass and Sampson, 1998; Yue et al., 1999]. Although the carboxylate residues in N732D and N732E appear ionized (see below), their presence apparently lends no advantage to CDH. Moreover, both substitutions result in a much higher K_m for cellobiose than is exhibited by the other variants, suggesting that the binding of substrate is significantly weakened in the N732E and N732D variants. Two possible explanations can be proposed. First, the presence of a negative charge may significantly alter the hydrogen-bonding network within the active site, inducing steric and/or electrostatic hindrances for binding of the substrate. A second explanation is based on an extended hydrogen-bonding network from Asn732 to Thr584 via Gln582. These residues are in close contact with Arg586, which forms two hydrogen bonds with the substrate in the enzyme–cellobiose complex (Fig. 5.4). Disruption of this hydrogen-

bonding network, owing to a new negative charge, might alter the orientation of Arg586, thus weakening cellobiose binding. Overall, an Asn residue appears to be the optimal choice in the active site for CDH and in almost all other GMC oxidoreductases.

5.4.3 Lactose as Substrate

Lactose is an epimer of cellobiose, differing in configuration at the C4 of the non-reducing glucosyl unit (Glc2). In the cellobiose–enzyme complex, Glc2-C4 is located at the entrance of the substrate-binding site [Hallberg et al., 2002]. rCDH exhibits lower specificity towards lactose than cellobiose, which is attributed to the binding affinity for the substrates, i.e., the k_{cat} for oxidation is similar for both substrates, but the K_m is 15-fold higher for lactose (Tables 5.1 and 5.2). The cellobiose–enzyme model [Hallberg et al., 2002] indicates the aromatic ring of Phe282 is stacked against the α face of Glc2 (Fig. 5.4). For cellobiose, the hydroxyl at the Glc2-C4 position is oriented away from the aromatic ring of Phe282; whereas for lactose, this hydroxyl would be oriented toward the aromatic ring, hindering lactose binding. The kinetic data for the flavin variants with cellobiose suggest that Asn732 substitutions weaken the binding of the substrate, whereas the H689 variants exhibit a similar affinity for this substrate (Tables 5.1 and 5.2). The steady-state kinetic data for lactose oxidation with the flavin variants supports this (Tables 5.1 and 5.2). Furthermore, the K_m for lactose is greatly increased upon mutation of N732. Using the change in activation energy $\Delta(\Delta G^{\ddagger})$ as a quantitative measure of the difference in binding energy between the substrates cellobiose and lactose [Fersht et al., 1985], lactose binds 7.2 kJ mol^{-1} less favorably to the active site of rCDH than cellobiose (Table 5.2). This value is comparable to changes in free energy resulting from removal of a weak or strong hydrogen bond, shown to be 2–6 and 15–19 kJ mol^{-1}, respectively [Fersht et al., 1985; Street et al., 1986], and in CDH may be the result of the loss or weakening of hydrophobic, electrostatic, van der Waals or hydrogen bonding interactions between the enzyme and substrate. The additional 2–4 kJ mol^{-1} difference observed for the N732 variants suggests that an Asn residue may

partially compensate for the weaker binding of lactose, whereas the N732 substitutions apparently do not.

5.4.4 pH Dependence

The results with the H689 and N732 variants (Fig. 5.1) indicate that these residues do not control the pH profile of cellobiose oxidation. However, for an enzymatic reaction assisted by base catalysis, the protonation state of the base should be important. In CDH, His689 should be neutral in the catalytically active state. rCDH exhibits a pH optimum for cellobiose oxidation between 3 and 5 (Fig. 5.1A), implying a greatly perturbed His pKa from its value in aqueous solution ($\sim$6). It is known that amino acid bases and carboxylic acids in proteins can exhibit anomalous pKa, attributed to their microenvironments. For example, the general base His159 in the thiol protease papain exhibits an unusually low pKa of $\sim$3.4 [Johnson et al., 1981], attributed to a hydrophobic environment around the imidazole ring [Kamphuis et al., 1984]. In the case of CDH, His689 is indeed buried in a hydrophobic pocket of the active site, near the xylene moiety of the isoalloxazine ring [Hallberg et al., 2002]. The results for N732D and N732E may exemplify how the microenvironment around the general base, His689, can modulate its acid–base properties. The distance between Asn732-N^{δ} and His689-N^{ϵ} is $\sim$3.5 Å. The Asn732 carboxylate variants shift the pH optimum for cellobiose oxidation from pH 3–5 to 6–7 (Fig. 5.1A). The introduced carboxylate groups may be ionized, creating a negative charge near His689. This may raise the pKa of the His and thus shift the optimum to neutrality.

An alternative explanation for the maximum activity of the N732 variant at pH 7 could be changes of titration curves. While the unidentified source of the wt pH dependence, which maximizes at pH $<$ 5, may be unchanged, the added carboxylate group may provide an additional titration curve with pKa $\sim$ 4. The 30% activity observed in the variant at pH, relative to the wild-type at pH 7, may correspond to a mechanism similar to that in CHO, where a deprotonated carboxylate (Glu361) facilitate the deprotonation of the substrate hydroxylate group.

The shift in pH optimum upon introduction of a carboxylate group in the active site is of interest when comparing the catalytic properties of the CDHs from *P.*

chrysosporium and *Humicola insolens* [Schou et al., 1998], since the *H. insolens* CDH exhibits a pH optimum closer to neutrality [Schou et al., 1998]. While there is no crystal structure for the flavin domain from *H. insolens*, the primary sequence alignment of the six sequenced CDH genes [Raices et al., 1995; Li et al., 1996; Dumonceaux et al., 1998; Moukha et al., 1999; Subramaniam et al., 1999; Yoshida et al., 2002] suggests that the catalytic site is conserved in all CDHs, containing a His and an Asn. In addition, the N732E variant still exhibits an acidic pH optimum for cytochrome *c* reduction, whereas the alkaline CDH from *H. insolens* is most active at neutral/alkaline pH. Other differences in the active site may account for the different pH dependencies, rather than an amide to acid substitution.

5.4.5 Electronic Properties of the Flavin

The turnover rates for the two carboxylate variants, N732D and N732E, were somewhat surprising. Intuitively, the Glu substitution, which is electrostatically and sterically different from Asn, should have resulted in a weaker catalyst than the Asp mutation. In contrast, the N732E variant exhibits a higher k_{cat} (50-fold) than the N732D variant (Table 5.2). The microenvironment around the isoalloxazine ring modulates various chemical properties of the flavin, including its electronic structure and reactivity [Yagi et al., 1980]. For example, flavin enzymes often have a positively charged entity in close contact with the N1–C2=O2 locus of the flavin [Fraaije and Mattevi, 2000]. This regulates the redox properties of the cofactor, stabilizing the anionic form of the reduced flavin and thus raising its redox potential. The pH profile (Fig. 5.2) suggests that the carboxylate residues in the N732D and N732E variants are ionized, introducing a negative charge in the active site. This could significantly alter the electrostatic environment around the flavin, reducing the oxidizing power of the FAD cofactor. To probe the effect of these variants on the redox potential, the electronic absorption spectra of the truncated flavin domains of N732D and N732E were recorded and compared to rCDH and several of the other flavin variants (N732H/Q/A, H689Q/A). Previous mutant studies of flavin enzymes show that changes in the electronic absorption spectra are accompanied by changes in the redox properties of the flavin. For example, substitution of the catalytic Asn by

Leu in CHO results in a drop of 76 mV in the redox potential, and the UV spectrum has a 4 nm red-shifted γmax with respect to the wild type [Yin et al., 2001]. In the old yellow enzyme, Thr34 forms a hydrogen bond with FMN-O4 and the T37A variant has a lower redox potential, supporting the role of Thr34 in stabilizing the reduced state [Xu et al., 1999]. The shift in redox potential is accompanied by a shift in the absorption maxima to a shorter wavelength. Only the N732D variant exhibits a different flavin spectrum from rCDH, with absorption maxima blue-shifted to 383 and 452 nm (Fig. 5.3A). Therefore, the Asp substitution may affect the redox properties of the flavin in CDH. The N732E (and other variants) exhibit a similar spectrum, suggesting that their redox properties are not significantly altered.

5.5 CONCLUSIONS

Residues His689 and Asn732 are involved in catalysis by CDH from *P. chrysosporium*. The catalytic His appears to facilitate the oxidation of cellobiose and lactose and concomitant reduction of the flavin cofactor, functioning as a general base. The primary role of Asn732 appears to be that of positioning of the substrate 1α-H and 1β-OH relative to FAD and His689, respectively, which would promote deprotonation and oxidation. These conclusions are in agreement with those based on the crystal structure of the CDH flavoprotein in complex with a transition-state analog (C. Divne, personal communication). The results also suggest that the proximity of a neutral residue, like Asn732, to the His689 and the isoalloxazine ring may control the acidity of the general base and the electrostatic environment around the flavin.

CHAPTER 6
CONCLUSIONS AND FUTURE DIRECTIONS

Using the homologous expression system for cellobiose dehydrogenase (CDH) in *Phanerochaete chrysosporium* [Li et al., 2000], we have achieved efficient production of a number of variants of the cytochrome and flavin domain of this enzyme. All variants could be purified employing a simple and fast, two-step purification protocol, resulting in an approximately 50% yield (Chapter 2). We have addressed questions regarding the nature and role(s) of amino acid residues that were predicted to be involved in the axial ligation to the heme iron (Chapters 3 and 4) and oxidation of cellobiose (Chapter 5). Our findings are further supported by the independent determination of the tertiary structure of flavin and cytochrome domains of wild-type CDH from *P. chrysosporium* by C. Divne and coworkers [Hallberg et al., 2000; Hallberg et al., 2002a]. A number of structural, functional, and molecular aspects of CDH remain to be discovered, and the approach delineated in this thesis could be further extended to address those issues.

6.1 CELLOBIOSE AND CELLULOSE BINDING

Mutagenesis studies as described in Chapter 5 demonstrated the critical roles that residues His 689 and Asn 732 play in the oxidation of cellobiose, as was proposed by our group [Subramaniam et al., 1999]. The loss of His689 results in the absence of an active base that, otherwise, would deprotonate the anomeric hydroxyl of cellobiose, facilitating the oxidation of cellobiose and electron transfer to the flavin. The second residue, Asn 732, is important for productive binding of the substrate, and its substitution weakens the binding of substrate and/or the positioning of the anomeric carbon of cellobiose towards the FAD-N5 locus and general base. Based on

docking of cellobiose in the active site of CDH [Hallberg et al., 2002a] and the tertiary structure of the flavin domain of CDH complexed with the inhibitor, cellobiono-1,5-lactam [Hallberg et al., 2002b], several other residues in the active site have been proposed to be involved in binding of cellobiose. These include Glu279, Arg586, Ser687, Ans688 and Tyr609 (via two active site waters), which are within hydrogen bonding distance of the docked substrate. Finally, the aromatic ring of Phe282 may interact with the α-face of the glycosyl ring by a planar hydrophobic stacking interaction (Fig. 5.4). Future site-directed mutagenesis studies of these residues and kinetic characterization of the variants may validate these predictions and the role these residues play in the binding and oxidation of cellobiose. Interestingly, several of the residues, are not completely conserved among all CDHs. For example, Glu227 and Phe282 of *P. chrysosporium* are replaced by an Asn and Trp respectively, in the CDHs from *S. thermophile* and *H. insolens*.

In contrast to most fungal cellulases, the cellulose binding sequence of CDH_{PC} apparently resides within the catalytic (flavin) domain. Earlier it had been proposed that two stretches of approximately 50 amino acids might be involved in cellulose binding [Henriksson et al., 1997]. One stretch (residues 342 to 398) contains a conserved sequence, unique to CDHs [Subramaniam et al., 1999]. The second stretch (residues 251 to 299) contains nine aromatic residues, which, by analogy with cellulose binding domains of cellulases [Lindner and Teeri, 1997], could be involved in cellulose binding. However, in the present tertiary structure [Hallberg et al., 2002a], no obvious substructures or surface patches are present that could be assigned as cellulose binding sites. Moreover, the stretch of amino acid residues 251 to 299 forms a loop-and-lid structure, close the entrance of the active site, shielding the flavin-binding pocket and is the likely docking surface for the cytochrome domain [Hallberg et al., 2002a]. Future work using mutations within these regions and comparisons of the cellulose binding properties of these variants with the wild-type enzyme may shed light on the structural basis for the strong absorption of CDH to cellulose. In addition, the kinetic analysis (steady-state and stopped flow) of variants in the region 251 to 299 may probe the structural requirement for a possible docking

surface at the flavin domain for electron transfer between the two redox active groups.

6.2 INTERDOMAIN REGION IN CELLOBIOSE DEHYDROGENASE

A region of approximately 30 amino acid residues (aa 186-216) was proposed to connect the N-terminal cytochrome domain and C-terminal flavin domain in CDH_{PC} [Raices et al., 1995; Li et al., 1996]. This linker peptide is rich in prolines (4), threonines (10) and serines (6), providing a large number of potential *O*-glycosylation sites. This covalent hinge is critical for electron transfer between the two redox active groups, as electrons are not transferred between the two individual domains after proteolytically cleavage [Henriksson et al., 1991]. This suggests that the hinge is required for the proper orientation of the two domains, facilitating electron transfer.

Flavocytochrome b_2 has a domain organization similar to CDH, however, the enzyme contains a much shorter linker (10 amino acids versus 30 residues in CDH) with prolines, glycines and charged residues. The kinetic properties of variants containing elongation and deletion mutations in the linker suggested an important role for the length of the linker in efficient electron transfer between the two domains and between the flavocytochrome and cytochrome *c* [Sharp et al., 1994; Sharp et al., 1996b; Sharp et al., 1996a]. Construction of deletions and elongations within the linker of CDH, followed by steady-state and stopped flow studies will provide insight into the importance of the length of the linker in inter-domain electron transfer. Interestingly, a long linker region may not be necessary because the CDHs from *H. insolens* and *S. thermophile* appear to contain shorter linkers (by two to three residues).

Studies of the interdomain region can be extended further by probing the importance of prolines and hydroxyamino acid enrichment. The abundance of these residues is typical for most cellulolytic enzymes, although the exact sequences in these enzymes are not conserved [Gilkes et al., 1991]. It is believed that the proline residues and the extensive glycosylation provide rigidity, as well as protection against

proteolytic cleavage. A structure-function study on these residues, systematically replacing one or more residues, should test the merit of these ideas.

6.3 CONTACT SURFACE ON THE CYTOCHROME DOMAIN

In yeast flavocytochrome b_2, the flavin and cytochrome domains are closely associated, enabeling the heme and FAD cofactor to be positioned with an edge-to-edge distance of 9.7 Å, thus facilitating inter-domain electron transfer [Xia and Mathews, 1990]. A crystal structure for the holo-enzyme of CDH is currently not available. However, an organization similar to that in flavocytochrome b_2 is likely for CDH. Analysis of the heme-exposed face of the cytochrome domain of CDH and the active site entrance of the flavin domain shows that both surfaces are complementary and the binding interactions have a mainly non-ionic character [Hallberg et al., 2000; Hallberg et al., 2002a]. *In silico* docking experiments with the cytochrome and flavin domain might provide information about the interacting surface of both domains and possible residues involved. Future structure-function studies on these residues, including site-directed mutagenesis and kinetic analysis, could evaluate these predictions. The results can than be combined with the results from structure-function studies on the interdomain linker region, providing more structural information, indirectly obtained, for the association of the two domains and the role of the peptide linker.

6.4 FUNCTIONAL ANALYSIS OF THE GENOME OF *PHANEROCHAETE CHRYSOSPORIUM*

Recently, a draft of the approximately thirty million base-pair genome of the "model system" for microbial wood degradation, *P. chrysosporium*, has been reported [White-Rot Genome Project, 2002]. Although this basidiomycete is the best-studied member of the family of wood-rot fungi, compare to model systems, such the budding yeast *Saccharomyces cerevisiae*, the plant *Arabidopsis thaliana*, or the roundworm *Caenorhabditis elegans*, little is known at the molecular level. For example, only a

limited number of genes and proteins had been cloned, purified and/or analyzed, and these are almost exclusively extracellular, "directly" involved in the degradation of the polymeric compounds cellulose, lignin and hemicellulose. The draft provide a complete genomic blue-print of the white-rot fungus. Analysis of the genome should be focused on the molecular machinery behind the degradation of wood by the fungus. One of the next steps could be to validate predicted genes, for example by sequence analysis and the creation of a "complete" cDNA or Expressed Sequence Tag (EST) library of the fungus, grown under different culture conditions, in particular wood and the main polymeric compounds, lignin, cellulose and hemicellulose.

One of the important questions regarding the cellulolytic enzymes is its regulation at the molecular level. These enzymes are regulated at the transcriptional level [Bisaria and Mishra, 1989] and expression is induced in the presence of cellulose. Obviously, this insoluble substrate is not the inducer in the cell. One hypothesis is that soluble products, such as cellobiose and sophorose, are produced by the hydrolytic activity of low levels of constitutively expressed cellulases, and are transported into the cell, inducing cellulase expression [Beguin and Aubert, 1994]. Interestingly, studies of a CDH deficient-strain of *Trametes versicolor* suggested that CDH is important for growth on crystalline cellulose and wood invasion [Dumonceaux et al., 2001]. Thus, CDH may be involved in the initial stages of cellulose and wood degradation. Using the EST library (see above), an initial and "limited" DNA micro-array of *P. chrysosporium* could be created. Global gene expression profiling studies of *P. chrysosporium*, grown under various conditions (from grown on a well-defined media, such as cellulose and glucose, to a complex substrate as wood) can then be performed. These studies may identify (novel) proteins and enzymes involved in the induction and early degradation of cellulose and wood. Selected proteins should then be further investigated, for example by homologous expression in *P. chrysosporium* or heterologous expression in a suitable host (*E. coli*, *Pichia pastoris*, *Saccharomyces cerevisiae*), followed by biochemical characterization. These in vitro experiments should be complemented by *in vivo* approaches, such as immunolocalization and gene disruption. All these experiments may shed light on the complex interactions of the fungal wood-degrading "enzyme-

soup", and thus may lead us to obtain a better understanding of the roles of CDH and other intracellular and extracellular enzymes in the degradation of wood.

LITERATURE CITED

Akileswaran, L., M. Alic, E. K. Clark, J. L. Hornick, and M. H. Gold (1993) Isolation and transformation of uracil auxotrophs of the lignin-degrading basidiomycete *Phanerochaete chrysosporium*. *Curr. Genet.* **23**, 351-356.

Alic, M., J. R. Kornegay, D. Pribnow, and M. H. Gold (1989) Transformation by complementation of an adenine auxotroph of the lignin-degrading basidiomycete *Phanerochaete chrysosporium*. *Appl. Environ. Microbiol.* **55**, 406-411.

Alic, M., E. K. Clark, J. R. Kornegay, and M. H. Gold (1990) Transformation of *Phanerochaete chrysosporium* and *Neurospora crassa* with adenine biosynthetic genes from *Schizophyllum commune*. *Curr. Genet.* **17**, 305-311.

Alic, M., M. B. Mayfield, L. Akileswaran, and M. H. Gold (1991) Homologous transformation of the lignin-degrading basidiomycete *Phanerochaete chrysosporium*. *Curr. Genet.* **19**, 491-494.

Ander, P., C. Mishra, R. L. Farrell, and K. E. L. Eriksson (1990) Redox reactions in lignin degradation interactions between laccase different peroxidases and cellobiose:quinone oxidoreductase. *J. Biotechnol.* **13**, 189-198.

Andresen, P. A., I. Kaasen, O. B. Styrvold, G. Boulnois, and A. R. Strom (1988) Molecular cloning, physical mapping and expression of the bet genes governing the osmoregulatory choline-glycine betaine pathway of *Escherichia coli*. *J. Gen. Microbiol.* **134**, 1737-1746.

Antonini, E., and B. Brunori (1971) *Hemoglobin and myoglobin in their reaction with ligands*. North-Holland Publishing Co., Amsterdam.

Appelby, C. A., and R. K. Morton (1959) Lactic dehydrogenase and cytochrome b_2 of baker's yeast. Purification and crystallization. *Biochem. J.* **71**, 492-499.

Aubert, C., F. Guerlesquin, P. Bianco, G. Leroy, P. Tron, K. O. Stetter, and M. Bruschi (2001) Cytochromes c_{555} from the hyperthermophilic bacterium *Aquifex aeolicus*. 2. Heterologous production of soluble cytochrome c_{555} and investigation of the role of methionine residues. *Biochemistry* **40**, 13690-13698.

Ayers, A. R., S. B. Ayers, and K. E. Eriksson (1978) Cellobiose oxidase, purification and partial characterization of a hemoprotein from *Sporotrichum pulverulentum*. *Eur. J. Biochem.* **90**, 171-181.

Baminger, U., S. S. Subramaniam, V. Renganathan, and D. Haltrich (2001) Purification and characterization of cellobiose dehydrogenase from the plant pathogen *Sclerotium* (*Athelia*) *rolfsii*. *Appl. Environ. Microbiol.* **67**, 1766-1774.

Banci, L., I. Bertini, K. L. Bren, H. B. Gray, P. Sompornpisut, and P. Turano (1997a) Solution structure of oxidized *Saccharomyces cerevisiae* iso-1-cytochrome *c*. *Biochemistry* **36**, 8992-9001.

Banci, L., I. Bertini, F. Ferroni, and A. Rosato (1997b) Solution structure of reduced microsomal rat cytochrome b_5 *Eur. J. Biochem.* **249**, 270-279.

Bao, W., and V. Renganathan (1992) Cellobiose oxidase of *Phanerochaete chrysosporium* enhances crystalline cellulose degradation by cellulases. *FEBS. Lett.* **302**, 77-80.

Bao, W., S. N. Usha, and V. Renganathan (1993) Purification and characterization of cellobiose dehydrogenase, a novel extracellular hemoflavoenzyme from the white-rot fungus *Phanerochaete chrysosporium*. *Arch. Biochem. Biophys.* **300**, 705-713.

Barker, P. D., E. P. Nerou, M. R. Cheesman, A. J. Thomson, P. de Oliveira, and H. A. Hill (1996) Bis-methionine ligation to heme iron in mutants of cytochrome b_{562}. 1. Spectroscopic and electrochemical characterization of the electronic properties. *Biochemistry* **35**, 13618-13626.

Battaile, K. P., J. Molin-Case, R. Paschke, M. Wang, D. Bennett, J. Vockley, and J. J. Kim (2002) Crystal structure of rat short chain acyl-CoA dehydrogenase complexed with acetoacetyl-CoA: comparison with other acyl-CoA dehydrogenases. *J. Biol. Chem.* **277**, 12200-12207.

Bayer, E. A., H. Chanzy, R. Lamed, and Y. Shoham (1998) Cellulose, cellulases and cellulosomes. *Curr. Opin. Struct. Biol.* **8**, 548-557.

Beck von Bodman, S., M. A. Schuler, D. R. Jollie, and S. G. Sligar (1986) Synthesis, bacterial expression, and mutagenesis of the gene coding for mammalian cytochrome b_5. *Proc. Natl. Acad. Sci. U.S.A.* **83**, 9443-9447.

Beguin, P., and J. P. Aubert (1994) The biological degradation of cellulose. *FEMS Microbiol. Rev.* **13**, 25-58.

Berry, E. A., and B. L. Trumpower (1987) Simultaneous determination of hemes *a*, *b*, and *c* from pyridine hemochrome spectra. *Anal. Biochem.* **161**, 1-15.

Bisaria, V. S., and S. Mishra (1989) Regulatory aspects of cellulase biosynthesis and secretion. *Crit. Rev. Biotechnol.* **9**, 61-103.

Bjornberg, O., P. Rowland, S. Larsen, and K. F. Jensen (1997) Active site of dihydroorotate dehydrogenase A from *Lactococcus lactis* investigated by chemical modification and mutagenesis. *Biochemistry* **36**, 16197-16205.

Bourne, Y., and B. Henrissat (2001) Glycoside hydrolases and glycosyltransferases: families and functional modules. *Curr. Opin. Struct. Biol.* **11**, 593-600.

Bright, H. J., and M. Appleby (1969) The pH dependence of the individual steps in the glucose oxidase reaction. *J. Biol. Chem.* **244**, 3625-3634.

Bruice, T. C. (1980) Mechanisms of flavin catalysis. *Acc. Chem. Res.* **13**, 256-262.

Brunger, A. T., P. D. Adams, G. M. Clore, W. L. DeLano, P. Gros, R. W. Grosse-Kunstleve, J. S. Jiang, J. Kuszewski, M. Nilges, N. S. Pannu, R. J. Read, L. M. Rice, T. Simonson, and G. L. Warren (1998) Crystallography & NMR system: A new software suite for macromolecular structure determination. *Acta Crystallogr. D Biol. Crystallogr.* **54**, 905-921.

Burdsall, H. H., and W. Eslyn (1974) *Phanerochaete* with a *Chrysosporium* imperfect state. *Mycotaxon* **1**, 124.

Cameron, M. D., and S. D. Aust (2000) Kinetics and reactivity of the flavin and heme cofactors of cellobiose dehydrogenase from *Phanerochaete chrysosporium*. *Biochemistry* **39**, 13595-13601.

Cameron, M. D., S. Timofeevski, and S. D. Aust (2000) Enzymology of *Phanerochaete chrysosporium* with respect to the degradation of recalcitrant compounds and xenobiotics. *Appl. Microbiol. Biotechnol.* **54**, 751-758.

Canevascini, G., P. Borer, and J. L. Dreyer (1991) Cellobiose dehydrogenases of *Sporotrichum* (*Chrysosporium*) *thermophile*. *Eur. J. Biochem.* **198**, 43-52.

Cavener, D. R. (1992) GMC oxidoreductases. A newly defined family of homologous proteins with diverse catalytic activities. *J. Mol. Biol.* **223**, 811-814.

Chapman, S. K., S. Daff, and A. W. Munro (1997) Heme: the most versatile redox centre in biology. *Struct. Bonding* **88**, 39-70.

Chen, Z. W., M. Koh, G. Van Driessche, J. J. Van Beeumen, R. G. Bartsch, T. E. Meyer, M. A. Cusanovich, and F. S. Mathews (1994) The structure of flavocytochrome *c* sulfide dehydrogenase from a purple phototrophic bacterium. *Science* **266**, 430-432.

Choi, S., T. G. Spiro, K. C. Langry, K. M. Smith, D. L. Budd, and G. N. LaMar (1982) Structural correlations and vinyl influences in resonance Raman spectra of protoheme complexes and proteins. *J. Am. Chem. Soc.* **104**, 4345-4351.

Cohen, J. D., W. Bao, V. Renganathan, S. S. Subramaniam, and T. M. Loehr (1997) Resonance Raman spectroscopic studies of cellobiose dehydrogenase from *Phanerochaete chrysosporium*. *Arch. Biochem. Biophys.* **341**, 321-328.

Coudray, M. R., G. Canevascini, and H. Meier (1982) Characterization of a cellobiose dehydrogenase in the cellulolytic fungus *Sporotrichum (Chrysosporium) thermophile*. *Biochem. J.* **203**, 277-284.

Cox, M. C., M. S. Rogers, M. Cheesman, G. D. Jones, A. J. Thomson, M. T. Wilson, and G. R. Moore (1992) Spectroscopic identification of the haem ligands of cellobiose oxidase. *FEBS Lett.* **307**, 233-236.

Craig, D. H., T. Barna, P. C. Moody, N. C. Bruce, S. K. Chapman, A. W. Munro, and N. S. Scrutton (2001) Effects of environment on flavin reactivity in morphinone reductase: analysis of enzymes displaying differential charge near the N-1 atom and C-2 carbonyl region of the active-site flavin. *Biochem. J.* **359**, 315-323.

Cunane, L. M., Z. W. Chen, N. Shamala, F. S. Mathews, C. N. Cronin, and W. S. McIntire (2000) Structures of the flavocytochrome *p*-cresol methylhydroxylase and its enzyme-substrate complex: gated substrate entry and proton relays support the proposed catalytic mechanism. *J. Mol. Biol.* **295**, 357-374.

Daff, S., W. J. Ingledew, G. A. Reid, and S. K. Chapman (1996) New insights into the catalytic cycle of flavocytochrome b_2. *Biochemistry* **35**, 6345-6350.

Darrouzet, E., S. Mandaci, J. Li, H. Qin, D. B. Knaff, and F. Daldal (1999) Substitution of the sixth axial ligand of *Rhodobacter capsulatus* cytochrome c_1 heme yields novel cytochrome c_1 variants with unusual properties. *Biochemistry* **38**, 7908-7917.

Davis, C. A., I. K. Dhawan, M. K. Johnson, and M. J. Barber (2002) Heterologous expression of an endogenous rat cytochrome b_5/cytochrome b_5 reductase fusion protein: identification of histidines 62 and 85 as the heme axial ligands. *Arch. Biochem. Biophys.* **400**, 63-75.

Delgado-Nixon, V. M., G. Gonzalez, and M. A. Gilles-Gonzalez (2000) Dos, a heme-binding PAS protein from *Escherichia coli*, is a direct oxygen sensor. *Biochemistry* **39**, 2685-2691.

Divne, C., J. Stahlberg, T. Reinikainen, L. Ruohonen, G. Pettersson, J. K. Knowles, T. T. Teeri, and T. A. Jones (1994) The three-dimensional crystal structure of the catalytic core of cellobiohydrolase I from *Trichoderma reesei*. *Science* **265**, 524-528.

Divne, C., J. Stahlberg, T. T. Teeri, and T. A. Jones (1998) High-resolution crystal structures reveal how a cellulose chain is bound in the 50 Å long tunnel of cellobiohydrolase I from *Trichoderma reesei*. *J. Mol. Biol.* **275**, 309-325.

Dou, Y., S. J. Admiraal, M. Ikeda-Saito, S. Krzywda, A. J. Wilkinson, T. Li, J. S. Olson, R. C. Prince, I. J. Pickering, and G. N. George (1995) Alteration of axial coordination by protein engineering in myoglobin. Bisimidazole ligation in the His64-->Val/Val68-->His double mutant. *J. Biol. Chem.* **270**, 15993-16001.

Dumonceaux, T. J., K. A. Bartholomew, T. C. Charles, S. M. Moukha, and F. S. Archibald (1998) Cloning and sequencing of a gene encoding cellobiose dehydrogenase from *Trametes versicolor*. *Gene* **210**, 211-219.

Dumonceaux, T., K. Bartholomew, L. Valeanu, T. Charles, and F. Archibald (2001) Cellobiose dehydrogenase is essential for wood invasion and nonessential for kraft pulp delignification by *Trametes versicolor*. *Enzyme Microb. Technol.* **29**, 478-489.

Dutton, P. L. (1978) Redox potentiometry: determination of midpoint potentials of oxidation-reduction components of biological electron-transfer systems. *Methods Enzymol.* **54**, 411-435.

Dym, O., and D. Eisenberg (2001) Sequence-structure analysis of FAD-containing proteins. *Protein Sci.* **10**, 1712-1728.

Eriksson, K. E., and B. Pettersson (1975) Extracellular enzyme system utilized by the fungus *Sporotrichum pulverulentum* (*Chrysosporium lignorum*) for the breakdown of cellulose. 1. Separation, purification and physico-chemical characterization of five endo-1,4-β-glucanases. *Eur. J. Biochem.* **51**, 193-206.

Eriksson, K. E., B. Pettersson, and U. Westermark (1974) Oxidation: an important enzyme reaction in fungal degradation of cellulose. *FEBS Lett.* **49**, 282-285.

Eriksson, K.-E. L., R. A. Blanchette, and P. Ander (1990) *Microbial and Enzymatic Degradation of Wood and Wood Components*. Springer-Verlag, Berlin Heidelberg.

Evans, P. R. (1993) Data reduction. In *Proceedings of CCP4 Study Weekend, 1993, on Data Collection and Processing*, Science and Engineering Research Council, Daresbury Laboratory, Warrington, Cheshire, U.K., pp. 114-122.

Fagerstam, L. G., L. Goran Pettersson, and J. Ake Engstrom (1984) The primary structure of a 1,4-β-glucan cellobiohydrolase from the fungus *Trichoderma reesei* QM 9414. *FEBS Lett.* **167**, 309-315.

Fang, J., W. Liu, and P. J. Gao (1998) Cellobiose dehydrogenase from *Schizophyllum commune*: purification and study of some catalytic, inactivation, and cellulose-binding properties. *Arch. Biochem. Biophys.* **353**, 37-46.

Fersht, A. (1985) *Enzyme Structure and Mechanism*. W.H. Freeman and Company, New York, pp. 301-307.

Fersht, A. R., J. P. Shi, J. Knill-Jones, D. M. Lowe, A. J. Wilkinson, D. M. Blow, P. Brick, P. Carter, M. M. Waye, and G. Winter (1985) Hydrogen bonding and biological specificity analysed by protein engineering. *Nature* **314**, 235-238.

Field, J. A., E. de Jong, G. Feijoo-Costa, and J. A. M. de Bont (1993) Screening for ligninolytic fungi applicable to the biodegradation of xenobiotics. *Trends Biotech.* **11**, 44-49.

Fraaije, M. W., and A. Mattevi (2000) Flavoenzymes: diverse catalysts with recurrent features. *Trends Biochem. Sci.* **25**, 126-132.

Ghisla, S., and V. Massey (1989) Mechanisms of flavoprotein-catalyzed reactions. *Eur. J. Biochem.* **181**, 1-17.

Gilkes, N. R., B. Henrissat, D. G. Kilburn, R. C. Miller, Jr., and R. A. Warren (1991) Domains in microbial β-1, 4-glycanases: sequence conservation, function, and enzyme families. *Microbiol. Rev.* **55**, 303-315.

Gold, M. H., and M. Alic (1993) Molecular biology of the lignin-degrading basidiomycete *Phanerochaete chrysosporium*. *Microbiol. Rev.* **57**, 605-622.

Gold, M. H., and T. M. Cheng (1978) Induction of colonial growth and replica plating of the white rot basidiomycete *Phanerochaete chrysosporium*. *Appl. Environ. Microbiol.* **35**, 1223-1225.

Gold, M. H., and T. M. Cheng (1979) Conditions for fruit body formation in the white rot basidiomycete *Phanerochaete chrysosporium*. *Arch. Microbiol.* **121**, 37-41.

Gonzalez, G., E. M. Dioum, C. M. Bertolucci, T. Tomita, M. Ikeda-Saito, M. R. Cheesman, N. J. Watmough, and M. A. Gilles-Gonzalez (2002) Nature of the displaceable heme-axial residue in the EcDos protein, a heme-based sensor from *Escherichia coli*. *Biochemistry* **41**, 8414-8421.

Gray, H. B., and J. R. Winkler (1996) Electron transfer in proteins. *Annu. Rev. Biochem.* **65**, 537-561.

Gunner, M. R., E. Alexov, E. Torres, and S. Lipovaca (1997) The importance of the protein in controlling the electrochemistry of heme metalloproteins: methods of calculation and analysis. *J. Biol. Inorg. Chem.* **2**, 126-143.

Habu, N., M. Samejima, J. F. Dean, and K. E. Eriksson (1993) Release of the FAD domain from cellobiose oxidase by proteases from cellulolytic cultures of *Phanerochaete chrysosporium*. *FEBS Lett.* **327**, 161-164.

Hallberg, B. M., T. Bergfors, K. Backbro, G. Pettersson, G. Herriksson, and C. Divne (2000) A new scaffold for binding haem in the cytochrome domain of the extracellular flavocytochrome cellobiose dehydrogenase. *Structure* **8**, 79-88.

Hallberg, B. M., G. Henriksson, G. Pettersson, and C. Divne (2002) Crystal structure of the flavoprotein domain of the extracellular flavocytochrome cellobiose dehydrogenase. *J. Mol. Biol.* **315**, 421-434.

Hallberg, B. M., G. Henriksson, G. Pettersson, A. Vasella, and C. Divne (2003) Mechanism of the reductive half reaction in cellobiose dehydrogenase. *J. Biol. Chem.* **278**, 7160-7166.

Hampsey, D. M., G. Das, and F. Sherman (1988) Yeast iso-1-cytochrome *c*: genetic analysis of structural requirements. *FEBS Lett.* **231**, 275-283.

Harbury, H. A., J. R. Cronin, M. W. Fanger, T. P. Hettinger, A. J. Murphy, Y. P. Myer, and S. N. Vinogradov (1965a) Complex formation between methionine and a heme peptide from cytochrome *c*. *Proc. Natl. Acad. Sci. U.S.A.* **54**, 1658-1664.

Harbury, H. A., J. R. Cronin, M. W. Fanger, T. P. Hettinger, A. J. Murphy, Y. P. Myer, and S. N. Vinogradov (1965b) Complex formation between methionine and a heme peptide from cytochrome *c*. *Proc. Natl. Acad. Sci. U.S.A.* **54**, 1658-1664.

Hecht, H. J., H. M. Kalisz, J. Hendle, R. D. Schmid, and D. Schomburg (1993b) Crystal structure of glucose oxidase from *Aspergillus niger* refined at 2.3 Å resolution. *J. Mol. Biol.* **229**, 153-172.

Henriksson, G., G. Pettersson, G. Johansson, A. Ruiz, and E. Uzcategui (1991) Cellobiose oxidase from *Phanerochaete chrysosporium* can be cleaved by papain into two domains. *Eur. J. Biochem.* **196**, 101-106.

Henriksson, G., G. Johansson, and G. Pettersson (1993) Is cellobiose oxidase from *Phanerochaete chrysosporium* a one-electron reductase? *Biochim. Biophys. Acta* **1144**, 184-190.

Henriksson, G., P. Ander, B. Pettersson, and G. Pettersson (1995) Cellobiose dehydrogenase (cellobiose oxidase) from *Phanerochaete chrysosporium* as a wood-degrading enzyme. Studies on cellulose, xylan and synthetic lignin. *Appl. Microbiol. Biotechnol.* **42**, 790-796.

Henriksson, G., A. Salumets, C. Divne, and G. Pettersson (1997) Studies of cellulose binding by cellobiose dehydrogenase and a comparison with cellobiohydrolase I. *Biochem. J.* **324**, 833-838.

Henriksson, G., V. Sild, I. J. Szabo, G. Pettersson, and G. Johansson (1998) Substrate specificity of cellobiose dehydrogenase from *Phanerochaete chrysosporium*. *Biochim. Biophys. Acta.* **1383**, 48-54.

Henriksson, G., A. Nutt, H. Henriksson, B. Pettersson, J. Stahlberg, G. Johansson, and G. Pettersson (1999) Endoglucanase 28 (Cel12A), a new *Phanerochaete chrysosporium* cellulase. *Eur. J. Biochem.* **259**, 88-95.

Henriksson, G., G. Johansson, and G. Pettersson (2000) A critical review of cellobiose dehydrogenases. *J. Biotechnol.* **78**, 93-113.

Henrissat, B., and A. Bairoch (1993) New families in the classification of glycosyl hydrolases based on amino acid sequence similarities. *Biochem. J.* **293**, 781-788.

Henrissat, B., and A. Bairoch (1996) Updating the sequence-based classification of glycosyl hydrolases. *Biochem. J.* **316**, 695-696.

Henrissat, B., T. T. Teeri, and R. A. Warren (1998) A scheme for designating enzymes that hydrolyse the polysaccharides in the cell walls of plants. *FEBS Lett.* **425**, 352-354.

Higham, C. W., D. Gordon-Smith, C. E. Dempsey, and P. M. Wood (1994) Direct 1H NMR evidence for conversion of β-D-cellobiose to cellobionolactone by cellobiose dehydrogenase from *Phanerochaete chrysosporium*. *FEBS Lett.* **351**, 128-132.

Hines, V., and M. Johnston (1989) Mechanistic studies on the bovine liver mitochondrial dihydroorotate dehydrogenase using kinetic deuterium isotope effects. *Biochemistry* **28**, 1227-1234.

Igarashi, K., M. Samejima, Y. Saburi, N. Habu, and K. E. Eriksson (1997) Localization of cellobiose dehydrogenase in cellulose-grown cultures of *Phanerochaete chrysosporium*. *Fungal Genet. Biol.* **21**, 214-222.

Igarashi, K., M. Samejima, and K. E. Eriksson (1998) Cellobiose dehydrogenase enhances *Phanerochaete chrysosporium* cellobiohydrolase I activity by relieving product inhibition. *Eur. J. Biochem.* **253**, 101-106.

Igarashi, K., M. F. Verhagen, M. Samejima, M. Schulein, K. E. Eriksson, and T. Nishino (1999) Cellobiose dehydrogenase from the fungi *Phanerochaete chrysosporium* and *Humicola insolens*. A flavohemoprotein from *Humicola insolens* contains 6-hydroxy-FAD as the dominant active cofactor. *J. Biol. Chem.* **274**, 3338-3344.

Igarashi, K., I. Momohara, T. Nishino, and M. Samejima (2002) Kinetics of inter-domain electron transfer in flavocytochrome cellobiose dehydrogenase from the white-rot fungus *Phanerochaete chrysosporium*. *Biochem. J.* **365**, 521-526.

Illias, R. M., R. Sinclair, D. Robertson, A. Neu, S. K. Chapman, and G. A. Reid (1998) L-Mandelate dehydrogenase from *Rhodotorula graminis*: cloning, sequencing and kinetic characterization of the recombinant enzyme and its independently expressed flavin domain. *Biochem. J.* **333**, 107-115.

Itagaki, E., and L. P. Hager (1966) Studies on cytochrome b_{562} of *Escherichia coli*. I. Purification and crystallization of cytochrome b_{562}. *J. Biol. Chem.* **241**, 3687-3695.

Iverson, T. M., D. M. Arciero, B. T. Hsu, M. S. Logan, A. B. Hooper, and D. C. Rees (1998) Heme packing motifs revealed by the crystal structure of the tetra-heme cytochrome c_{554} from *Nitrosomonas europaea*. *Nat. Struct. Biol.* **5**, 1005-1012.

Iverson, T. M., D. M. Arciero, A. B. Hooper, and D. C. Rees (2001) High-resolution structures of the oxidized and reduced states of cytochrome c_{554} from *Nitrosomonas europaea*. *J. Biol. Inorg. Chem.* **6**, 390-397.

Jacq, C., and F. Lederer (1974) Cytochrome b_2 from bakers' yeast (L-lactate dehydrogenase) A double-headed enzyme. *Eur. J. Biochem.* **41**, 311-320.

Jensen, K. A., Jr., C. J. Houtman, Z. C. Ryan, and K. E. Hammel (2001) Pathways for extracellular Fenton chemistry in the brown rot basidiomycete *Gloeophyllum trabeum*. *Appl. Environ. Microbiol.* **67**, 2705-2711.

Jensen, K. A., Z. C. Ryan, A. Vanden Wymelenberg, D. Cullen, and K. E. Hammel (2002) An NADH:quinone oxidoreductase active during biodegradation by the brown-rot basidiomycete *Gloeophyllum trabeum*. *Appl. Environ. Microbiol.* **68**, 2699-2703.

Johnson, F. A., S. D. Lewis, and J. A. Shafer (1981) Perturbations in the free energy and enthalpy of ionization of histidine-159 at the active site of papain as determined by fluorescence spectroscopy. *Biochemistry* **20**, 52-58.

Jones, T. A., J. Y. Zou, S. W. Cowan, and Kjeldgaard (1991) Improved methods for building protein models in electron density maps and the location of errors in these models. *Acta Crystallogr. A* **47**, 110-119.

Kamiya, N., Y. Okimoto, Z. Ding, H. Ohtomo, M. Shimizu, A. Kitayama, H. Morii, and T. Nagamune (2001) How does heme axial ligand deletion affect the structure and the function of cytochrome b(562)? *Protein Eng.* **14**, 415-419.

Kamphuis, I. G., K. H. Kalk, M. B. Swarte, and J. Drenth (1984) Structure of papain refined at 1.65 Å resolution. *J. Mol. Biol.* **179**, 233-256.

Kass, I. J., and N. S. Sampson (1998) Evaluation of the role of His447 in the reaction catalyzed by cholesterol oxidase. *Biochemistry* **37**, 17990-18000.

Kassner, R. J. (1972) Effects of nonpolar environments on the redox potentials of heme complexes. *Proc. Natl. Acad. Sci. U.S.A.* **69**, 2263-2267.

Kerem, Z., A. J. Jensen, and K. E. Hammel (1999) Biodegradative mechanism of the brown rot basidiomycete *Gloeophyllum trabeum*: evidence for an extracellular hydroquinone-driven fenton reaction. *FEBS Lett.* **446**, 49-54.

Keys, L. D., III, and M. Johnson (1985) Stereoselectivity in the enzymic oxidation and nonenzymic hydrogen-exchange reactions of dihydroorotate. *J. Am. Chem. Soc* **107**, 486.

Kiess, M., H. J. Hecht, and H. M. Kalisz (1998) Glucose oxidase from *Penicillium amagasakiense*. Primary structure and comparison with other glucose-methanol-choline (GMC) oxidoreductases. *Eur. J. Biochem.* **252**, 90-99.

Kim, J. J., and J. Wu (1988) Structure of the medium-chain acyl-CoA dehydrogenase from pig liver mitochondria at 3 Å resolution. *Proc. Natl. Acad. Sci. U.S.A.* **85**, 6677-6681.

Kinoshita, K., K. Sadanami, A. Kidera, and N. Go (1999) Structural motif of phosphate-binding site common to various protein superfamilies: all-against-all structural comparison of protein-mononucleotide complexes. *Protein Eng.* **12**, 11-14.

Kirk, T. K., E. Schultz, W. J. Connors, L. F. Lorenz, and J. G. Zeikus (1978) Influence of culture parameters on lignin metabolism by *Phanerochaete chrysosporium*. *Arch. Microbiol.* **177**, 277-285.

Kleman-Leyer, K. M., N. R. Gilkes, R. C. Miller, Jr., and T. K. Kirk (1994) Changes in the molecular-size distribution of insoluble celluloses by the action of recombinant *Cellulomonas fimi* cellulases. *Biochem. J.* **302**, 463-469.

Kleywegt, G. J. (2000) Validation of protein crystal structures. *Acta Crystallogr. D Biol. Crystallogr.* **56**, 249-265.

Kleywegt, G. J., and T. A. Jones (1996) Phi/psi-chology: Ramachandran revisited. *Structure* **4**, 1395-1400.

Kleywegt, G. J., J. Y. Zou, C. Divne, G. J. Davies, I. Sinning, J. Stahlberg, T. Reinikainen, M. Srisodsuk, T. T. Teeri, and T. A. Jones (1997) The crystal structure of the catalytic core domain of endoglucanase I from *Trichoderma reesei* at 3.6 Å resolution, and a comparison with related enzymes. *J. Mol. Biol.* **272**, 383-397.

Klyosov, A. A. (1990) Trends in biochemistry and enzymology of cellulose degradation. *Biochemistry* **29**, 10577-10585.

Koenig, J. W. (1974) Production of hydrogen peroxide by wood-rotting fungi in wood and its correlation with weight loss, depolymerizaton, and pH changes. *Arch. Microbiol.* **99**, 129-145.

Koenig, J. W. (1975) Hydrogen peroxide and iron: a microbial cellulolytic system. *Biotechnol. Bioeng. Symp.* 154-159.

Koshland, D. E. (1953) Stereochemistry and the mechanisme of enzymatic reactions. *Biol. Rev.* **28**, 416-436.

Kraulis, J., G. M. Clore, M. Nilges, T. A. Jones, G. Pettersson, J. Knowles, and A. M. Gronenborn (1989) Determination of the three-dimensional solution structure of the C-terminal domain of cellobiohydrolase I from *Trichoderma reesei*. A study using nuclear magnetic resonance and hybrid distance geometry-dynamical simulated annealing. *Biochemistry* **28**, 7241-7257.

Kremer, S. M., and P. M. Wood (1992a) Evidence that cellobiose oxidase from *Phanerochaete chrysosporium* is primarily an Fe(III) reductase. Kinetic comparison with neutrophil NADPH oxidase and yeast flavocytochrome b_2. *Eur. J. Biochem.* **205**, 133-138.

Kremer, S. M., and P. M. Wood (1992b) Production of Fenton's reagent by cellobiose oxidase from cellulolytic cultures of *Phanerochaete chrysosporium*. *Eur. J. Biochem.* **208**, 807-814.

Laemmli, U. K. (1970) Cleavage of structural proteins during the assembly of the head of bacteriophage T4. *Nature* **227**, 680-685.

Lario, P. I., N. Sampson, and A. Vrielink (2003) Sub-atomic resolution crystal structure of cholesterol oxidase: what atomic resolution crystallography reveals about enzyme mechanism and the role of the FAD cofactor in redox activity. *J. Mol. Biol.* **326,** 1635-1650.

Ledeboer, A. M., L. Edens, J. Maat, C. Visser, J. W. Bos, C. T. Verrips, Z. Janowicz, M. Eckart, R. Roggenkamp, and C. P. Hollenberg (1985) Molecular cloning and characterization of a gene coding for methanol oxidase in *Hansenula polymorpha*. *Nucleic Acids Res.* **13**, 3063-3082.

Lehner, D., P. Zipper, G. Henriksson, and G. Pettersson (1996) Small-angle X-ray scattering studies on cellobiose dehydrogenase from *Phanerochaete chrysosporium*. *Biochim. Biophys. Acta* **1293**, 161-169.

Leys, D., A. S. Tsapin, K. H. Nealson, T. E. Meyer, M. A. Cusanovich, and J. J. Van Beeumen (1999) Structure and mechanism of the flavocytochrome *c* fumarate reductase of *Shewanella putrefaciens* MR-1. *Nat. Struct. Biol.* **6,** 1113-1117.

Li, B. (1999) Cloning and characterization of cellobiose dehydrogenase from *Phanerochaete chrysosporium*. Ph.D. Dissertation, Oregon Graduate Institute of Science & Technology, Beaverton, Oregon, pp. 59-75.

Li, B., S. R. Nagalla, and V. Renganathan (1996) Cloning of a cDNA encoding cellobiose dehydrogenase, a hemoflavoenzyme from *Phanerochaete chrysosporium*. *Appl. Environ. Microbiol.* **62**, 1329-1335.

Li, B., S. R. Nagalla, and V. Renganathan (1997) Cellobiose dehydrogenase from *Phanerochaete chrysosporium* is encoded by two allelic variants. *Appl. Environ. Microbiol.* **63**, 796-799.

Li, B., F. A. J. Rotsaert, M. H. Gold, and V. Renganathan (2000) Homologous expression of recombinant cellobiose dehydrogenase in *Phanerochaete chrysosporium*. *Biochem. Biophys. Res. Commun.* **270**, 141-146.

Li, D., H. L. Youngs, and M. H. Gold (2001) Heterologous expression of a thermostable manganese peroxidase from *Dichomitus squalens* in *Phanerochaete chrysosporium*. *Arch. Biochem. Biophys.* **385**, 348-356.

Li, J., A. Vrielink, P. Brick, and D. M. Blow (1993) Crystal structure of cholesterol oxidase complexed with a steroid substrate: implications for flavin adenine dinucleotide dependent alcohol oxidases. *Biochemistry* **32**, 11507-11515.

Linder, M., M. L. Mattinen, M. Kontteli, G. Lindeberg, J. Stahlberg, T. Drakenberg, T. Reinikainen, G. Pettersson, and A. Annila (1995) Identification of functionally important amino acids in the cellulose-binding domain of *Trichoderma reesei* cellobiohydrolase I. *Protein Sci.* **4**, 1056-1064.

Lindner, M., and T. T. Teeri (1997) The roles and function of cellulose-binding domain. *J. Biotechnol.* **57**, 15-28.

Lloyd, E., D. P. Hildebrand, K. M. Tu, and A. G. Mauk (1995) Conversion of myoglobin into a reversible electron transfer protein that maintains bis-histidine axial ligation. *J. Am. Chem. Soc.* **117**, 6433-6438.

Lu, Y., D. R. Casimiro, K. L. Bren, J. H. Richards, and H. B. Gray (1993) Structurally engineered cytochromes with unusual ligand-binding properties: expression of *Saccharomyces cerevisiae* Met-80 → Ala iso-1-cytochrome *c*. *Proc. Natl. Acad. Sci. U.S.A.* **90**, 11456-11459.

Mansfield, S. D., E. De Jong, and N. Saddler John (1997) Cellobiose dehydrogenase, an active agent in cellulose depolymerization. *Appl. Environ. Microbiol.* **63**, 3804-3809.

Marcus, R. A., and N. Sutin (1985) DNA damage through long-range electron transfer. *Biochem. Biophys. Acta* **811**, 265-275.

Martinez, S. E., D. Huang, A. Szczepaniak, W. A. Cramer, and J. L. Smith (1994) Crystal structure of chloroplast cytochrome *f* reveals a novel cytochrome fold and unexpected heme ligation. *Structure* **2**, 95-105.

Massey, V. (1995) Introduction: flavoprotein structure and mechanism. *FASEB J.* **9**, 473-475.

Mathews, F. S., Z. W. Chen, H. D. Bellamy, and W. S. McIntire (1991) Three-dimensional structure of *p*-cresol methylhydroxylase (flavocytochrome *c*) from *Pseudomonas putida* at 3.0 Å resolution. *Biochemistry* **30**, 238-247.

Mattevi, A., M. A. Vanoni, F. Todone, M. Rizzi, A. Teplyakov, A. Coda, M. Bolognesi, and B. Curti (1996) Crystal structure of D-amino acid oxidase: a case of active site mirror-image convergent evolution with flavocytochrome b_2. *Proc. Natl. Acad. Sci. U.S.A.* **93**, 7496-7501.

Mattevi, A., M. W. Fraaije, A. Mozzarelli, L. Olivi, A. Coda, and W. J. van Berkel (1997) Crystal structures and inhibitor binding in the octameric flavoenzyme vanillyl-alcohol oxidase: the shape of the active-site cavity controls substrate specificity. *Structure* **5**, 907-920.

Mattinen, M. L., M. Kontteli, J. Kerovuo, M. Linder, A. Annila, G. Lindeberg, T. Reinikainen, and T. Drakenberg (1997) Three-dimensional structures of three engineered cellulose-binding domains of cellobiohydrolase I from *Trichoderma reesei*. *Protein Sci.* **6**, 294-303.

Mauk, A. G., and G. R. Moore (1997) Control of metalloprotein redox potentials: what does site-directed mutagenesis of hemoproteins tell us? *J. Biol. Inorg. Chem.* **2**, 119-125.

Mayfield, M. B., K. Kishi, M. Alic, and M. H. Gold (1994) Homologous expression of recombinant manganese peroxidase in *Phanerochaete chrysosporium*. *Appl. Environ. Microbiol.* **60**, 4303-4309.

McPherson, A. (1982) *Preparation and Analysis of Protein Chrystals*. John Wiley and Sons, New York.

Mewies, M., W. S. McIntire, and N. S. Scrutton (1998) Covalent attachment of flavin adenine dinucleotide (FAD) and flavin mononucleotide (FMN) to enzymes: the current state of affairs. *Protein Sci.* **7**, 7-20.

Miles, C. S., F. D. Manson, G. A. Reid, and S. K. Chapman (1993) Substitution of a haem-iron axial ligand in flavocytochrome b_2. *Biochim. Biophys. Acta* **1202**, 82-86.

Miller, G. T., B. Zhang, J. K. Hardman, and R. Timkovich (2000) Converting a *c*-type to a *b*-type cytochrome: Met61 to His61 mutant of *Pseudomonas* cytochrome c_{551}. *Biochemistry* **39**, 9010-9017.

Moore, G. R., and G. W. Pettigrew (1990) *Cytochrome c: Evolutionary, Structural, and Physiochemical Aspects*. Springer-Verlag, Berlin.

Moore, G. R., and R. J. Williams (1977) Structural basis for the variation in redox potential of cytochromes. *FEBS Lett.* **79**, 229-232.

Moore, G. R., R. J. Williams, J. Peterson, A. J. Thomson, and F. S. Mathews (1985) A spectroscopic investigation of the structure and redox properties of *Escherichia coli* cytochrome b_{562}. *Biochim. Biophys. Acta* **829**, 83-96.

Morpeth, F. F. (1985) Some properties of cellobiose oxidase from the white-rot fungus *Sporotrichum pulverulentum*. *Biochem. J.* **228**, 557-564.

Morpeth, F. F., and G. D. Jones (1986) Resolution, purification and some properties of the multiple forms of cellobiose:quinone dehydrogenase from the white-rot fungus *Sporotrichum pulverulentum*. *Biochem. J.* **236**, 221-226.

Moukha, S. M., T. J. Dumonceaux, E. Record, and F. S. Archibald (1999) Cloning and analysis of *Pycnoporus cinnabarinus* cellobiose dehydrogenase. *Gene* **234**, 23-33.

Mowat, C. G., C. S. Miles, A. W. Munro, M. R. Cheesman, L. G. Quaroni, G. A. Reid, and S. K. Chapman (2000) Changing the heme ligation in flavocytochrome b_2: substitution of histidine-66 by cysteine. *J. Biol. Inorg. Chem.* **5**, 584-592.

Munoz, I. G., W. Ubhayasekera, H. Henriksson, I. Szabo, G. Pettersson, G. Johansson, S. L. Mowbray, and J. Stahlberg (2001) Family 7 cellobiohydrolases from *Phanerochaete chrysosporium*: crystal structure of the catalytic module of Cel7D

(CBH58) at 1.32 Å resolution and homology models of the isozymes. *J. Mol. Biol.* **314**, 1097-1111.

Murshudov, G. N., A. A. Vagin, and E. J. Dodson (1997) Refinement of macromolecular structures by the maximum-likelyhood method. *Acta Crystallogr. D Biol. Crystallogr.* **53**, 240-255.

Okamura, K. (1991) Structure of cellulose. In *Wood and Cellulosic Chemistry* (Hon and Shiraishi, eds.), Marcel Dekker, New York, Basel, pp. 89-112.

Ostermeier, C., A. Harrenga, U. Ermler, and H. Michel (1997) Structure at 2.7 Å resolution of the *Paracoccus denitrificans* two-subunit cytochrome *c* oxidase complexed with an antibody FV fragment. *Proc. Natl. Acad. Sci. U.S.A.* **94**, 10547-10553.

Ozols, J., and P. Strittmatter (1964) The interaction of porphyrins and metalloporphyrins with apocytochrome b_5. *J. Biol. Chem.* **239**, 1018-1023.

Paoli, M., J. Marles-Wright, and A. Smith (2002) Structure-function relationships in heme-proteins. *DNA Cell. Biol.* **21**, 271-280.

Pascal, R. A., Jr., and C. T. Walsh (1984) Mechanistic studies with deuterated dihydroorotates on the dihydroorotate oxidase from *Crithidia fasciculata*. *Biochemistry* **23**, 2745-2752.

Paszczynski, A., R. Crawford, D. Funk, and B. Goodell (1999) De novo synthesis of 4,5-dimethoxycatechol and 2, 5-dimethoxyhydroquinone by the brown rot fungus *Gloeophyllum trabeum*. *Appl. Environ. Microbiol.* **65**, 674-679.

Powell, H. R. (1999) The Rossmann Fourier autoindexing algorithm in MOSFLM. *Acta Crystallogr. D Biol. Crystallogr.* **55**, 1690-1695.

Pratima, B. P., and P. K. Bajpai (2001) Status of biotechnology in pulp and paper industry. *http://www.inpaper.com/*

Qin, J., G. N. La Mar, Y. Dou, S. J. Admiraal, and M. Ikeda-Saito (1994) 1H NMR study of the solution molecular and electronic structure of engineered distal myoglobin His64(E7) Val/Val68(E11) His double mutant. Coordination of His64(E11) at the sixth position in both low-spin and high-spin states. *J. Biol. Chem.* **269**, 1083-1090.

Raices, M., E. Paifer, J. Cremata, R. Montesino, J. Stahlberg, C. Divne, J. Szabo Istvan, G. Henriksson, G. Johansson, and G. Pettersson (1995) Cloning and characterization of a cDNA encoding a cellobiose dehydrogenase from the white rot fungus *Phanerochaete chrysosporium*. *FEBS Lett.* **369**, 233-238.

Raices, M., R. Montesino, J. Cremata, B. Garcia, W. Perdomo, I. I. Szabo, G. Henriksson, B. M. Hallberg, G. Pettersson, and G. Johansson (2002) Cellobiose: quinone oxidoreductase from the white rot fungus *Phanerochaete chrysosporium* is produced by intracellular proteolysis of cellobiose dehydrogenase. *Biochim. Biophys. Acta* **1576**, 15-22.

Ramakrishnan, C., and G. N. Ramachandran (1965) Stereochemical criteria for polypeptide and protein chain conformations. II. Allowed conformations for a pair of peptide units. *Biophys. J.* **5**, 909-933.

Raphael, A. L., and H. B. Gray (1989) Axial ligand replacement in horse heart cytochrome *c* by semisynthesis. *Proteins* **6**, 338-340.

Receveur, V., M. Czjzek, M. Schulein, P. Panine, and B. Henrissat (2002) Dimension, shape and conformational flexibility of a two domain fungal cellulase in solution probed by small angle solution X-ray scattering. *J. Biol. Chem.* **277**, 40887-40892.

Reddy, G. V. B., and M. H. Gold (2000) Degradation of pentachlorophenol by *Phanerochaete chrysosporium*: Intermediates and reactions involved. *Microbiology* **146**, 405-413.

Reid, L. S., F. T. Taniguschi, H. B. Gray, and A. G. Mauk (1982) Oxidation-reduction equilibrium of cytochrome b_5. *J. Am. Chem. Soc.* **104**, 7516-7519.

Reid, G. A., S. White, M. T. Black, F. Lederer, F. S. Mathews, and S. K. Chapman (1988) Probing the active site of flavocytochrome b_2 by site-directed mutagenesis. *Eur. J. Biochem.* **178**, 329-333.

Reinikainen, T., L. Ruohonen, T. Nevanen, L. Laaksonen, P. Kraulis, T. A. Jones, J. K. Knowles, and T. T. Teeri (1992) Investigation of the function of mutated cellulose-binding domains of *Trichoderma reesei* cellobiohydrolase I. *Proteins* **14**, 475-482.

Renganathan, V., and W. Bao (1994) Cellobiose dehydrogenase. A hemoflavoenzyme from *Phanerochaete chrysosporium*. *ACS Symp. Ser.* **566**, 179-187.

Renganathan, V., S. N. Usha, and F. Lindenburg (1990) Cellobiose oxidizing enzymes from the lignocellulose degrading basidiomycete *Phanerochaete chrysosporium* interaction with microcrystalline cellulose. *Appl. Microbiol. Biotechnol.* **32**, 609-613.

Rodriguez, J. C., and M. Rivera (1998) Conversion of mitochondrial cytochrome b_5 into a species capable of performing the efficient coupled oxidation of heme. *Biochemistry* **37**, 13082-13090.

Roth, J. P., and J. P. Klinman (2003) Catalysis of electron transfer during activation of O_2 by the flavoprotein glucose oxidase. *Proc. Natl. Acad. Sci. U.S.A.* **100**, 62-67.

Rouvinen, J., T. Bergfors, T. Teeri, J. K. Knowles, and T. A. Jones (1990) Three-dimensional structure of cellobiohydrolase II from *Trichoderma reesei*. *Science* **249**, 380-386.

Rowland, P., F. S. Nielsen, K. F. Jensen, and S. Larsen (1997) The crystal structure of the flavin containing enzyme dihydroorotate dehydrogenase A from *Lactococcus lactis*. *Structure* **5**, 239-252.

Rowland, P., O. Bjornberg, F. S. Nielsen, K. F. Jensen, and S. Larsen (1998) The crystal structure of *Lactococcus lactis* dihydroorotate dehydrogenase A complexed with the enzyme reaction product throws light on its enzymatic function. *Protein Sci.* **7**, 1269-1279.

Roy, B. P., M. G. Paice, F. S. Archibald, S. K. Misra, and L. E. Misiak (1994) Creation of metal-complexing agents, reduction of manganese dioxide, and promotion of manganese peroxidase-mediated Mn(III) production by cellobiose:quinone oxidoreductase from *Trametes versicolor*. *J. Biol. Chem.* **269**, 19745-19750.

Roy, B. P., T. Dumonceaux, A. A. Koukoulas, and F. S. Archibald (1996) Purification and characterization of cellobiose dehydrogenases from the white rot fungus *Trametes versicolor*. *Appl. Environ. Microbiol.* **62**, 4417-4427.

Sadana, J. C., and R. V. Patil (1985) The purification and properties of cellobiose dehydrogenase from *Sclerotium rolfsii* and its role in cellulolysis. *J. Gen. Microb.* **131**, 1917-1923.

Samejima, M., and K. E. Eriksson (1991) Mechanisms of redox interactions between lignin peroxidase and cellobiose:quinone oxidoreductase. *FEBS Lett.* **292**, 151-153.

Samejima, M., and K. E. Eriksson (1992) A comparison of the catalytic properties of cellobiose:quinone oxidoreductase and cellobiose oxidase from *Phanerochaete chrysosporium*. *Eur. J. Biochem.* **207**, 103-107.

Samejima, M., R. S. Phillips, and K. E. Eriksson (1992) Cellobiose oxidase from *Phanerochaete chrysosporium*. Stopped-flow spectrophotometric analysis of pH-dependent reduction. *FEBS Lett.* **306**, 165-168.

Samejima, M., T. Ohkubo, K. Igarashi, A. Isogai, S. Kuga, J. Sugiyama, and L. Eriksson Karl-Erik (1997) The behavior of *Phanerochaete chrysosporium* cellobiose dehydrogenase on adsorption to crystalline and amorphous celluloses. *Biotechnol. Appl. Biochem.* **25**, 135-141.

Sampson, N. S., and I. J. Kass (1997) Isomerization, but not oxidation, is suppressed by a single point mutation, E361Q, in the reaction catalyzed by cholesterol oxidase. *J. Am. Chem. Soc.* **119**, 855-862.

Schmidhalter, D. R., and G. Canevascini (1993) Isolation and characterization of the cellobiose dehydrogenase from the brown-rot fungus *Coniophora puteana* (Schum ex Fr.) Karst. *Arch. Biochem. Biophys.* **300**, 559-563.

Schou, C., M. H. Christensen, and M. Schulein (1998) Characterization of a cellobiose dehydrogenase from *Humicola insolens*. *Biochem. J.* **330**, 565-571.

Schulein, M. (2000) Protein engineering of cellulases. *Biochim. Biophys. Acta.* **1543**, 239-252.

Sharp, R. E., P. White, S. K. Chapman, and G. A. Reid (1994) The use of deletion mutants in the hinge region as functional probes of flavocytochrome b_2. *Biochem. Soc. Trans.* **22**, 281S.

Sharp, R. E., S. K. Chapman, and G. A. Reid (1996a) Deletions in the interdomain hinge region of flavocytochrome b_2: effects on intraprotein electron transfer. *Biochemistry* **35**, 891-899.

Sharp, R. E., S. K. Chapman, and G. A. Reid (1996b) Modulation of flavocytochrome b_2 intraprotein electron transfer via an interdomain hinge region. *Biochem. J.* **316**, 507-513.

Silverman, R. B., S. J. Hoffman, and W. B. Catus III (1980) A mechanism for mitochondrial monoamine oxidase catalyzed amine oxidation. *J. Am. Chem. Soc.* **102**, 7126-7128.

Sligar, S. G., and K. D. Egeberg (1987) Alteration of heme axial ligands by site-directed mutagenesis: a cytochrome becomes a catalytic demethylase. *J. Am. Chem. Soc.* **109**, 7896-7897.

Smith, P. K., R. I. Krohn, G. T. Hermanson, A. K. Mallia, F. H. Gartner, M. D. Provenzano, E. K. Fujimoto, N. M. Goeke, B. J. Olson, and D. C. Klenk (1985) Measurement of protein using bicinchoninic acid. *Anal. Biochem.* **150**, 76-85.

Sollewijn Gelpke, M. D., M. Mayfield-Gambill, G. P. L. Cereghino, and M. H. Gold (1999) Homologous expression of recombinant lignin peroxidase in *Phanerochaete chrysosporium*. *Appl. Environ. Microbiol.* **65**, 1670-1674.

Spiro, T. G., and X. Li (1988) Resonanance Raman spectroscopy of heme and metalloproteins. In *Biological Application of Raman Spectroscopy*, Vol. 3 (T. G. Spiro. ed.), John Wiley & Sons, New York, pp 1-37.

Spiro, T. G., J. D. Stong, and P. Stein (1979) Porphyrin core expansion and doming in heme proteins: new evidence from resonance Raman spectra of six-coordinate high-spin iron(III) hemes. *J. Am. Chem. Soc.* **101**, 2648-2655.

Stenberg, K., and Y. Lindqvist (1997) Three-dimensional structures of glycolate oxidase with bound active-site inhibitors. *Protein Sci.* **6**, 1009-1015.

Street, I. P., C. R. Armstrong, and S. G. Withers (1986) Hydrogen bonding and specificity. Fluorodeoxy sugars as probes of hydrogen bonding in the glycogen phosphorylase-glucose complex. *Biochemistry* **25**, 6021-6027.

Su, Q., and J. P. Klinman (1999) Nature of oxygen activation in glucose oxidase from *Aspergillus niger*: the importance of electrostatic stabilization in superoxide formation. *Biochemistry* **38**, 8572-8581.

Subramaniam, S. S. (1999) Cloning and biochemical characterization of a thermostable cellobiose dehydrogenase from *Sporotrichum thermophile* and its role in cellulose degradation. Ph.D. Dissertation, Oregon Graduate Institute of Science & Technology, Beaverton, OR, pp. 96-116.

Subramaniam, S. S., S. R. Nagalla, and V. Renganathan (1999) Cloning and characterization of a thermostable cellobiose dehydrogenase from *Sporotrichum thermophile*. *Arch. Biochem. Biophys.* **365**, 223-230.

Sukumar, N., Y. Xu, D. L. Gatti, B. Mitra, and F. S. Mathews (2001) Structure of an active soluble mutant of the membrane-associated (S)-mandelate dehydrogenase. *Biochemistry* **40**, 9870-9878.

Sun, W., C. H. Williams, Jr., and V. Massey (1996) Site-directed mutagenesis of glycine 99 to alanine in L-lactate monooxygenase from *Mycobacterium smegmatis*. *J. Biol. Chem.* **271**, 17226-17233.

Tamura, M., T. Asakura, and T. Yonetani (1972) Heme-modification studies on horseradish peroxidase. *Biochim. Biophys. Acta* **268**, 292-304.

Teeri, T. T. (1997) Crystalline cellulose degradation: new insight into the function of cellobiohydrolases. *Trends Biotechnol.* **15**, 160-167.

Temp, U., and C. Eggert (1999) Novel interaction between laccase and cellobiose dehydrogenase during pigment synthesis in the white rot fungus *Pycnoporus cinnabarinus*. *Appl. Environ. Microbiol.* **65**, 389-395.

Thomas, R. J. (1991) *Wood Structure and Composition*. Marcel Dekker, New York.

Tokimatsu, T., Y. Nagai, T. Hattori, and M. Shimada (1998) Purification and characteristics of a novel cytochrome c dependent glyoxylate dehydrogenase from a wood-destroying fungus *Tyromyces palustris*. *FEBS Lett.* **437**, 117-121.

Tomme, P., A. J. Warren, R. C. Miller, D. G. Kilburn, and N. R. Gilkes (1995) *Cellulose-Binding Domains: Classification and Properties*. American Chemical Society, New York.

Umhau, S., L. Pollegioni, G. Molla, K. Diederichs, W. Welte, M. S. Pilone, and S. Ghisla (2000) The X-ray structure of D-amino acid oxidase at very high resolution identifies the chemical mechanism of flavin-dependent substrate dehydrogenation. *Proc. Natl. Acad. Sci. U.S.A.* **97**, 12463-12468.

Uzcategui, E., G. Johansson, B. Ek, and G. Pettersson (1991) The 1,4-β-D-glucan glucanohydrolases from *Phanerochaete chrysosporium*. Re-assessment of their significance in cellulose degradation mechanisms. *J. Biotechnol.* **21**, 143-159.

Vallim, M. A., B. J. Janse, J. Gaskell, A. A. Pizzirani-Kleiner, and D. Cullen (1998) *Phanerochaete chrysosporium* cellobiohydrolase and cellobiose dehydrogenase transcripts in wood. *Appl. Environ. Microbiol.* **64**, 1924-1928.

van Beilen, J. B., G. Eggink, H. Enequist, R. Bos, and B. Witholt (1992) DNA sequence determination and functional characterization of the OCT-plasmid-encoded alkJKL genes of *Pseudomonas oleovorans*. *Mol. Microbiol.* **6**, 3121-3136.

Vogels, H. J. (1964) Distribution of lysine pathways among fungi: evolutionary implications. *Am. Nat.* **98**.

von Jagow, G., and W. Sebald (1980) *b*-Type cytochromes. *Annu. Rev. Biochem.* **49**, 281-314.

Vrielink, A., L. F. Lloyd, and D. M. Blow (1991a) Crystal structure of cholesterol oxidase from *Brevibacterium sterolicum* refined at 1.8 Å resolution. *J. Mol. Biol.* **219**, 533-554.

Wallace, C. J., and I. Clark-Lewis (1992) Functional role of heme ligation in cytochrome *c*. Effects of replacement of methionine 80 with natural and non-natural residues by semisynthesis. *J. Biol. Chem.* **267**, 3852-3861.

Walsh, C. (1980) Flavin coenzymes: at the crossroads of biological redox chemistry. *Acc. Chem. Res.* **13**, 148-155.

Weibel, M. K., and H. J. Bright (1971) The glucose oxidase mechanism. Interpretation of the pH dependence. *J. Biol. Chem.* **246**, 2734-2744.

Westermark, U., and K. E. Eriksson (1975) Purification and properties of cellobiose: quinone oxidoreductase from *Sporotrichum pulverulentum*. *Acta Chem. Scand. [B]* **29**, 419-424.

Whetten, R., E. Organ, P. Krasney, D. Cox-Foster, and D. Cavener (1988) Molecular structure and transformation of the glucose dehydrogenase gene in *Drosophila melanogaster*. *Genetics* **120**, 475-484.

White-Rot Genome Project (2002) Joint Genome Institute, U.S Department of Energy. *http://www.jgi.doe.gov/programs/whiterot.htm*

Wierenga, R. K., P. Terpstra, and W. G. Hol (1986) Prediction of the occurrence of the ADP-binding beta alpha beta-fold in proteins, using an amino acid sequence fingerprint. *J. Mol. Biol.* **187**, 101-107.

Witt, S., M. Singh, and H. M. Kalisz (1998) Structural and kinetic properties of nonglycosylated recombinant *Penicillium amagasakiense* glucose oxidase expressed in *Escherichia coli*. *Appl. Environ. Microbiol.* **64**, 1405-1411.

Witt, S., G. Wohlfahrt, D. Schomburg, H. J. Hecht, and H. M. Kalisz (2000) Conserved arginine-516 of *Penicillium amagasakiense* glucose oxidase is essential for the efficient binding of β-D-glucose. *Biochem. J.* **347**, 553-559.

Wohlfahrt, G., S. Witt, J. Hendle, D. Schomburg, H. M. Kalisz, and H. J. Hecht (1999) 1.8 and 1.9 Å resolution structures of the *Penicillium amagasakiense* and *Aspergillus niger* glucose oxidases as a basis for modelling substrate complexes. *Acta Crystallogr. D Biol. Crystallogr.* **55**, 969-977.

Wood, J. D., and P. M. Wood (1992) Evidence that cellobiose:quinone oxidoreductase from *Phanerochaete chrysosporium* is a breakdown product of cellobiose oxidase. *Biochim. Biophys. Acta* **1119**, 90-96.

Xavier, A. V., E. W. Czerwinski, P. H. Bethge, and F. S. Mathews (1978) Identification of the haem ligands of cytochrome b_{562} by X-ray and NMR methods. *Nature* **275**, 245-247.

Xia, Z. X., and F. S. Mathews (1990) Molecular structure of flavocytochrome b_2 at 2.4 Å resolution. *J. Mol. Biol.* **212**, 837-863.

Xu, D., R. M. Kohli, and V. Massey (1999) The role of threonine 37 in flavin reactivity of the old yellow enzyme. *Proc. Natl. Acad. Sci. U.S.A.* **96**, 3556-3561.

Xu, F., E. J. Golightly, K. R. Duke, S. F. Lassen, B. Knusen, S. Christensen, K. M. Brown, S. H. Brown, and M. Schulein (2001) *Humicola insolens* cellobiose

dehydrogenase: cloning, redox chemistry, and "logic gate"-like dual functionality. *Enzyme Microb. Technol.* **28**, 744-753.

Xu, G., and B. Goodell (2001) Mechanisms of wood degradation by brown-rot fungi: chelator-mediated cellulose degradation and binding of iron by cellulose. *J. Biotechnol.* **87**, 43-57.

Yagi, K., N. Ohishi, K. Nishimoto, J. D. Choi, and P. S. Song (1980) Effect of hydrogen bonding on electronic spectra and reactivity of flavins. *Biochemistry* **19**, 1553-1557.

Yamashita, M., M. Toyama, H. Ono, I. Fujii, N. Hirayama, and Y. Murooka (1998) Separation of the two reactions, oxidation and isomerization, catalyzed by *Streptomyces* cholesterol oxidase. *Protein Eng.* **11**, 1075-1081.

Yasin, M., and C. A. Fewson (1993) L(+)-Mandelate dehydrogenase from *Rhodotorula graminis*: purification, partial characterization and identification as a flavocytochrome *b*. *Biochem. J.* **293**, 455-460.

Yin, Y., N. S. Sampson, A. Vrielink, and P. I. Lario (2001) The presence of a hydrogen bond between asparagine 485 and the π system of FAD modulates the redox potential in the reaction catalyzed by cholesterol oxidase. *Biochemistry* **40**, 13779-13787.

Yoshida, M., T. Ohira, K. Igarashi, H. Nagasawa, K. Aida, B. M. Hallberg, C. Divne, T. Nishino, and M. Samejima (2001) Production and characterization of recombinant *Phanerochaete chrysosporium* cellobiose dehydrogenase in the methylotrophic yeast *Pichia pastoris*. *Biosci. Biotechnol. Biochem.* **65**, 2050-2057.

Yoshida, M., T. Ohira, K. Igarashi, H. Nagasawa, and M. Samejima (2002) Molecular cloning and characterization of a cDNA encoding cellobiose dehydrogenase from the wood-rotting fungus *Grifola frondosa*. *FEMS Microbiol. Lett.* **217**, 225-230.

Yue, Q. K., I. J. Kass, N. S. Sampson, and A. Vrielink (1999) Crystal structure determination of cholesterol oxidase from *Streptomyces* and structural characterization of key active site mutants. *Biochemistry* **38**, 4277-4286.

Zaric, S. D., D. M. Popovic, and E. W. Knapp (2001) Factors determining the orientation of axially coordinated imidazoles in heme proteins. *Biochemistry* **40**, 7914-7928.

Zechel, D. L., and S. G. Withers (2000) Glycosidase mechanisms: anatomy of a finely tuned catalyst. *Acc. Chem. Res.* **33**, 11-18.

Zou, J., G. J. Kleywegt, J. Stahlberg, H. Driguez, W. Nerinckx, M. Claeyssens, A. Koivula, T. T. Teeri, and T. A. Jones (1999) Crystallographic evidence for substrate ring distortion and protein conformational changes during catalysis in cellobiohydrolase Ce16A from *Trichoderma reesei*. *Struct. Fold. Des.* **7**, 1035-1045.

BIOGRAPHICAL SKETCH

The author was born on November 16, 1971, in Waregem, Belgium. In 1996, he received his M.S. in Chemical engineering from Delft University of Technology in The Netherlands. In the spring of 1998, he received his M.S. without thesis in Biochemistry and Molecular Biology at the OGI School of Science and Engineering at Oregon Health & Science University (formerly the Oregon Graduate Institute of Science & Engineering). That same year, he joined the laboratory of Drs. V. Renganathan and M. H. Gold to pursue his Ph.D.

Publications

Li, B., Rotsaert, F.A.J., Gold, M.H., and Renganathan, V. (2000) Homologous expression of recombinant cellobiose dehydrogenase in *Phanerochaete chrysosporium*. *Biochem. Biophys. Res. Commun.* **270:**141–146.

Rotsaert, F.A.J., Li, B., Renganathan, V., and Gold, M.H. (2001) Site-directed mutagenesis of the heme axial ligands in the hemoflavoenzyme cellobiose dehydrogenase. *Arch. Biochem. Biophys.* **390:**206–214.

van Amsterdam, I.M.C., Ubbink, M., van den Bosch, M., Rotsaert, F., Sanders-Loehr, J., and Canters, G.W. (2002) A new type 2 copper cysteinate azurin. Involvement of an engineered exposed cysteine in copper binding through internal rearrangement. *J. Biol. Chem.* **277:**44121–44130.

Rotsaert, F.A.J., Pikus, J.D., Fox, B.G., Markley, J.L., and Sanders-Loehr, J. (2003) N-Isotope effects on the Raman spectra of Fe_2S_2 ferredoxins and Rieske ferredoxins: evidence of structural rigidity of metal sites. *J. Biol. Inorg. Chem.* **8:** 318–326.

Rotsaert, F.A.J., Renganathan, V., and Gold, M.H. (2003) Role of the flavin domain residues, His 689 and Asn732, in the catalytic mechanism of cellobiose dehydrogenase from *Phanerochaete chrysosporium*. *Biochemistry* **42:**4049–4056.